UNIVERSITEIT VAN PRETORIA
UNIVERSITY OF PRETORIA
YUNIBESITHI YA PRETORIA

Faculty of Natural and Agricultural Sciences

Fungal diversity in Namibian *Stipagrostis* 'fairy circles' including the description of new *Curvularia* species

By

Nicole Innike van Vuuren

Submitted in partial fulfilment of the requirements for the degree

Magister Scientiae

In the faculty of Natural and Agricultural Sciences

Department of Biochemistry, Genetics and Microbiology

Forestry and Agricultural Biotechnology Institute at the University of Pretoria, Pretoria, South Africa

August 2022

DECLARATION OF ORIGINALITY

UNIVERSITY OF PRETORIA

I**, Nicole Innike van Vuuren** declare that the dissertation , which I hereby submit for the degree Magister Scientae at the Univeristy of Pretoria, is my own work and has not previously been submitted by me for a degree at this or any other tertiary institution.

SIGNATURE: 

DATE: 18 August 2022

Table of Contents

List of tables and figures

Acknowledgements

I would firstly like to acknowledge my supervisors, who not only devoted an immense number of hours to my project but supported me throughout the process.

To Dr Neriman Yilmaz, it has been a great pleasure to be your student. Thank you for your patience, guidance, motivation, and support throughout my studies. You have taught me so many valuable lessons and given me so many wonderful opportunities. You have always been there for me, and I could not imagine completing a task such as this without you. I am truly grateful for the impact you as a mentor had on me as an individual, allowing me to grow as a scientist.

To Prof. Cobus Visagie, thank you for always being willing to assist me. Thank you for your positivity and guidance when I was unsure of things. Thank you for setting up the many important systems that we use for our groups data. Without the systems, this task would be very challenging.

To Prof. Mike Wingfield, thank you for sharing your enthusiasm for my project with me. Thank you for your positivity and insight. I am so grateful for the opportunities that you have provided me with. Thank you for gifting me with something so special as visiting Namibia, the home of my project.

Thank you to my lab collogues. Thank you for your input when I needed advice. Thank you for creating a welcoming environment that we could share.

I would also like to thank my family, and friends. Thank you for believing in me. Thank you for your support throughout my studies, I truly cherish it. To my fiancé, thank you for your patience and the things you have taught me that have allowed me to flourish as an individual. I value the motivation I have received from you, and without your support, this task could not be accomplished.

I would like to thank the admin team, culture collection, as well as the sequencing facility team at the Forestry Agricultural and Biotechnology Institute (FABI) of South Africa, who made this possible through their respective roles in the institution. Thank you for all of the time spent managing the facilities and admin that go along with them.

I would like to thank the Applied Mycology group for their support throughout my project. Thank you for attending my presentations and giving input where possible. I appreciate it dearly.

This project was funded by a research grant from Prof M Wingfield. To my funding body, I would like to say thank you for supporting me throughout this degree.

Preface

The world's oldest dryland, the Namib desert, is home to the phenomena of "fairy circles". Fairy circles are barren, almost-circular, patches of land that are often surrounded at their margins by flourishing tufts of grasses or other plants. There are many hypotheses that surround the formation and maintenance of these circles, including the non-scientific such as "rolling spots" for zebras or meteorite impacts, and those with a scientific basis including insect activity, abiotic factors, vegetation self-organisation, or microbial phytopathogens. However, there has not been any firm conclusion regarding their cause or maintenance. One of the recent hypotheses has evoked the involvement of microbial phytopathogens. This prompted the present study that in which I have explored the fungal diversity associated with fairy circles.

The first chapter of the dissertation provides a literature overview of the nature, distribution and life-cycle of Namib fairy circles. This includes consideration of the differences between fairy circles and other similar vegetation patterns. In addition, the different hypotheses that have been raised to explain fairy circle formation and maintenance are discussed.

The second chapter considers the fungal diversity associated with *Stipagrostis ciliata* (*Poaceae*) grasses collected from fairy circles. An important consideration here is that previous research has focused only on soils. The fungal diversity associated with these grasses was studied using classical morphological approaches and final identifications based on DNA sequence data.

The aim of studies in the third chapter was to identify the *Curvularia* species (*Pleosporaceae*, *Pleosporales*) isolated from *Stipagrostis ciliata* and associated rhizosphere collected in the Namib desert fairy circles. Strains belonging to putative new species were compared to known ones using both phylogenetic trees generated from multi-locus sequences and morphological features.

The broad aim of the studies included in this dissertation was to gain an improved understanding of the fungi associated with the Namib fairy circles. It is important to emphasize that this had no specific bearing whether fungi might be involved in causing these enigmatic phenomena. That question would require a much more detailed study and at some point, pathogenicity tests with putative pathogens. What this study has provided is the first in-depth consideration of fungi associated with the fairy circles and it is my hope that they will stimulate future research on them.

Chapter 1: Literature review

“Fairy circles” – the unresolved mystery

Abstract

In the Namib desert, the term “fairy circles” refers to barren, almost circular patches of land that are distributed in a honeycomb-like fashion and occur in a narrow arid climatic region. They are surrounded by tufts of flourishing grass and other plant species. There are numerous hypotheses regarding their formation and maintenance that have been proposed since the first scientific report of the circles by Tinley in 1971. These hypotheses range from “non-scientific” such as rolling spots for zebras or unidentified flying objects to scientific ones such as vegetation self-organisation, termite and ant involvement, and allelopathic compounds. One of the more recent hypotheses is that of microbe involvement in the form of soil-borne phytopathogens. The exploration of this hypothesis has indicated that the fungal diversity related to fairy circles is largely unexplored. A recent review of hypotheses as to the cause of fairy circles considered the involvement of termites and ants, vegetation self-organisation, allelopathic compounds, and gas, however, it did not include microbe-related hypotheses. The aim of this review is thus to consider the characteristics, distribution, and lifecycles of Namib fairy circles as well as the hypotheses proposed as to their cause, including those related to microbes.

Introduction

In the Namib desert, “fairy circles” refer to barren, almost-circular vegetation patterns distributed in a hexagonal or honeycomb-like fashion, lack an insect nest at the centre of the circle, and occur in a limited climatic region (Getzin et al. 2021b). Vegetation patterns such as these have been documented from other areas of the world, including arid and semi-arid regions like those in Angola, Australia, China, USA and South Africa (Borgogno et al. 2009; Getzin et al. 2016; Lovegrove and Siegfried 1986; Rietkerk and Koppel 2008; van Rooyen et al. 2004). These reports range from written accounts to drawings, such as the Ui-Ais petroglyphs of fairy circles in Namibia (Meyer et al. 2021). In contrast to those mentioned above, the mima-like mounds in South Africa, known as “Heuweltjies”, the Australian “fairy circles”, and other similar vegetation patterns display differences from fairy circles in Namibia.

Numerous hypotheses have been proposed with regards to fairy circle formation and maintenance since they were first documented by Tinley (1971). However, no conclusion has yet been reached as to their true origin. The hypotheses range from unidentified flying objects and meteorite impact sites to others such as termite activity and vegetative patterns (Albrecht et al. 2001).

Fairy circles occur in a broken belt from the Orange River in South Africa (Northern Cape) to southern Angola (Cramer and Barger 2013; Getzin et al. 2015a; Juergens 2013; van Rooyen et al. 2004), where most recently fairy circles have been observed in south-eastern Namibia and the Kalahari Desert (Getzin et al. 2021a; Meyer et al. 2021). These almost circular, barren patches of land are embedded in matrix vegetation of sparse grass and are characteristically surrounded by a margin of flourishing grass species (Grube 2002).

Grasses such as *Schmidtia kalahariensis* Stent., *Stipagrostis uniplumis* (Licht.) De Winter, *S. ciliata* (Desf.) De Winter, *S.giessii* Kers, *S. obtuse* (Delile) Nees, and *S. hochstetteriana* (Beck ex Hack.) De Winter have been associated with fairy circles in Namibia (Becker and Getzin 2000; Cramer and Barger 2013; Getzin et al. 2015a; Tschinkel 2012). These circles exhibit a decrease in diameter in a gradient from North to South (Getzin et al. 2015a). They are believed to have a lifespan of 40 to 60 years, with stages including ‘birth’, ‘maturation’ and ‘death’ (Tschinkel 2012).

The topic of fairy circles in Namibia has attracted substantial attention in recent years. A recent review of hypotheses as to their cause was published by Meyer et al. (2021) that considers the involvement of ants and termites, allelopathy, gas, as well as the so-called self-organisation hypotheses. The review also discusses the characteristics of fairy circles and whether they could be attributed to the hypotheses discussed. However, Meyer et al. (2021) do not address microbe-related hypotheses that have also been raised. The aim of this review is consequently to consider the distribution and characteristics of Namib fairy circles, their lifecycle, as well as the hypotheses that have been proposed over the last 50 years, including those relating to microbes. The similarities and differences between Namib fairy circles and other vegetation patterns are also briefly considered.

Distribution and characteristics

Fairy circles in Namibia have been likened to several other vegetation patterns elsewhere in the world. Despite their similarities, each of these patterns display unique attributes that distinguish them from the Namib fairy circles. ‘Baba’ circles in the Namibé Province of Southwest Angola are larger and less densely distributed in their surrounding vegetation, with different zones of vegetation, central protrusions and outer depressions (Jürgens et al. 2020). Fairy circles in the Pilbara region of Western Australia are less uniform in distribution, shape, and size, in comparison to Namib fairy circles. Australian circles are smaller (4m), occur in clay-rich soils and in areas with higher mean annual precipitation (37–619 mm), and the matrix has a higher water content than that of Namib fairy circles (Al-Sarayreh et al. 2016; Getzin et al. 2020; Getzin et al. 2016; Getzin et al. 2019). ‘Heuweltjies’ in South Africa and the ‘prairie pimples’ in the USA are convex in shape, have a larger diameter (> 25 m), and are covered in vegetation, whereas fairy circles are concave and mostly devoid of vegetation (Cramer and Midgley 2015; Dietz 1945; Lovegrove and Siegfried 1986; Moore and Picker 1991). The salt-marsh circles of coastal regions such as those in China display concentric rings, are irregular in shape, and transient in nature, where fairy circles are almost circular (Zhao et al. 2021). ‘Collective plant rings’ that were discovered in Donkerhuk, Namibia, are smaller, disordered, annual grass rings with a diameter of up to 100 cm (Getzin et al. 2021b). ‘Collective plant rings’ occur after rainfall and have a lower soil water content when compared to their surrounding vegetation (Getzin et al. 2021b). Like the fairy circles of the Namib desert, these patterns have eluded scientists, with numerous hypotheses being proposed, but no consensus reached yet.

Namib fairy circles are mostly found in areas approximately 60–120 km inland at altitude ranges of 500–1000 m above sea level (van Rooyen et al. 2004) in a transition area between the great escarpment and the Namib desert, known as the pro-Namib. They are limited to areas with a mean annual precipitation of 50–150 mm (Cramer and Barger 2014; Getzin et al. 2015a; Juergens 2013; van Rooyen et al. 2004) and are mostly restricted to sandy soils (Juergens 2013). These barren patches occur in a broken belt from the North-West Province of South Africa through the pro-Namib to southern Angola, interrupted only by the vast dune and mountain areas (Albrecht et al. 2001; Becker and Getzin 2000; van Rooyen et al. 2004) (Figure 1A).

The Namib fairy circles are most continuously distributed in an area approximately 25 km North-West of Orupembe, just off the Hartmann's Valley area (Becker and Getzin 2000) (Figure 1B). This area is approximately 80 km in length from North to South and 25 km in width from East to West (Becker and Getzin 2000). The density of fairy circles decreases in a gradient from East to West, linked to an increase in precipitation (Becker and Getzin 2000). The Westernmost documentation of fairy circles is just West of the Skeleton Coast Park border (Becker and Getzin 2000). This area is separated from the Hartmann's Valley by an area of vast dunes, which do not have any fairy circles (Becker and Getzin 2000).

The distribution of fairy circles varies with their environment. Within homogeneous environments – environments which exhibit uniform properties such as grass species coverage, soil moisture content, and sandy soil type – fairy circles are distributed in a regular, hexagonal fashion with reference to a focal circle (Albrecht et al. 2001; Jüergens et al. 2015; van Rooyen et al. 2004). In atypical, or heterogeneous environments – environments that do not exhibit uniform properties such as those of homogenous environments – fairy circles are distributed randomly, such as in the case of "mega-circles", which are observed in the southern parts of the Giribes Plains. Mega circles are elongated with lengths spanning 32.5 m and widths of only 7.7 m (Getzin and Yizhaq 2019). These mega-circles have been observed upon the closely gathered chain-like development of fairy circles (Getzin and Yizhaq 2019). Mega circles may also display distances ranging between 5 m and 50 m between one another (Getzin and Yizhaq 2019).

Fairy circles have a characteristic almost-circular shape, which may be altered by human movement and structures such as vehicle tracks and fences (Getzin and Yizhaq 2019; Tschinkel 2012). The diameters of these circles vary markedly, from as large as 20 m to as small as 2 m (Getzin et al. 2015a). These fairy circle diameters decrease in a gradient from North to South, associated with a decline in aridity (Cramer and Barger 2013; Fernandez-Oto et al. 2014). In the Hartmann's valley (North-West) circle diameters average 10 m, in the Marienfluss area (North-East) circles have an average diameter of 7.5 m, circles in the Giribes Plain (South-East) display an average diameter of 6.2 m, further South in the Tsondab Vlei, at the Escourt Experimental Farm, circle diameter averages at 5 m, whereas, in the Northern Cape Province of South Africa in the Richtersveld area, circles have an average diameter of only 2 m (van Rooyen et al. 2004). Along with a decrease in diameter, the margins of these circles has been said to be less

pronounced, and even absent in the circles that occur in the Southernmost areas (van Rooyen et al. 2004).

The vegetation surrounding fairy circles in the Namib desert, known as the margin or circle periphery, vary from that making up the areas between circles, which is known as the matrix vegetation as the periphery of *Stipagrostis* species and other plants thrive notably in comparison to the sparely covered matrix vegetation (Grube 2002) (Figure 1C–F). The periphery may be absent, in which the matrix grasses define the circle by formation of a halo-like structure. The predominant species of *Stipagrostis* found on the margins of circles are *S. ciliata* (Desf.) De Winter*, S. hochstetteriana* (Beck ex Hack.) De Winter and *S. giessii* Kers., whereas the predominant species of *Stipagrostis* in the matrix vegetation are *S. obtuse* (Delile) Nees and *S. uniplumis* (Licht.) De Winter (Albrecht et al. 2001; Cramer and Barger 2013; Eicker et al. 1982; Tschinkel 2012).

Fairy circles have a characteristic concave shape. This has been attributed to wind erosion (Albrecht et al. 2001; Becker and Getzin 2000; Tschinkel 2012). The surrounding matrix soils have been thought to be protected from wind erosion by the tussocks of grasses that populate the area (Becker and Getzin 2000). The concavity of these circles is not stable, however, and varies between stages of the circle, ranging from a depth of 1.3–15 cm (Tschinkel 2012). However, exceptions to this have been noted in the South of Namibia near Garub, where fairy circles with diameters of approximately 3 m displayed a convex shape which may be attributed to the deposition of sand from once present *Euphorbia gummifera* shrubs (Meyer et al. 2015).

The concavity of fairy circles allows for water to collect in their centres, causing a ‘water trap’, resulting in the storage of water for many years. The absence of plants in the centres of circles reduce the loss of water that would have occurred through the process of transpiration. Additionally, the large pore sizes between sand particles, which allows percolation of water to deeper soil layers, have also been suggested to play a role in trapping water through prevention of water evaporation (Albrecht et al. 2001; Juergens 2013). However, the soil-water content of fairy circles and their surrounding vegetation may vary in heterogeneous environments (Getzin and Yizhaq 2019). In the dry seasons, the water content of fairy circle soil is significantly higher than that of the surrounding matrix vegetation, however, in heterogeneous environments there is no significant difference in soil-water content between fairy circles and their surrounding matrix vegetation (Getzin and Yizhaq 2019). Additionally, convexly shaped fairy circles near

Garub displayed a lower soil-water content than that of their surrounding matrix vegetation, which was attributed to the increased water evaporation of heaps compared to soils of the matrix vegetation (Getzin and Yizhaq 2019).

As these fairy circles collect and store water in their centres, they have been thought to increase biodiversity markedly in comparison to their surrounding matrix vegetation, through supporting the better growth of their surrounding margin grasses (Juergens 2013).

Lifecycle of fairy circles

Fairy circles are non-permanent structures that have been suggested to have a so-called “life-cycle” in which they traverse through stages of “birth”, “growth” or “maturation”, “death”, and eventual “extinction” (Albrecht et al. 2001; Tschinkel 2012). A life cycle proceeds for approximately 60 years, depending on the size of the circle (Tschinkel 2012). The “birth” stage of the circles is characterized by the appearance of a bare circular patch of soil. Thereafter, the “maturation” stage occurs, typified by the development of a margin of taller grass and is sometimes accompanied by enlargement of the circle, known as the “growth stage’’. Finally, the “death” stage is characterized by the revegetation of the barren centres of the circles, with the eventual “extinction” of the circle, leaving little sign of their existence. The concavity of circles, thought to be caused by wind erosion (Becker and Getzin 2000), remains after the “death” phase, giving rise to the name “ghost circles” (Tschinkel 2012). Tschinkel (2012) documented a “ghost” circle, which appeared as a new circle within four years, suggesting that the “birth” stage of these circles occurs within a space of four years, whereas “maturation” and “revegetation” occur in approximately five years (Tschinkel 2012). Fairy circles have been estimated to have a lifespan of up to 60 years (Tschinkel 2012), however, their genesis has never been recorded in the field (Getzin et al. 2015a).

Hypotheses explaining the existence of fairy circles

Since the first reports of the fairy circles of the Namib Desert in the 1970s, several hypotheses have been proposed with regards to their origin and or maintenance (Meyer et al. 2021; Tinley 1971). Despite this, there remains no consensus and is still a topic of debate (Sahagian 2017). Other hypotheses that have been proposed include rolling spots of zebras, possible rodent activity such as that of gerbils, locations of traditional huts, landmines, meteorite impact sites, and unidentified flying objects (Albrecht et al. 2001; Becker and Getzin 2000). Scientific hypotheses include termite activity, allelopathic compounds, radioactivity, geochemical compound seepage as well as microbe related hypotheses (Block 1).

Block 1. Summary of research and hypotheses regarding the cause of fairy circles in the Namib

	Date	Hypothesis or research	Reference
	1971	Fairy circles are as a result of fossil termitaria in a time where precipitation was higher.	(Tinley 1971)
	1979	Fairy circle result from allelopathic compounds released from *Euphorbia darana.*	(Theron 1979)
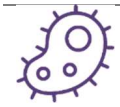	1982	The microbial diversity of fairy circles was studied. No hypotheses were suggested.	(Eicker et al. 1982)
	1987	Radioactivity was thought to be involved in the formation of fairy circles in different “zones”.	(Fraley 1987)
	1994	Termite casts inside fairy circles resembled those of *Hodotermes mossambicus*, even though these termites were not observed in field studies. The barren centres of circles were as a result of the lack of seeds due to foraging activities of the termites.	(Moll 1994)
	1995	Vegetation and self-organisation were proposed to be the causal agent of fairy circles through clonal replication.	(Danin and Orshan 1995)
	2000	*Hodotermes mossambicus* was found in fairy circles in field studies and the termite species is	(Becker and Getzin 2000)

		proposed as a causal agent due to the correlation between their characteristic harvesting activities and fairy circle patterns.	
	2001	A semi-volatile compound associated with termites was proposed to be the causal agent of fairy circles as seedlings were able to grow in soil from the outer and margin of circles, but not the inner soils.	(Albrecht et al. 2001)
	2002	Argument against the termite hypothesis – where the harvesting activities of the termites were not accurately accounted for in the given environmental conditions in Etosha Park fairy circles.	(Grube 2002)
	2004	The termite harvesting activity hypothesis was argued against due to emergence of short-lived seedlings after periods of rain and the lack of termite galleries in fairy circles. A phytotoxic compound was proposed to be the causal agent of fairy circles.	(van Rooyen et al. 2004)
	2007	The termite hypothesis was argued against, stating that the lack of seedlings in circle centres was not as a result of harvesting activities but rather the lack of nutrients. Additionally, no termite galleries were observed in fairy circles. The harvesting activities of *Hodotermes mossambicus* were said to differ in different environments, explaining why Grube (2002) stated that these circles were not caused by the species. The inhibition of seedling growth in potting trials was said to be as a result of a lack of nutrients and not termites.	(Becker 2007)
	2008	The geochemical displacement of air as well as the involvement of a microbes and a phytotoxic compound were proposed.	(Jankowitz et al. 2008)

	2011	Gas seepage was proposed as the causal agent for fairy circle formation.	(Naudé et al. 2011)
	2012	Fairy circle life-span calculation. Support of the vegetation self-organisation hypothesis.	(Tschinkel 2012)
	2012	*Anoplolepsis steingroeveri* ants were found at 10 times higher concentrations in circle centres than in matrix vegetation.	(Picker et al. 2012)
	2013	The involvement of the termite *Pogonomyrmex allocerus* was proposed as it is distributed in all fairy circle areas, in all life stages.	(Juergens 2013)
	2013	Resource competition resulting in self-organisation was proposed as the causal agent of fairy circles.	(Cramer and Barger 2013)
	2014	Water transport and competition results in the formation of fairy circles through mathematical modelling approaches.	(Fernandez-Oto et al. 2014)
	2014	Bacterial and fungal communities were studied through T-RFLP, indicating fairy circles has distinctive communities between one another and their surrounding matrix. Soil-borne microorganisms were hypothesised to be involved in fairy circle formation.	(Ramond et al. 2014)
	2015	An allelopathic chemical from *Euphorbia gummifera* was proposed as the causal agent for fairy circles.	(Meyer et al. 2015)
	2015	Spatial and self-organisation was supported as no difference between plant growth was noted upon supplementation with micronutrients.	(Tschinkel 2015)
	2015	*Pogonomyrmex allocerus* foraging activities result in fairy circle formation.	(Vlieghe et al. 2015)
	2015	Mathematical modelling of spatial distribution of fairy circles indicate that fairy circles result from competition for resources such as water.	(Getzin et al. 2015a)

	2015	The desert microbial ecology was studied, indicating a gap in research of fungal communities.	(Makhalanyane et al. 2015)
	2016	The microbial communities of the gravel plain and dune fairy circles were compared using high throughput sequencing methods, suggesting that fungal pathogens are involved in fairy circle formation.	(van der Walt et al. 2016)
	2016	Plant competition and interaction was proposed given that fairy circles occur in soils with a high water flux.	(Cramer et al. 2017)
	2016	Discovery of Australian fairy circles, supporting the vegetation self-organisation hypothesis through mathematical modelling.	(Getzin et al. 2016)
	2017	Soil dumps of *Hodotermes mossambicus* were noted in the matrix and fairy circles at the same frequency. No termite activity, past or present was noted.	(Ravi et al. 2017)
	2017	Mathematical modelling of the formation of fairy circles revealed the pattern formation as a result of termite activity in conjunction with scale dependent feedback vegetation patterning.	(Tarnita et al. 2017)
	2017	Microbial community assemblage was studied indicating the majority of OTUs recovered were fungal.	(Johnson et al. 2017)
	2019	The high temperatures of the desert were thought to contribute to the formation of fairy circles.	(Vlieghe and Picker 2019)
	2019	Mathematical modelling introduced to reproduce the pattern formation considering faunal and floral interactions and their significance in fairy circle formation.	(Getzin et al. 2019)
	2020	Activity of an unknown termite species in “Baba” fairy circles.	(Jürgens et al. 2020)

	2020	*Euphorbia* species were investigated and said to release a toxic latex compound that changes the rhizosphere and inhibits *Stipagrostis* seedling germination. The size and distribution of fairy circles that co-occur with *Euphorbia* was seen to be similar to other fairy circles.	(Meyer et al. 2020)
	2021	*Euphorbia* and fairy circles did not display similar distribution patterns or sizes. The infiltration rate of water between circle centres and matrix soils did not show a consistent difference. Seedling germination was not inhibited under *Euphorbia* shrubs.	(Getzin et al. 2021a)
	2021	Review of the hypotheses.	(Meyer et al. 2021)
	2021	Definition of the term “fairy circles” and how they differ from other vegetation patterns as well as the discovery of collective plant rings.	(Getzin et al. 2021b)

Legend Social insect related hypotheses, Allelopathic compound related hypotheses, Microbial related hypotheses, Radiation hypothesis, Vegetation self-organisation hypotheses, Abiotic factor related hypotheses, Review of hypotheses and definition of fairy circles.

The role of termites and ants

The involvement of social insects, such as termites and ants, has been considered in the formation of fairy circles (Albrecht et al. 2001; Becker 2007; Becker and Getzin 2000; Juergens 2013; 2015; Jüergens et al. 2015; Moll 1994; Picker et al. 2012; Sahagian 2017; Tinley 1971; Vlieghe et al. 2015). The social insect hypothesis was the first scientific hypothesis and was proposed by Tinley (1971) and has since been elaborated on. These hypotheses range from fossil termitaria, semi-volatile gasses associated with termite nests, to ants.

Termites

One of the hypotheses that has been provided for the formation of Namib fairy circles is that harvester termites, such as *Hodotermes mossambicus* ("Grass-cutting termite" (Becker 2007)), *Microhodotermes viator*, *Psammotermes allocerus*, and even an undescribed *Hodotermitidae* species, may be involved in the formation of the fairy circles (Becker and Getzin 2000; Juergens 2013; Jürgens et al. 2020). These termites mainly feed on grasses, inhabiting dry grass- and bushland areas in which grass cover is variable, subject to external factors such as grazing and fire (Becker and Getzin 2000; Coaton 1958). Termite distribution is widespread, ranging from Ethiopia to South Africa (Coaton and Sheasby 1972). However, only the species *P. allocerus* is associated with fairy circles throughout their entire distribution and in every life stage, but fairy circles do not occur across the distribution of *P. allocerus* (Getzin et al. 2015b). In contrast, *H. mossambicus* and *M. viator* are restricted to summer and winter rainfall climates respectively (Juergens 2013).

Tinley (1971) proposed that the barren patches known as fairy circles were fossil termitaria. Later, a study conducted by Moll (1994) found termite casts within fairy circles and proposed that *H. mossambicus* may be involved in their formation. Subsequently, *H. mossambicus* were found in field studies, concurring with this hypothesis (Becker and Getzin 2000; Moll 1994). The nest size and galleries of these termites observed by Moll (1994) matched those of *H. mossambicus* (Coaton and Sheasby 1972) and the fairy circle appearance matched that of long- lived barren patches caused by these termites under similar environmental conditions (Becker and Getzin 2000; Coaton 1958).

It has been suggested that diameters of barren patches resulting from termite activity are dependent on environmental factors affecting harvester termites, such as heat and rainfall (Coaton 1958), as their harvesting patterns may vary with environmental conditions (Albrecht et al. 2001; Coaton 1958). Environmental changes, such as changes in precipitation, can result in altered foraging patterns, as seen in the Etosha-Park area, where termite involvement in fairy circle formation has been debated (Becker 2007; Grube 2002). In years with average precipitation, *H. mossambicus* forages within its immediate environment, whereas when rainfall is lower than normal, their tunnelling systems extend further to reach food sources, allowing for revegetation of the previously denuded patches (Becker and Getzin 2000).

There are many findings that contradict the involvement of termites in the formation and maintenance of fairy circles. This include the absence of termites and their galleries in some circles, but evidence of their presence in matrix vegetation (Meyer et al. 2020; Ravi et al. 2017; Sahagian 2017; van Rooyen et al. 2004). This was argued against however, as it was thought that the absence of termite galleries in the fairy circles could be attributed to the fact that termites such as *H. mossambicus* do not seal their galleries and are thus easily destroyed, leaving no trace of their presence. Additionally, it was suggested that digging for tunnels by researchers may result in destruction of the once present tunnels (Becker 2007).

The barren centres of fairy circles have been attributed to the absence of seeds resulting from termite foraging. An argument against this view is that short-lived seedlings emerge after periods of rainfall (Moll 1994; van Rooyen et al. 2004). Additionally, foraging activities of termites leave grasses with serrated, cut-off edges as they do not consume the whole plant, which is not observed for grasses of circle peripheries, implying that termite foraging does not result in fairy circles (Becker 2007). However, it has been suggested that the cut-off edges resulting from termite foraging would only be seen for new fairy circles and not those abandoned by termites (Becker 2007).

The hexagonal distribution of fairy circles argues against the termite hypothesis because insects such as termites are thought not to be capable of establishing such large-scale, and regular patterns (Getzin et al. 2015b). This led to the implementation of mathematical modelling approaches for the analysis of faunal (insect) and floral (fairy ring grass) interactions and how these might explain fairy circle formation (Tarnita et al. 2017). Tarnita et al. (2017) showed that competition between termites can indeed generate large-scale regular patterns, similar to fairy circles, and interestingly, when termite based models are merged with vegetation self-organisation models, the large-scale fairy circle patterns are computationally predicted more accurately than when either of the models are applied separately.

A hypothesis related to termites but not to their feeding patters is one concerning semi-volatile compounds associated with these insects. In this case, Albrecht et al. (2001) postulated that soils from within circles contain a semi-volatile compound associated with termite nests and that this compound inhibits the resistance plants have to dehydration. However, the authors were not able to determine the nature or source of the chemical compound.

Field observations and soil excavations of fairy circles and their surrounding vegetation of up to 2.2 m deep and 3 m into the matrix vegetation have been conducted in many studies, all of which found no termite nests or activity in fairy circles (Getzin et al. 2021b; Meyer et al. 2020; Moll 1994; Ravi et al. 2017; Theron 1979; Tschinkel 2012; van Rooyen et al. 2004). Consequently, Getzin et al. (2021b) defined "fairy circles as vegetation patterns which lack a central insect nest, thus contradicting the termite hypothesis.

Ants

Some ant species such as those classified in *Pogonomyrmex*, have also been suggested to aid in the formation and maintenance of these circles due to the similar denuded patches formed by their foraging activities (Picker et al. 2012; Sahagian 2017; Vlieghe et al. 2015). Bare patches created by these ants have a higher soil moisture content than the surrounding matrix vegetation, a flourishing margin of *Stipagrostis* species, and similar lifecycle and lifespan to that of fairy circles (Picker et al. 2012). These ants, however, do not occur throughout fairy circle distribution (Juergens 2013)

The distribution of ants has been studied to determine the possible involvement of ants in the fairy circle phenomenon. Ants such as *Anoplolepsis steingroeveri* were found at 10 times the frequency, within fairy circles than in the associated matrix vegetation. This was suggested to be related to fairy circle formation (Picker et al. 2012). However, species distribution maps indicate that only three species, namely, *A. steingroeveri*, *Messor denticornis*, and *Tetramorium* sp. are associated with some fairy circles. Consequently, ants cannot be a causal agent of fairy circles (Juergens 2013).

Ants have also been involved in the fairy circle hypotheses through chemistry. Compounds associated with fairy circles, such as alkanes, may be from the Dufour's gland of the ants (Picker et al. 2012). These compounds are important in foraging trails and have thus been suggested to result in the characteristic shape of these fairy circles (Picker et al. 2012). The formation of fairy circles by ants, however, does not concur with the definition of a fairy circle provided by Getzin et al. (2021b).

Allelopathic compounds

Allelopathy refers to inhibition of a plant species, resulting from the release of a chemical and or toxic compound by an adjacent plant species. An allelopathic effect caused by *Euphorbia* species, which are highly toxic latex-containing plants, has been implicated in

the fairy circle phenomenon (Theron 1979). Sites observed by Theron (1979) where *E. damarana* plants were in various stages of death, Fairy circles, matrix areas, and dead branches of *E. damarana* within the matrix, were also marked. Furthermore, the total diameters of the above-ground plant material were compared to fairy circles. Theron (1979) found that the diameters of the *E. damarana* and fairy circles were similar and concluded that an inorganic compound within the aboveground *E. damarana* tissues results in an allelopathic effect on adjacent grass species after the *Euphorbia* plants die.

More than 35 years after the report of Theron (1979), other researchers provided evidence in support of the allelopathy hypothesis (Meyer et al. 2020; Meyer et al. 2015). In inter-dune valleys, the presence of compounds released by dead *E. gummifera* was suggested to result in soil toxicity leading to fairy circle formation in the sandy soils adjacent to *Euphorbia* plants (Meyer et al. 2015). These authors found that a compound known as euphol, released from dead *Euphorbia* plants, was abundant in most fairy circle centres. In addition to euphol, other compounds such as phytane, α- and β-amyrin, betulin, heptacosanol, lanosterol, lucenin 2, lupeol and lupeol acetate, and quinic acid have been found in association with *Euphorbia* species. These compounds have antibacterial activity, and it was suggested that they may affect the microbial rhizosphere of *Stipagrostis*, and ultimately affect grass growth (Meyer et al. 2020).

The allelopathic and other compounds identified by Meyer et al. (2020) could also affect the water infiltration and soil properties observed in fairy circles. They suggested that the hydrophobicity and faster infiltration rates of fairy circle soils were induced in matrix soils through the addition of *Euphorbia* shrub latex substances, implying that barren centres are a result of *Euphorbia* compounds (Meyer et al. 2020). Additionally, they suggested that grass species seed germination could be inhibited by water stress conditions when exposed to *E. gummifera* extracts (Meyer et al. 2020).

There have been several arguments against the allelopathy hypothesis. For example, Getzin et al. (2021a) suggested that if these compounds were present, a constant difference would be noted between circle centres and matrix vegetation soils, which was not the case in the study by these authors.

The appearance of *E. damarana, E. gummifera* and *E. gregaria* shrubs may coincide with that of fairy circles (Meyer et al. 2020; Meyer et al. 2015), however, there are areas of fairy circles where no *Euphorbia* species are present (Becker and Getzin 2000; Getzin et

al. 2021a). Theron (1979) suggested that the average size and distribution patterns of fairy circles correlated with the size of the *Euphorbia* species. Getzin et al. (2021a), however, showed that this was not true. Analysis of satellite imagery, drone imagery and confirmation of the sites originally marked by Theron, showed that all *Euphorbia* sites contained tufts of grass around and at the metal pins Theron originally used to mark the *E. damarana* sites, indicating that *E. damarana* did not inhibit grass growth (Getzin et al. 2021a).

In a long-term study of approximately 20 years duration, the relationship between fairy circles and *E. damarana* was assessed (van Rooyen et al. 2004). In this study, fairy circles and *E. damarana* sites were marked with metal droppers. The authors observed that no new fairy circles formed at sites where *E. damarana* had died and that none of the fairy circles had undergone revegetation. These authors also performed Bioassay analysis of the topsoil beneath living and dead *E. damarana* plants and showed no inhibition of root or shoot growth (van Rooyen et al. 2004). It could be argued that allelopathic compounds from *Euphorbia* would degrade; and their presence, despite the absence of the plant, would be unlikely (van Rooyen et al. 2004). However, *Euphorbia* may take longer than 40 years to degrade (Meyer et al. 2020), which may have an effect on the degradation time of the compounds.

Radioactivity

Radioactivity has been suggested as being involved in fairy circle formation (van Rooyen et al. 2004). This is due to the presence of radioactive elements in Namib desert sand (van Rooyen et al. 2004). The observed pattern of fairy circles is closely mimicked by the radiation zones observed by Fraley (1987), who investigated the effects of chronic radiation over a nine-year period on shortgrass (grasses of short stature). One of these zones was the ‘lethal’ zone where vegetation was eradicated. A second zone, the “effects zone” referred to areas where visible changes could be seen. A third zone was defined as a ‘no effects’ zone, in which no changes were observed (Fraley 1987). However, this hypothesis was refuted by van Rooyen et al. (2004), as samples analysed by the South African Bureau of Standards showed no difference in the radiation levels of soils.

Temperature

Temperature and water play important roles in seed germination. Due to the extremely high temperatures that the Namib desert can reach, the effect of temperature on seed germination and development of grasses was assessed in the matrix and fairy circles of the Namib desert. The minimum, maximum, average daily and daytime temperatures of the matrix and fairy circles in the NamibRand Nature reserve were measured. The optimum temperature for germination and growth of *S. ciliata* was determined to be between 35–37 °C (Vlieghe and Picker 2019). However, the soil temperatures within barren centres at depths of 15 cm where grass seeds would be situated, averaged at 36.8 °C (Vlieghe and Picker 2019). This negates the fact that temperature would play a role in fairy circle formation and maintenance (Vlieghe and Picker 2019).

Spatial distribution, competition, and vegetation patterns

Vegetation self-organisation refers to a process where random or periodic ordered spatial arrangements arise from initially disordered states through local interactions, which may be inhibitory or negative (competition), or positive (facilitation) (Rietkerk and Koppel 2008). When both interaction mechanisms exist at two different spatial scales, vegetation patterns can form, the extent of which is determined by the interactions between the mechanisms (Bordeu et al. 2016; Borgogno et al. 2009; Lefever and Lejeune 1997; Lejeune and Tlidi 1999).

These interactions and the resulting vegetation patterns are affected by environmental factors such as precipitation (Fernandez-Oto et al. 2014; Tlidi et al. 2008). Models considering size of fairy circles suggest that increased aridity results in increased circle diameter, and with decreased aridity, a decrease in circle diameter (Fernandez-Oto et al. 2014). Despite the lack of evidence supporting this hypothesis, there is evidence that fairy circles disappear after periods of above-average rainfall and appear after periods of decreased rainfall, sometimes not in the same location as before (Getzin et al. 2015a; Jüergens et al. 2015; Meyer et al. 2020; Zelnik et al. 2015).

Vegetation patterns have been observed in clonal plants occurring in several environments, including deserts (Bonanomi et al. 2014). The mechanism by which these clones replicate mimics the shape, lifespan, and distribution of fairy circles where plants die at the centres of the circles and expand outwards, leaving a lush periphery (Bonanomi

et al. 2014; Cartenì et al. 2012; Cramer and Barger 2013; Kappel et al. 2020). Models of ring formations in clonal plants indicate that other factors such as resource depletion, clonal senescence and competition play a role in vegetation pattern formation (Cain et al. 1991). Perennial grasses such as *S. ciliata,* a prominent species that makes up fairy circles, are amongst the most prevalent ring-forming plants (Bonanomi et al. 2014; Cramer and Barger 2013; Danin and Orshan 1995) and it could therefore be thought that fairy circles are produced through the replication of clonal plants. However, genetic information at the peripheries of fairy circles indicates that the grasses belong to numerous genetically distinct individuals (Kappel et al. 2020), indicating clonal plants are not the cause of fairy circles.

The self-organisation hypothesis suggests that the hexagonal distribution pattern of fairy circles is achieved by inhibitory interactions where plants compete for resources (Meyer et al. 2020). To overcome this competition, plants within ecosystems concentrate resources in their immediate environment in areas known as “fertility islands”, “resource islands”, “localized structures” or “localized patches”, allowing them to persist in unfavourable conditions such as increased aridity (Deblauwe et al. 2008; Meron et al. 2007; Rietkerk and Koppel 2008). These areas in turn increase plant growth through positive feedback systems, which represent fairy circles (Cramer and Barger 2013).

Fairy circles can be likened to fertility islands, where water is concentrated in circle centres in so-called “water-traps”, through paths left by previous root systems and rapid percolation of water through large pores between sand particles (Juergens 2013; Meyer et al. 2020). The higher water content within these circles coupled with the length of availability of the water facilitates the formation of the flourishing plants at the periphery of the fairy circles. The periphery plants are better suited for resource competition than those in the matrix vegetation, due to their deep roots growing towards the centre of the circle, enabling them to tap into the water supplies at the circle centres (Cramer and Barger 2013; Fernandez-Oto et al. 2014; Juergens 2013; Kinast et al. 2014; Ravi et al. 2017). This would result in larger spaces between individual plants and finally, in gaps known as fairy circles.

Water run-off and sub-surface seepage at the centres of the circles enhance the growth of plants at the periphery of the circle even further and may result in the expansion of the circles (Cramer and Barger 2013). Run-off towards the periphery of these circles, which has been attributed to the hydrophobicity or water-repelling nature of these soils, may

lead to water concentration differences, resulting in water-gradients that exist between fairy circles and their matrix vegetation (Meyer et al. 2020; Picker et al. 2012). However, these water gradients are a result of existing fairy circles and are not the cause of new circles (Jüergens et al. 2015).

Micronutrients and a lack thereof have also been proposed as being involved in the formation of fairy circles. The chemical properties of soils within circles and in the surrounding matrix vegetation were compared in soil transfer experiments to test this hypothesis (Albrecht et al. 2001; Cramer and Barger 2013; Juergens 2013; Tschinkel 2015; van Rooyen et al. 2004). The levels of micronutrients, such as magnesium, nitrogen, potassium, phosphorous, sodium, and pH, were seen to be insignificant in fairy circle formation (Grabovsky 2018). But the results of different pot trials have been contradictory and seem to depend on the source of the soil samples and when they were collected (Jankowitz et al. 2008; van Rooyen et al. 2004).

Abiotic factors

A wide range of hydrocarbon compounds such as carbon monoxide and oil are able to escape from geological sources and migrate to the surface of the soil through processes such as diffusion, effusion and buoyancy, resulting in what is known as micro-seepage (near-surface effects that may or may not be visible and may present in many forms) or macro-seepage (visible effects) (Naudé et al. 2011). Micro-seepage may result in a change of soil chemistry due to an associated increase in microbial activity, resulting in plant stress in the form of reduced growth, chlorosis and even plant death (Naudé et al. 2011). These micro-seepage rates can change drastically over periods of time, appearing and disappearing, just as fairy circles do.

Geochemical seepages have been suggested to form fairy circles due to the presence of hydrocarbons in circles (Naudé et al. 2011). The inhibition of grass growth resulting in a barren, circular patch was proposed by Albrecht et al. (2001) and later supported using a pot trial by Jankowitz et al. (2008) and van Rooyen et al. (2004), to originate from an abiotic factor that could be semi-volatile. The centres of these barren patches, thought to be created by peak hydrocarbon seepage, have a diminished oxygen concentration, which not only alters the soil physiochemical properties but creates an unfavourable environment for plant growth (Naudé et al. 2011). Geochemical micro-seepage also

results in the enrichment of the soils at the edges of the seep with calcium, resulting in an outer ring, just like those of fairy circles (Naudé et al. 2011).

Juergens (2015) proposed an alternative explanation for the hydrocarbons in fairy circle centres and suggested that termites and or the associated organisms within these fairy circles produce these gasses. He measured the gas composition from sand termite nests, soils of the fairy circles, and soils of matrix vegetation. The concentration of carbon monoxide and methane within the termite nests was found to be much higher than the other soils. This suggested that the compounds originated from within the sand termite nests (Jüergens et al. 2015). The role of microorganisms in the production of these compounds has also been considered (Juergens 2015). Alkanes present in fairy circles are attributed to the presence of alkene-reducing bacteria (Naudé et al. 2011). It has thus been suggested that microbes such as these could be associated with the intestinal tract of termites (Juergens 2015; Naudé et al. 2011).

Microbes

Ecosystem productivity is largely influenced by soil-borne microbial processes (Makhalanyane et al. 2015). In the absence of plants, soil-borne microbial communities contribute to most of the nitrogen, phosphorous and carbon cycling (Makhalanyane et al. 2015). Microbial communities are affected by environmental conditions such as climate, soil physiochemical properties as well as geographical spatial scales. The biological distribution of these microbes has been suggested to be driven by the “plant-island” hypothesis, in which the presence of plants increases soil fertility and thus promotes microbial heterogeneity (Herman et al. 1995). Furthermore, many perennial plants harbour endophytic fungal communities, which function to ameliorate the impacts of stresses (Wenndt et al. 2021). These endophytes may mediate the plant stress response through, for instance, the production of compounds that promote tolerance to the stress, thus negating the impacts of the stress (Porras-Alfaro and Bayman 2011).

Eicker et al. (1982) reported on the bacterial and fungal diversity of Namib fairy circle inner, margin, and outer soils. They, however, did not propose a hypothesis regarding fairy circle formation. In a consideration of soils collected in the upper 30 mm below the surface, they noted that margin soils had the highest aerobic bacterial density, whereas anaerobic bacterial density was greatest in soils from the circle centre (Eicker et al. 1982). The microbial density was consistent with that of the higher plants within the soils except

for the higher anaerobic bacterial density within the barren centres of the soils (Eicker et al. 1982). The higher alkene emission within fairy circles in comparison to the surrounding matrix vegetation has been attributed to a reduction of alkanes caused by anaerobic bacteria (Grossi et al. 2008; Naudé et al. 2011). Eicker et al. (1982) recorded 63 species of fungi belonging to 37 genera in these soils, with the greatest numbers found at the margins, followed by the matrix vegetation and lastly from the circle centres. The most prevalent fungi isolated were species of *Aspergillus*, *Cladosporium* and *Penicillium* (Eicker et al. 1982). Species of *Fusarium, Trichoderma, Epicoccum, Alternaria* and *Phoma,* amongst others, were also found but they were not as common (Eicker et al. 1982).

As fairy circles are non-permanent structures and proceed through stages of a life-cycle, the presence of a phytotoxic compound produced by microbes and resulting in plant necrosis is well-suited (van der Walt et al. 2016; Walsh et al. 1999), bringing about the microbial plant pathogen hypothesis (Ramond et al. 2014) as both members of bacteria and fungi have been seen to be phytopathogenic. Ramond et al. (2014) investigated the role of soil-borne plant pathogens in the maintenance and formation of gravel plain fairy circles. In their study they used a terminal restriction fragment length polymorphism approach (T-RFLP) to study both bacteria and fungi. Two fungal OTUs were observed in samples from the margin and/or centres of all fairy circles studied, but were not observed in the surrounding matrix, suggesting that these are “fairy circle related fungi” (Ramond et al. 2014; Walsh et al. 1999). However, the fingerprinting technique applied did not allow for the allocation of identities of all the fungi, and their pathogenicity could not be confirmed (Ramond et al. 2014).

van der Walt et al. (2016) elaborated on the soil-borne phytopathogenic microorganism hypothesis using a next generation high-throughput sequencing approach of the 16S rRNA and internal transcribed spacer (ITS) regions to determine bacterial, fungal and archaeal diversity respectively. In their study, Namib desert gravel plain and dune fairy circles were compared (van der Walt et al. 2016). The results showed that bacterial and archaeal communities had high levels of species richness but there were no substantial differences between sampling zones (van der Walt et al. 2016). But fungal communities indicated high species richness across sampling zones, and unique ‘zone-specific’ operational taxonomic units (OTUs) were identified (van der Walt et al. 2016). In this study, only 50% of the fungal OTUs could be classified due to the lack of representative

databases, however, members of *Aspergillus*, *Calcarisporiella, Clitopilus, Curvularia, Periconia, Phoma, Stachybotrys,* and *Rhizophlyctis*, were identified (van der Walt et al. 2016). This study emphasises the fact that fungi within and associated with these fairy circles are largely understudied.

The edaphic bacterial, fungal and archaeal community assemblage and structure of gravel plains, salt pans, riverbeds and dunes of the Namib desert were assessed through a T-RFLP approach, using the 16s rRNA and internal transcribed spacer (ITS) for bacterial, archaeal and fungal diversity (Johnson et al. 2017). Here, 300 unique microbial OTUs were recovered (Johnson et al. 2017). Bacterial OTUs were ubiquitous whereas fungal OTUs were diverse and not detected in slopes and dune tops. Of the 300 unique microbial OTUs, 147 were of fungi, 93 archaea and only 60 represented bacteria implying that fungi are the most prevalent group of microorganisms present in these environments. The soil physiochemistry of these distinct soil habitats indicated that, although, the bacteria, fungi and archaea may share drivers such as carbon content, bacterial and archaeal communities were shaped by soil moisture and ion concentration (Johnson et al. 2017). In contrast, the fungal component was shaped by soil structure, suggesting that the fungal communities are shaped by deterministic and not stochastic assembly mechanisms implying that there are strong selective pressures that act on edaphic fungal communities (Johnson et al. 2017). Although this study did not include fairy circle soils directly, fairy circles do occur in similar substrates.

The microbial communities associated with the Namib Sand Sea grass, *S. sabulicola* was assessed through a culture-dependent approach (Jacobson et al. 2015). Fungal taxa identified included members of *Aspergillus, Aureobasidium, Chaetomium, Fusarium*, and *Thielavia* (Jacobson et al. 2015). Following on this study, the microbial communities of *S. sabulicola,* were assessed using both culture-independent and -dependent approaches in different moisture conditions between sampling sites in the East and West of Namibia. Sampling sites in the West were Gobabeb and Rooibank, and those in the East included Far East Dune and Euphorbia Hill. In this study by Wenndt et al. (2021), 20 taxa were identified using a culture-dependent approach, whereas 168 endophytic taxa were retrieved with a culture-independent approach. Amongst others, species of *Aspergillus, Chaetomium, Thielavia, Alternaria and Curvularia* were isolated from both sampling regions (Wenndt et al. 2021). The fungal species richness obtained from the culture-independent approaches was considerably greater than that observed from the culture-

dependent approach, however, both approaches yielded similar community structures (Wenndt et al. 2021). Both approaches indicated that the endophytic communities are not only widely diverse in this grass, but that they consist mostly of latent saprophytic fungal taxa, the majority of which actively participate in decomposition of senesced plant matter (Wenndt et al. 2021).

Conclusions

The cause of fairy circles in the Namib desert have eluded scientists for many years. Numerous hypotheses relating to the nature and origin of these circles have been proposed. These include termite and ant related hypotheses, allelopathic compound release, geochemical and radioactivity related hypotheses, vegetation pattern and self-organisation hypotheses, microbe related hypotheses, temperature, as well as other 'non-scientific' hypotheses.

The recent review of hypotheses by Meyer et al. (2021) addressed the most popular of the hypotheses but did not consider that of microbes, which was considered in this review. There is no clear evidence emerging from this review, however, that fungi are directly involved in the formation of fairy circles. Despite this, it is clear that very little is known regarding this topic and the environment provides a superb opportunity to study the fungi. The research chapters following this review will therefore explore the fungal diversity of these fairy circles using culture-based approaches.

References

Al-Sarayreh M, Moayed Z, Bollard-Breen B, Ramond J-B, Klette R (2016) Detection and spatial analysis of fairy circles. IEEE, 1–6 pp.

Albrecht C, Joubert JJ, Rycke P (2001) Origin of the enigmatic, circular, barren patches ('Fairy Rings') of the pro-Namib. South African Journal of Science 97: 23–27.

Becker T (2007) The phenomenon of fairy circles in Kaokoland (NW Namibia). Basic and Applied Dryland Research 1: 121–137.

Becker T, Getzin S (2000) The fairy circles of Kaokoland (North-West Namibia) origin, distribution, and characteristics. Basic and Applied Ecology 1: 149–159.

Bonanomi G, Incerti G, Stinca A, Cartenì F, Giannino F, Mazzoleni S (2014) Ring formation in clonal plants. Community Ecology 15: 77–86.

Bordeu I, Clerc MG, Couteron P, Lefever R, Tlidi M (2016) Self-replication of localized vegetation patches in scarce environments. Scientific Reports 6: 1–11.

Borgogno F, D'Odorico P, Laio F, Ridolfi L (2009) Mathematical models of vegetation pattern formation in ecohydrology. Reviews of Geophysics 47: 8755–1209.

Cain ML, Pacala SW, Silander JA (1991) Stochastic simulation of clonal growth in the tall goldenrod, *Solidago altissima*. Oecologia 88: 477–485.

Cartenì F, Marasco A, Bonanomi G, Mazzoleni S, Rietkerk M, Giannino F (2012) Negative plant soil feedback explaining ring formation in clonal plants. Journal of Theoretical Biology 313: 153–161.

Coaton WGH (1958) The hodotermitid harvester termites of South Africa. Dept. of Agriculture, Union of South Africa, Pretoria, South Africa, 112 pp.

Coaton WGH, Sheasby JL (1972) Preliminary report on a survey of the termites (Isoptera) of South West Africa. State Museum, Windhoek [South West Africa],

Cramer M, Barger N (2014) Are mima-like mounds the consequence of long-term stability of vegetation spatial patterning? Palaeogeography, Palaeoclimatology, Palaeoecology 409: 72–83.

Cramer M, Midgley J (2015) The distribution and spatial patterning of mima-like mounds on South Africa suggests genesis through vegetation induced Aeolian sediment deposition. Journal of Arid Environments 119: 16–26.

Cramer MD, Barger NN (2013) Are Namibian “Fairy Circles” the consequence of self-organizing spatial vegetation patterning? PLOS ONE 8: e70876.

Cramer MD, Barger NN, Tschinkel WR (2017) Edaphic properties enable facilitative and competitive interactions resulting in fairy circle formation. Ecography 40: 1210–1220.

Danin A, Orshan G (1995) Circular arrangement of *Stipagrostis ciliata* clumps in the Negev, Israel and near Gokaeb, Namibia. Journal of Arid Environments 30: 307–313.

Deblauwe V, Barbier N, Couteron P, Lejeune O, Bogaert J (2008) The global biogeography of semi-arid periodic vegetation patterns. Global Ecology and Biogeography 17: 715–723.

Dietz RS (1945) The small mounds of the gulf coastal plain. Science 102: 596–597.

Eicker A, Theron G, Grobbelaar N (1982) ’n Mikrobiologiese studie van ‘kaal kolle’in die Giribesvlakte van Kaokoland, SWA-Namibië. South African Journal of Botany 1: 69–74.

Fernandez-Oto C, Tlidi M, Escaff D, Clerc MG (2014) Strong interaction between plants induces circular barren patches: fairy circles. Philosophical Transactions of the Royal Society A: Mathematical, Physical and Engineering Sciences 372: 1–5.

Fraley L (1987) Response of shortgrass plains vegetation to gamma radiation—III. Nine years of chronic irradiation. Environmental and Experimental Botany 27: 193–201.

Getzin S, Erickson TE, Yizhaq H, Muñoz-Rojas M, Huth A, Wiegand K (2020) Bridging ecology and physics: Australian fairy circles regenerate following model assumptions on ecohydrological feedbacks. Journal of Ecology n/a: 1–18.

Getzin S, Nambwandja A, Holch S, Wiegand K (2021a) Revisiting Theron’s hypothesis on the origin of fairy circles after four decades: Euphorbias are not the cause. BMC Ecology and Evolution 21: 1–23.

Getzin S, Wiegand K, Wiegand T, Yizhaq H, von Hardenberg J, Meron E (2015a) Adopting a spatially explicit perspective to study the mysterious fairy circles of Namibia. Ecography 38: 1–11.

Getzin S, Wiegand K, Wiegand T, Yizhaq H, Von Hardenberg J, Meron E (2015b) Clarifying misunderstandings regarding vegetation self-organisation and spatial patterns of fairy circles in Namibia: a response to recent termite hypotheses. 40: 669–675.

Getzin S, Yizhaq H (2019) Unusual Namibian fairy circle patterns in heterogeneous and atypical environments. Journal of Arid Environments 164: 85–89.

Getzin S, Yizhaq H, Bell B, Erickson TE, Postle AC, Katra I, Tzuk O, Zelnik YR, Wiegand K, Wiegand T, Meron E (2016) Discovery of fairy circles in Australia supports self-organization theory. Proceedings of the National Academy of Sciences 113: 3551–3556.

Getzin S, Yizhaq H, Muñoz-Rojas M, Wiegand K, Erickson TE (2019) A multi-scale study of Australian fairy circles using soil excavations and drone-based image analysis. Ecosphere 10: e02620.

Getzin S, Yizhaq H, Tschinkel WR (2021b) Definition of “fairy circles” and how they differ from other common vegetation gaps and plant rings. Journal of Vegetation Science 32: e13092.

Grabovsky VI (2018) A model of vegetation cover in conditions of resource scarcity: Fairy rings in Namibia. Biology Bulletin Reviews 8: 169–180.

Grossi V, Cravo-Laureau C, Guyoneaud R, Ranchou-Peyruse A, Hirschler-Réa A (2008) Metabolism of n-alkanes and n-alkenes by anaerobic bacteria: A summary. Organic Geochemistry 39: 1197–1203.

Grube S (2002) The fairy circles of Kaokoland (Northwest Namibia) – is the harvester termite *Hodotermes mossambicus* the prime causal factor in circle formation? Basic and Applied Ecology 3: 367–370.

Herman RP, Provencio KR, Herrera-Matos J, Torrez RJ (1995) Resource islands predict the distribution of heterotrophic bacteria in chihuahuan desert soils. Applied and Environmental Microbiology 61: 1816–1821.

Jacobson K, van Diepeningen A, Evans S, Fritts R, Gemmel P, Marsho C, Seely M, Wenndt A, Yang X, Jacobson P (2015) Non-rainfall moisture activates fungal decomposition of surface litter in the Namib Sand Sea. PLOS ONE 10: e0126977.

Jankowitz WJ, Rooyen MWV, Shaw D, Kaumba JS, Rooyen NV (2008) Mysterious circles in the Namib Desert. South African Journal of Botany 74: 332–334.

Johnson RM, Ramond J-B, Gunnigle E, Seely M, Cowan DA (2017) Namib Desert edaphic bacterial, fungal and archaeal communities assemble through deterministic processes but are influenced by different abiotic parameters. Extremophiles 21: 381–392.

Juergens N (2013) The biological underpinnings of Namib Desert fairy circles. Science 339: 1618–1621.

Juergens N (2015) Exploring common ground for different hypotheses on Namib fairy circles. Ecography 38: 12–14.

Jüergens N, Vlieghe KEP, Bohn C, Erni B, Gunter F, Oldeland J, Rudolph B, Picker MD (2015) Weaknesses in the plant competition hypothesis for fairy circle formation and evidence supporting the sand termite hypothesis. Ecological Entomology 40: 661–668.

Jürgens N, Gunter F, Oldeland J, Groengroeft A, Henschel JR, Oncken I, Picker MD (2020) Largest on earth: Discovery of a new type of fairy circle in Angola supports a termite origin. Ecological Entomology n/a: 1–13.

Kappel C, Illing N, Huu CN, Barger NN, Cramer MD, Lenhard M, Midgley JJ (2020) Fairy circles in Namibia are assembled from genetically distinct grasses. Communications Biology 3: 1–8.

Kinast S, Zelnik YR, Bel G, Meron E (2014) Interplay between turing mechanisms can increase pattern diversity. Physical Review Letters 112: 078701.

Lefever R, Lejeune O (1997) On the origin of tiger bush. Bulletin of Mathematical Biology 59: 263–294.

Lejeune O, Tlidi M (1999) A model for the explanation of vegetation stripes (tiger bush). Journal of Vegetation Science 10: 201–208.

Lovegrove B, Siegfried W (1986) Distribution and formation of Mima-like earth mounds in the western Cape Province of South Africa. South African Journal of Science 82: 432–436.

Makhalanyane TP, Valverde A, Gunnigle E, Frossard A, Ramond J-B, Cowan DA (2015) Microbial ecology of hot desert edaphic systems. FEMS Microbiology Reviews 39: 203–221.

Meron E, Yizhaq H, Gilad E (2007) Localized structures in dryland vegetation: Forms and functions. Chaos: An Interdisciplinary Journal of Nonlinear Science 17: 037109.

Meyer J, Schutte C, Hurter J, Galt N, Degashu P, Breetzke G, Baranenko D, Meyer N (2020) The allelopathic, adhesive, hydrophobic and toxic latex of *Euphorbia* species is the cause of fairy circles investigated at several locations in Namibia. BMC Ecology 20: 1–23.

Meyer JJM, Schutte CS, Galt N, Hurter JW, Meyer NL (2021) The fairy circles (circular barren patches) of the Namib Desert - What do we know about their cause 50 years after their first description? South African Journal of Botany 140: 226–239.

Meyer JJM, Senejoux F, Heyman HM, Meyer NL, Meyer MA (2015) The occurrence of triterpenoids from *Euphorbia gummifera* inside the fairy circles of Garub in the southern Namibian pro-desert. South African Journal of Botany 98: 10–15.

Moll E (1994) The origin and distribution of fairy rings in Namibia, 1203–1209 pp.

Moore JM, Picker MD (1991) Heuweltjies (earth mounds) in the Clanwilliam district, Cape Province, South Africa: 4000-year-old termite nests. Oecologia 86: 424–432.

Naudé Y, van Rooyen MW, Rohwer ER (2011) Evidence for a geochemical origin of the mysterious circles in the Pro-Namib desert. Journal of Arid Environments 75: 446–456.

Picker MD, Ross-Gillespie V, Vlieghe K, Moll E (2012) Ants and the enigmatic Namibian fairy circles – cause and effect? Ecological Entomology 37: 33–42.

Porras-Alfaro A, Bayman P (2011) Hidden fungi, emergent properties: Endophytes and microbiomes. Annual Review of Phytopathology 49: 291–315.

Ramond J-B, Pienaar A, Armstrong A, Seely M, Cowan DA (2014) Niche-partitioning of edaphic microbial communities in the Namib Desert gravel plain fairy circles. PLOS ONE 9: e109539.

Ravi S, Wang L, Kaseke KF, Buynevich IV, Marais E (2017) Ecohydrological interactions within “fairy circles” in the Namib Desert: Revisiting the self-organization hypothesis. Journal of Geophysical Research: Biogeosciences 122: 405–414.

Rice EL (1995) Biological control of weeds and plant diseases: advances in applied allelopathy. University of Oklahoma Press,

Rietkerk M, Koppel Jvd (2008) Regular pattern formation in real ecosystems. Trends in Ecology and Evolution 23: 169–175.

Sahagian D (2017) The magic of fairy circles: Built or created? Journal of Geophysical Research: Biogeosciences 122: 1294–1295.

Tarnita CE, Bonachela JA, Sheffer E, Guyton JA, Coverdale TC, Long RA, Pringle RM (2017) A theoretical foundation for multi-scale regular vegetation patterns. Nature 541: 398–401.

Theron G (1979) Die verskynsel van kaal kolle in Kaokoland, Suidwes-Afrika. Journal of the South African Biological Society 20: 43–53.

Tinley KL (1971) Etosha and the Kaokoveld. African Wild Life 25: 1–16.

Tlidi M, Lefever R, Vladimirov A (2008) On vegetation clustering, localized bare soil spots and fairy circles. Dissipative Solitons: From Optics to Biology and Medicine. Springer Berlin Heidelberg, Berlin, Heidelberg, 1–22.

Tschinkel WR (2012) The life cycle and life span of namibian fairy circles. PLOS ONE 7: e38056.

Tschinkel WR (2015) Experiments testing the causes of Namibian fairy circles. PLOS ONE 10: e0140099.

van der Walt AJ, Johnson RM, Cowan DA, Seely M, Ramond J-B (2016) Unique microbial phylotypes in Namib desert dune and gravel plain fairy circle soils. Applied and Environmental Microbiology 82: 4592–4601.

van Rooyen MW, Theron GK, van Rooyen N, Jankowitz WJ, Matthews WS (2004) Mysterious circles in the Namib Desert: review of hypotheses on their origin. Journal of Arid Environments 57: 467–485.

Vlieghe K, Picker M (2019) Do high soil temperatures on Namibian fairy circle discs explain the absence of vegetation? PloS one 14: e0217153. doi:10.1371/journal.pone.0217153

Vlieghe K, Picker M, Ross-Gillespie V, Erni B (2015) Herbivory by subterranean termite colonies and the development of fairy circles in SW Namibia. Ecological Entomology 40: 42–49.

Walsh B, Ikeda SS, Boland GJ (1999) Biology and management of dollar spot (*Sclerotinia homoeocarpa*): An important disease of turfgrass. HortScience 34: 13–21.

Wenndt AJ, Evans SE, van Diepeningen AD, Logan JR, Jacobson PJ, Seely MK, Jacobson KM (2021) Why plants harbor complex endophytic fungal communities: Insights from perennial bunchgrass *Stipagrostis sabulicola* in the Namib sand sea. Frontiers in Microbiology 12.

Zelnik YR, Meron E, Bel G (2015) Gradual regime shifts in fairy circles. Proceedings of the National Academy of Sciences 112: 12327–12331.

Zhao L-X, Zhang K, Siteur K, Li X-Z, Liu Q-X, van de Koppel J (2021) Fairy circles reveal the resilience of self-organized salt marshes. Science Advances 7: eabe1100.

Figures

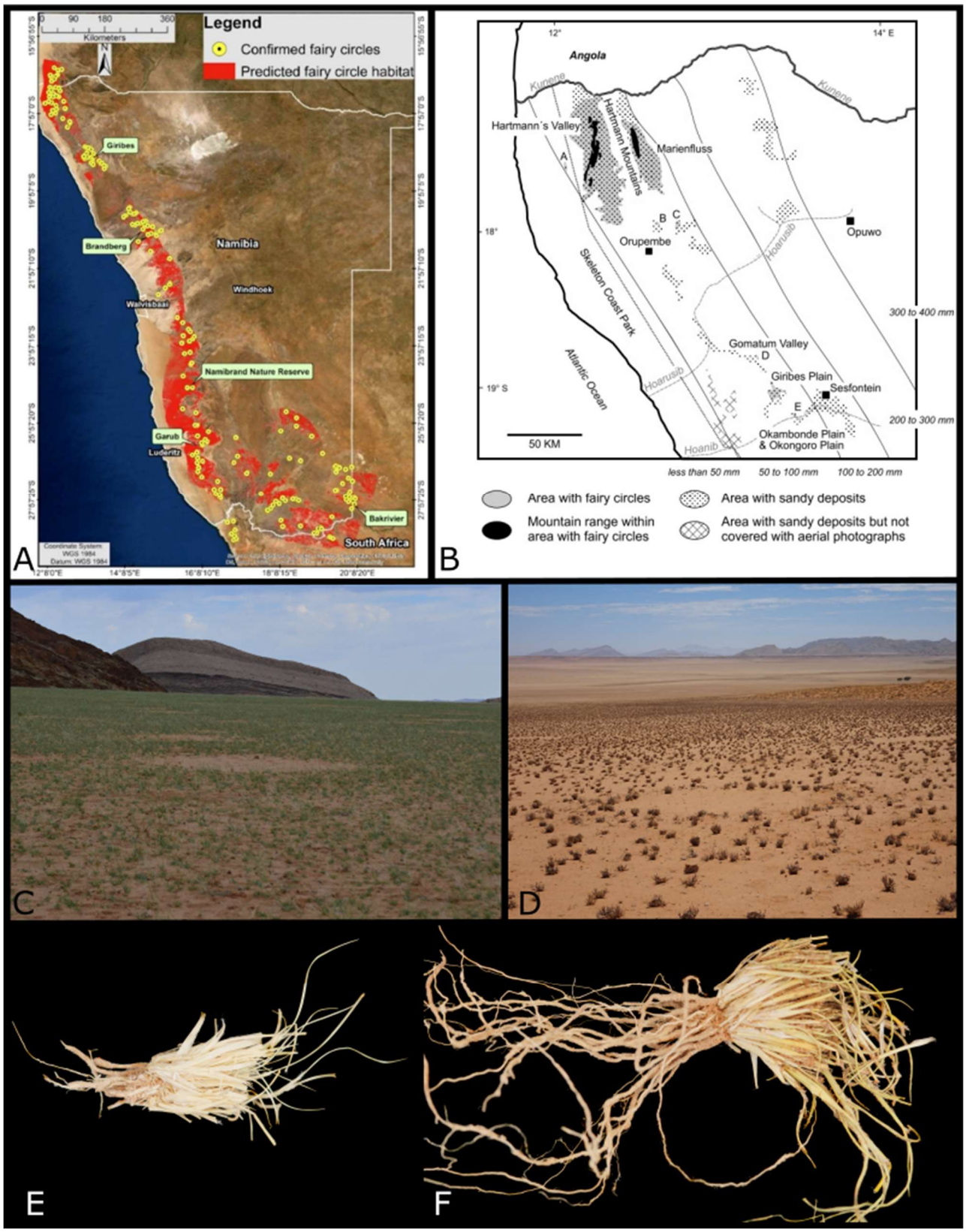

Figure 1. A Distribution of predicted (red) and confirmed (yellow) fairy circles throughout Namibia and parts of South Africa and Botswana (taken from Meyer et al. (2021)) **B** The Kaokoland and its fairy circles (taken from Becker and Getzin (2000)); **C**–**D** Fairy circles

in Namibia indicating the barren centre and sparse matrix; **E** Grass from the inside of a fairy circle in Namibia; **F** Grass from the matrix vegetation around fairy circles in Namibia.

Chapter 2

Fungal diversity associated with *Stipagrostis ciliata* in Namib desert ‘fairy circles’

Abstract

Desert ecosystems, such as the Namib desert, may contain a rich diversity of fungi that remain unexplored. So-called "fairy circles" are limited to the arid climatic regions in the Namib desert and are poorly understood. These almost circular barren patches of land are distributed in a regular hexagonal fashion and surrounded by flourishing tufts of *Stipagrostis ciliata* (*Poaceae*). Culture-independent approaches have been used to consider the microbial diversity of the fairy circle rhizosphere and soil, however, none have been conducted on the *Stipagrostis* plants associated with circles. In this study, we thus used a culture-dependent approach to study the fungal diversity of *Stipagrostis* in the "Mirabib" and "Far East" regions of the Namib. A total of 485 strains, representing 54 genera and 113 species were isolated and identified based on DNA sequencing of *BenA, CaM, GAPDH,* LSU, ITS, *RPB2,* and/or *TEF1* loci. The most prevalent fungal genera were *Curvularia* (73 strains) and *Fusarium*, (73 strains), respectively. The results indicate that the Namib desert fairy circles hold a wealth of fungal diversity that deserves more intense study.

Introduction

Deserts are commonly typified by fluctuating temperatures, low amounts of precipitation, is highly saline and acidic, and are exposed to high levels of ultraviolet irradiation (Makhalanyane et al. 2015; Whitford and Wade 2002). These factors combined provide a harsh living environment for organisms like fungi that inhabit it. The Namib is one of the oldest and driest deserts on earth and home to fairy circles, a strange phenomenon of barren patches of land that is regularly spaced and hexagonally distributed (i.e. a honeycomb like structure) (Getzin et al. 2021). These barren patches were first described from the Namib desert in 1971. These fairy circles commonly have a ring of flourishing grass (*Stipagrostis ciliata*; *Poaceae*) at its margins (Albrecht et al. 2001). The topic of fairy circles has received much attention in recent years, but their origin remains unexplained.

Very little is known about the fungi occurring in the Namib desert. In this regard, some of the most intensive work has been done on the so-called fairy circles. One of the more recent hypotheses surrounding its formation is that of soil-borne microbial phytopathogens (Ramond et al. 2014). In their research, Ramond et al. (2014) found that fungal operational taxonomic units (OTUs) occurred in a higher proportion than those of bacteria. Furthermore, Ramond et al. (2014) found that of the fungal OTUs, two were uniquely observed in all fairy circles studied, including both at the margin and inside circles, but were not detected in the matrix plot. These fungal OTUs where subsequently considered as ‘fairy circle specific fungi’ (Ramond et al. 2014). This was later elaborated on by van der Walt et al. (2016) who identified ‘zone-specific’ fungal OTUs, i.e., fungal species that were seen to differ between sampling locations and between the fairy circle and the surrounding matrix. Their results also indicated that species richness of fungi was significantly higher than bacteria and archaea in Namib desert dune and gravel fairy circles, indicating a wealth of fungi deserving further study.

The current application of high-throughput sequencing (HTS) or culture-independent approaches to survey fungi, mostly cannot identify OTUs to species-level. This is due to the lack of variability, and thus resolution, in the ITS DNA barcode region for many genera (Schoch et al. 2012). Incomplete or inaccurate reference sequence databases is a further complication (Kõljalg et al. 2013; Nilsson et al. 2015). The aim of this study was thus to complete a fungal survey of *Stipagrostis ciliata* plants associated with fairy circles in the Namib desert using a culture-based approach. Collections were made from two distinct

locations, namely Mirabib and Far East. After isolations, fungi were identified based on morphology and DNA sequence analyses. In this paper, we report on the species diversity and compare the fungal communities from different sampling regions, and different zones (i.e. margin, inside and matrix) of the circles.

Materials and Methods

Sample collection

Stipagrostis ciliata plants were collected from two sampling sites, namely Mirabib (23°28.75'S; 15°20.1' E) and the Far East (23°43.95'S; 15°46.50'E) (Figure 1). At each circle, five plants were collected at the margin and five from the inside. Two fairy circles were sampled in the Far East, one in the Mirabib, and five control plants were collected from the matrix vegetation between the circles where plants were growing normally.

Isolations and morphological identifications

Samples were cut into ~1 cm pieces and subsequently surface disinfested in 2 % sodium hypochlorite (bleach) (v/v) for 3 min, 70 % ethanol (v/v) for 30 sec and rinsed in distilled water for 10 sec. Samples were allowed to dry on sterile paper towels before being plated onto Fusarium Selective Media (FSM) [15 g/L peptone powder, 1 g/L Potassium Phosphate (KH_2PO_4), 0.5 g/L Magnesium Sulphate Heptahydrate ($MgSO_4.7H_2O$), 20 g/L agar, 1 g/L Pentachloronitrobenzene (PCNB) dissolved in acetone, and 100 ppm Chloramphenicol] for the selection of *Fusarium* species (Leslie and Summerell 2006a; Nash and Snyder 1962), 18 % Dichloran-Glycerol Agar (DG18) [31.6 g/L Dichloran-glycerol agar, 220 g/L glycerol, supplemented with 100ppm Chloramphenicol] for the selection of fungi that grow in a low water activity, and Malt Extract Agar (MEA) [20 g/L malt extract, 20 g/L agar, supplemented with 50ppm Streptomycin] as a generalist isolation medium. Five samples were plated in triplicate on each of the media. Samples were incubated for a period of 1–3 wks at ±21 °C, after which isolates were purified onto ¼ Potato Dextrose Agar (¼ PDA) (10 g/L Potato Dextrose Agar, 12 g/L agar). Isolates were maintained for a further 1–3 wks under the same conditions.

Isolates were observed using a Zeiss Stemi 508 stereomicroscope and a Zeiss Axio Imager A2 compound microscope and subsequently morpho-grouped and identified to genus level, where possible, based on colony appearance and micromorphology.

Cultures were accessioned and preserved in the CN working collection of the Applied Mycology group and representative strains in the CMW culture collection, both housed at the Forestry and Agriculture Biotechnology Institute (FABI), at the University of Pretoria. Depending on the genus, preservation methods included cryopreservation, mineral oil and water plugs, slants and/or freeze-drying. Photo plates of representatives of each genus identified were constructed using Affinity Designer and Affinity Photo v1.10.4 (Serif (Europe) Ltd.). Sampling maps were generated using images from Google Earth v. 9.163.0.0.

DNA extraction, sequencing, and molecular identifications

Subsequently, DNA was extracted using two different techniques. For fungi with hyaline conidia, DNA was extracted using PrepMan™ Ultra Sample Preparation Reagent (Applied Biosystems, Foster City, CA, USA). Modifications to the manufacturer's protocols were made as follow: mycelium was suspended in 70 µL of PrepMan™ Reagent and agitated in a vortex mixer for 30 sec. The reactions were incubated at 100 °C for 10 min after which they were centrifuged at 21 130 rcf for 7.5 min to pellet cell debris. The supernatant was transferred to a clean 1.5 mL Eppendorf tube. DNA from pigmented fungi such as *Penicillium, Aspergillus,* and *Talaromyces*, was extracted using the Zymo Quick-DNA™ Fungal/Bacterial miniprep (Zymo Research, Irvine, CA, USA) kit. All DNA was accessioned and stored at -20 °C in the CN-DNA collection of the Applied Mycology group at FABI.

PCR amplification was performed of various gene regions typically used for DNA sequence-based identifications of fungal genera and included: translation elongation factor 1-alpha (*TEF1*) for *Fusarium* (O'Donnell et al. 2015); calmodulin (*CaM*) for *Aspergillus* (Samson et al. 2014); beta-tubulin (*BenA*) for *Penicillium* (Visagie et al. 2014); Glyceraldehyde-3-phosphate dehydrogenase (*GAPDH)* for *Alternaria*, *Curvularia*, *Exserohilum,* and *Bipolaris* (Hernández-Restrepo et al. 2018; Manamgoda et al. 2012; Woudenberg et al. 2013); RNA polymerase II second largest subunit (*RPB2*) for *Didymellaceae* (Hou et al. 2020), and the internal transcribed spacer rDNA region (ITS) for all other strains (Schoch et al. 2012). The 28S large subunit rDNA (LSU) region was amplified in cases where strains could not be identified to genus or species level using ITS. Primer sequences are listed in Table 1.

PCRs were set up with in total reaction volumes of 25 µL, made up by: 17.3 µL Milli-Q® water (Millipore Corporation), 2.5 µL 10x FastStart™ Taq PCR reaction buffer with 20 mM $MgCl_2$ (Sigma-Aldrich, Roche Diagnostics), 2.5 µL of 100 mM of each deoxynucleotide (New England Biolabs®, Inc), 0.5 µL for each primer (10 µM) , 0.5 µL 25 mM $MgCl_2$ (Sigma-Aldrich, Roche Diagnostics), 0.2 µL of 5 U/µL FastStart™ Taq DNA Polymerase (Sigma-Aldrich, Roche Diagnostics) and 1 µL DNA. Amplification cycles varied according to the primers used for the gene regions for different fungal genera (see Table 1). Amplicon sizes were determined using 1 % Agarose (SeaKem® LE Agarose, Lonza Bioscience) gel electrophoresis at 80 V for 30 min. PCR products were stained using GelRed® Nucleic Acid Gel Stain (Biotium, Hayward, CA, USA) and electrophoresed alongside a 0.5 µg/µL GeneRuler 100 bp DNA ladder (Thermo Fisher Scientific). Results were visualised under UV light using a Bio-Rad Gel Doc™ EZ Imager (Bio-Rad Laboratories, Inc., USA).

PCR products were cleaned for sequencing reactions using ExoSAP. In PCR strip tubes, 5 µL PCR product was combined with 2 µL ExoSAP-IT™ PCR clean-up reagent (1 U/µL FastAP™ Thermosensitive Alkaline Phosphatase (Thermo Fisher Scientific), 20 U/µL Exonuclease I (Thermo Fisher Scientific)) and incubated at 37 °C for 15 min and then at 85 °C for a further 15 min. Reactions were stored at 4 °C until used.

Bidirectional sequencing reactions were performed in 96 well plates. Reactions were set up to a total volume of 13 µL and were made up by 7.4 µL Milli-Q® water, 2.1 µL 5x BigDye™ Terminator v3.1 Sequencing buffer (Applied Biosystems, Foster City, CA, USA), 0.5 µL BigDye™ Terminator v3.1 Cycle Sequencing Ready Reaction Mix (Applied Biosystems, Foster City, CA, USA), 1 µL primer, and 2 µL ExoSap product. A silicone cover was used to seal the plate. Initial denaturation was performed at 94 °C for 5 min, followed by 40 cycles of denaturation at 96 °C for 30 sec, annealing at 50 °C for 10 sec and elongation at 60 °C for 4 min. Reactions were kept at 4 °C in foil until precipitation.

Reactions were precipitated with sodium acetate. A volume of 60 µL of a sodium acetate master mix [6 000 µL absolute ethanol, 240 µL 3 M sodium acetate (pH 4.6), and 960 µL of Milli-Q] was transferred to each reaction and the sealed plate centrifuged 3220 x g at 4 °C for 30 min. The supernatant was discarded, and the plate inverted on a paper towel and centrifuged for 15 sec at 180 x g. The pellet was washed with 100 µL freshly prepared 70 % (v/v) ethanol. The plate was incubated at room temperature for 5 min and then centrifuged for 10 min at 3220 x g. The ethanol was discarded, and the plate inverted and

centrifuged as before. The wash step was repeated, and the plate inverted and centrifuged as before for 30 sec. Excess ethanol was allowed to evaporate by air drying in a laminar flow for 10 min. A plastic film was used to seal the plate wells. The reactions were kept at 4 °C in foil until Sanger sequencing.

Sequencing was conducted at the Sanger Sequencing Facility of the University of Pretoria (Bioinformatics and Computational Biology Unit, v 19.8.22) using an ABI PRISM™ 3500xl Auto-sequencer (Applied Biosystems, Foster City, CA, USA).

Contigs were assembled and base-calling done where needed in Geneious Prime® v.2019.2.3 (Biomatters, Ltd., Auckland, New Zealand). Sequences were compared to the NCBI GenBank (National Centre for Biotechnology Information, USA) database using BLASTn to obtain preliminary identifications to species level. Table 2 summarises identifications and gene regions sequenced for each strain.

Results

Isolations

A total of 485 fungal strains were isolated during this survey (Table 2). These included 193 strains from the Mirabib (102 from margin, 91 from inside), 202 from Far East (114 from margins, 88 from insides), and 90 from the matrix.

Identifications

A total of 54 genera and 113 species were identified (Table 3). Community composition data is shown to genus level in Figure 2. Figure 2A displays genera that have more than three strains (in total, 23 genera), and Figure 2B shows genera that have equal to or below three (in total, 31 genera). *Curvularia* (n = 73) and *Fusarium* (n = 73) were the most commonly isolated, followed by *Alternaria* (n = 29), *Aspergillus* (n = 7), *Aureobasidium* (n = 31), *Bipolaris* (n = 5), *Canariomyces* (n = 14), *Chaetomium* (n = 6), *Chrysocorona* (n = 5), *Daldinia* (n = 7), *Darksidea* (n = 13), *Didymella* (n = 27), *Eutypa* (n = 29), *Exserohilum* (n = 12), *Monosporascus* (n = 41), *Penicillium* (n = 17), *Pseudopithomyces* (n = 17), and *Talaromyces* (n = 8). Other genera isolated represented, respectively, less than 1% of the total and are shown in Figure 2B. Cultural characteristics of representatives for each genus are shown in Figure 3.

Of the 113 species identified, the most commonly isolated were *Aureobasidium pullulans* (n = 20), *Curvularia moringae* (n = 30), *Didymella dimorpha* (n = 14), *Fusarium chlamydosporum* (n = 62), *Monosporascus eutypoides* (n = 21), and *Pseudopithomyces atro-olivaceous* (n = 16). *Aureobasidium pullulans* and *Curvularia moringae* occurred in all samples. *Didymella dimorpha* was isolated from the Mirabib fairy circle and matrix, as well as from the margins of one of the Far East fairy circles. Species belonging to the genus *Fusarium* (mostly *F. chlamydosporum* species complex) were isolated from all samples. *Monosporascus eutypoides* occurred in all samples from the Mirabib region, as well as the inside of one of the Far East fairy circles. *Pseudopithomyces atro-olivaceous* was isolated from the margins of Far East fairy circles, and the inside of the Mirabib fairy circle, as well as the matrix, but was not identified from the insides of Far East fairy circles, nor the margin of the Mirabib fairy circle. Species identified are listed in Table 3.

Community comparisons

Fairy circle specific genera

We found 16 genera to be 'fairy circle specific', namely, *Achroiostachys, Acremonium, Acrophialophora, Amesia, Ascotricha, Aspergillus, Clypeosphaeria, Corynascella, Cyclaneusma, Eutypella, Preussia, Pseudothielavia, Rosellinia, Talaromyces, Trametes* and *Trichoderma,* along with an unidentified member in the order *Agaricales.* These genera were unique to the Mirabib fairy circles and were not found in the matrix. The Far East region was not included in the determination of 'fairy circle specific' fungi as the matrix control area was not sampled in the Far East region. Ten genera, namely *Achaetomium, Canariomyces, Chaetomium, Chrysocorona, Eutypa, Penicillium, Phaeodothis, Phoma, Pseudophialophora,* and *Thielavia* were shared between the fairy circles in the Far East and Mirabib fairy circles but did not occur in the matrix area and are considered fairy circle specific genera (Figure 4BC).

Mirabib genera

Sixteen genera were found to be unique to the Mirabib region (Figure 4B). Genera isolated from the margin and inside of the circle were distributed as follows: *Achroiostachys*, *Acremonium, Acrophialophora, Amesia, Aspergillus, Clypeosphaeria, Corynascella, Cyclaneusma, Pseudothielavia, Rosellinia, Talaromyces,* and *Trichoderma* were found only from the margin samples in the Mirabib fairy circle. *Ascotricha, Eutypella,*

Preussia, and *Trametes* were found only from the inside of the same circle along with a member of *Agaricales*.

Far East genera

Twelve genera were isolated only from Far East fairy circles (Figure 4C), and were distributed amongst the insides and margins of the fairy circles as follows: *Allocryptovalsa, Bipolaris, Coniochaeta, Hypocopra, Microsphaeropsis,* and *Naganishia* were isolated from the inside of fairy circles, whereas *Allocanariomyces, Camilea, Daldinia, Nothophoma, Pestalotiopsis,* and *Spadicoides,* were isolated only from margins of fairy circles.

Matrix

The genera *Diatrypella, Neokalmusia,* and *Paraconiothyrium* were found to be unique to the matrix without fairy circles as seen in Figure 4A.

The genera *Alternaria, Aureobasidium, Curvularia, Darksidea, Didymella, Exserohilum, Fusarium, Lentithecium, Monosporascus, Pseudopithomyces,* and *Pyricularia* were shared between fairy circles in the Mirabib and Far East region, but were also isolated from the matrix region in Mirabib, as depicted in Figure 4ABC and are not fairy circle or matrix specific.

Discussion

A total of 485 strains representing 54 genera and 113 species were identified during this survey of fungi associated with *Stipagrostis ciliata* collected from fairy circles in two distinct areas of the Namib desert. The results of this study indicate a rich diversity of fungi which are associated with grasses of fairy circles, and differences in diversity between sampling sites and zones of circles.

Community composition differences were observed between the Far East and Mirabib collection sites. Sixteen genera were unique to the Mirabib fairy circle, twelve genera unique to the Far East samples, and ten genera shared between the fairy circles in the regions. Three genera were isolated only from the matrix and eleven genera were isolated from all areas. The community composition differences observed between localities and zones of fairy circles indicate that some fungi may play specific roles in fairy circles, whilst some fungi may be ubiquitous or completely absent from fairy circles. The concept of

‘fairy circle specific’ fungi was introduced by Ramond et al. (2014) where two unique fungal OTUs were found to be associated only with the margin and/or the centres of fairy circles and not associated with the surrounding matrix vegetation soils. Later, van der Walt et al. (2016) reported 57 unique fungal phylotypes that were ‘fairy circle specific’. Although van der Walt et al. (2016) could not identify 33 of the 57 OTUs below the kingdom level, they did identify, to genus level, those in *Ascomycota* to *Aspergillus flavus, Calcarisporiella, Curvularia, Periconia, Phoma,* and *Stachybotrys microspora*. In our study, only sixteen genera were found to be ’fairy circle specific’, including the genus *Aspergillus,* however, the species *A. flavus* was not identified.

We observed a large degree of overlap between our results and those of a previous fairy circle soil fungal survey (Eicker et al. 1982). In their study, *Alternaria, Aspergillus*, *Cladosporium*, *Fusarium*, *Penicillium*, and *Trichoderma* were the most prevalent genera, followed by *Aureobasidium*, *Chaetomium*, *Curvularia*, *Epicoccum, Humicola*, *Phoma*, and *Pseudopithomyces*. Our survey of endophytic fungi of *Stipagrostis ciliata* found *Aureobasidium, Curvularia*, *Fusarium,* and *Monosporascus* to be the most prevalent in fungal genera. Our study also report members of *Alternaria, Aspergillus, Chaetomium, Exserohilum, Penicillium, Talaromyces* and *Thielavia*. These genera were, additionally, detected with culture-dependent and -independent approaches for the analysis of latent-saprotrophs from *Stipagrostis sabulicola* plant litter in the Namib (Jacobson et al. 2015; Wenndt et al. 2021).

Many dematiaceous fungi were isolated during this survey and include *Alternaria, Aureobasidium, Curvularia, Darksidea, Didymella, Exserohilum,* and *Phoma*. These fungi typically contain large amounts of melanin or melanin-like pigments in the walls of hyphae and/or spores (Eisenman and Casadevall 2012; Gessler et al. 2014; Porras-Alfaro et al. 2008). Melanin acts as a protection mechanism against harmful Ultra-violet (UV) irradiation, dehydration stress, and harmful free radicals (Belozerskaya et al. 2017). Additionally, melanin assists in thermal regulation, cellular reinforcement as well as host colonization and pathogenicity (Belozerskaya et al. 2017; Cordero and Casadevall 2017; Eisenman and Casadevall 2012). Chlamydospores is another mechanism fungi can use to protect themselves from harsh environments. These survival structures are typically resistant to desiccation and extreme temperatures These structures are produced by some fungi isolated during this study, such as *Aureobasidium, Chaetomium*, *Curvularia* and *Fusarium* (Crous et al. 2021; Kiss et al. 2020; Marin-Felix et al. 2020; Ramos and

García Acha 1975). Both melanin and chlamydospore is thought to give fungi a competitive advantage in the harsh conditions of the Namib, and explains to some degree the species found.

Curvularia was one of the most commonly isolated genera, with sixteen species identified. Four of these did not conform to any known species and these will be formally described in a future paper. The genus is ubiquitous and several species are important pathogens of *Poaceae* members (e.g. maize, wheat etc). Of the 73 strains, 30 were identified as *C. moringae,* a species recently described from Namibia (Crous et al. 2020). This is the first report of *C. moringae* in *Stipagrostis ciliata* tissues. The prevalence of *Curvularia,* given the fact that it produces both melanin and chlamydospores, is not surprising in such a harsh environment.

Fusarium was also most commonly isolated, and is typically cosmopolitan in its distribution (Leslie and Summerell 2006b). *Fusarium chlamydosporum* (n = 62) was the most commonly found species and characterised by its production of chlamydospores. The prevalence of *F. chlamydosporum* as opposed to other species of the genus is consistent with other studies conducted in arid environments (Burgess and Summerell 1992; Jacobson et al. 2015; Sangalang et al. 1995; Wenndt et al. 2021) and is not surprising given the harsh environment that the Namib desert presents.

Monosporascus was the second most commonly isolated genus. The genus is cosmopolitan in its distribution and causes disease of melons and cucurbits known as '*Monosporascus* root rot and vine decline' (MRRVD) (Cavalcante et al. 2020). Our strains were identified as *Monosporascus cannonballus, M. eutypoides* and *M. ibericus* , however, some strains could not be identified to species level and could represent undescribed species that require further analysis. *Monosporascus* is reported to be associated with grasses, particularly in arid environments as members display resistance to high temperatures and salinity, as well as pH values of 5 to 9 (Herrera et al. 2010; Martyn and Miller 1996; Porras-Alfaro et al. 2008), which allow *Monosporascus* to inhabit harsh environments such as that of the Namib desert.

Curvularia, Fusarium and *Monosporascus* have been associated with grasses as endophytes or plant pathogens. Many authors have suggested that endophytic genera are latent saprotrophs, and function to decompose plant matter and return of nutrients to the soil (Porras-Alfaro and Bayman 2011). Whether these fungi result in disease on the

Stipagrostis ciliata of the fairy circles in the Namib desert, or adopt a latent saprotrophic lifestyle is not known and can be studied in future.

The identification of fungi present in the grasses associated with Namib fairy circles was explored for the first time in this study and thus contributes to the current knowledge of biodiversity of arid environments. The most recent studies of microbes of fairy circles have been based on culture-independent techniques on soil (Ramond et al. 2014; van der Walt et al. 2016). Both techniques have their advantages and disadvantages regarding the estimation of biodiversity, and the application of both methods in future diversity studies will allow for a better understanding of what fungi are present and what roles they play in this environment (Porras-Alfaro and Bayman 2011; Selbmann et al. 2021). Our results indicate that a wealth of undescribed fungi remain undiscovered from the Namib and fungal diversity warrant further study.

References

Al-Sarayreh M, Moayed Z, Bollard-Breen B, Ramond J-B, Klette R (2016) Detection and spatial analysis of fairy circles. IEEE, 1–6 pp.

Albrecht C, Joubert JJ, Rycke P (2001) Origin of the enigmatic, circular, barren patches ('Fairy Rings') of the pro-Namib. South African Journal of Science 97: 23–27.

Almaguer M, Rojas TI, Rodríguez-Rajo FJ, Aira MJ (2012) Airborne fungal succession in a rice field of Cuba. European Journal of Plant Pathology 133: 473–482.

Barde AK, Singh SM (1983) A case of onychomycosis caused by *Curvularia lunata* (Wakker) Boedijn. Mycoses 26: 311–316.

Becker T (2007) The phenomenon of fairy circles in Kaokoland (NW Namibia). Basic and Applied Dryland Research 1: 121–137.

Becker T, Getzin S (2000) The fairy circles of Kaokoland (North-West Namibia) origin, distribution, and characteristics. Basic and Applied Ecology 1: 149–159.

Belozerskaya TA, Gessler NN, Aver‘yanov AA (2017) Melanin pigments of fungi. In: Mérillon J-M, Ramawat KG (Eds) Fungal Metabolites. Springer International Publishing, Switzerland, 263–291.

Berbee M, Pirseyedi M, Hubbard S (1999) *Cochliobolus* phylogenetics and the origin of known, highly virulent pathogens, inferred from ITS and glyceraldehyde-3-phosphate dehydrogenase gene sequences. Mycologia 91: 964–977.

Boedjin K (1933) Ueber einige phragmospren Dematiazeen. Bulletin du Jardin botanique de Buitenzord 13: 120–134.

Bonanomi G, Incerti G, Stinca A, Cartenì F, Giannino F, Mazzoleni S (2014) Ring formation in clonal plants. Community Ecology 15: 77–86.

Bordeu I, Clerc MG, Couteron P, Lefever R, Tlidi M (2016) Self-replication of localized vegetation patches in scarce environments. Scientific Reports 6: 1–11.

Borgogno F, D'Odorico P, Laio F, Ridolfi L (2009) Mathematical models of vegetation pattern formation in ecohydrology. Reviews of Geophysics 47: 8755–1209.

Burgess LW, Summerell BA (1992) Mycogeography of *Fusarium*: survey of *Fusarium* species in subtropical and semi-arid grassland soils from Queensland, Australia. Mycological Research 96: 780–784.

Cain ML, Pacala SW, Silander JA (1991) Stochastic simulation of clonal growth in the tall goldenrod, *Solidago altissima*. Oecologia 88: 477–485.

Carbone I, Kohn LM (1999) A method for designing primer sets for speciation studies in filamentous ascomycetes. Mycologia 91: 553–556.

Cartenì F, Marasco A, Bonanomi G, Mazzoleni S, Rietkerk M, Giannino F (2012) Negative plant soil feedback explaining ring formation in clonal plants. Journal of Theoretical Biology 313: 153–161.

Carter E, Boudreaux C (2004) Fatal cerebral phaeohyphomycosis due to *Curvularia lunata* in an immunocompetent patient. Journal of Clinical Microbiology 42: 5419–5423.

Cavalcante ALA, Negreiros AMP, Tavares MB, Barreto ÉDS, Armengol J, Sales Júnior R (2020) Characterization of five new *Monosporascus* species: adaptation to environmental factors, pathogenicity to cucurbits and sensitivity to fungicides. Journal of fungi (Basel, Switzerland) 6: 1–14.

Coaton WGH (1958) The hodotermitid harvester termites of South Africa. Dept. of Agriculture, Union of South Africa, Pretoria, South Africa, 112 pp.

Coaton WGH, Sheasby JL (1972) Preliminary report on a survey of the termites (Isoptera) of South West Africa. State Museum, Windhoek [South West Africa],

Coleine C, Stajich JE, Selbmann L (2022) Fungi are key players in extreme ecosystems. Trends in Ecology & Evolution 37: 517–528.

Cordero RJB, Casadevall A (2017) Functions of fungal melanin beyond virulence. Fungal Biology Reviews 31: 99–112.

Cramer M, Barger N (2014) Are mima-like mounds the consequence of long-term stability of vegetation spatial patterning? Palaeogeography, Palaeoclimatology, Palaeoecology 409: 72–83.

Cramer M, Midgley J (2015) The distribution and spatial patterning of mima-like mounds on South Africa suggests genesis through vegetation induced Aeolian sediment deposition. Journal of Arid Environments 119: 16–26.

Cramer MD, Barger NN (2013) Are namibian “fairy circles” the consequence of self-organizing spatial vegetation patterning? PLOS ONE 8: e70876.

Cramer MD, Barger NN, Tschinkel WR (2017) Edaphic properties enable facilitative and competitive interactions resulting in fairy circle formation. Ecography 40: 1210–1220.

Crous PW, Cowan DA, Maggs-Kölling G, Yilmaz N, Larsson E, Angelini C, Brandrud TE, Dearnaley JDW, Dima B, Dovana F, Fechner N, García D, Gené J, Halling RE, Houbraken J, Leonard P, Luangsa-Ard JJ, Noisripoom W, Rea-Ireland AE, Ševčíková H, Smyth CW, Vizzini A, Adam JD, Adams GC, Alexandrova AV, Alizadeh A, Duarte E, Andjic V, Antonín V, Arenas F, Assabgui R, Ballarà J, Banwell A, Berraf-Tebbal A, Bhatt VK, Bonito G, Botha W, Burgess TI, Caboň M, Calvert J, Carvalhais LC, Courtecuisse R, Cullington P, Davoodian N, Decock CA, Dimitrov R, Di Piazza S, Drenth A, Dumez S, Eichmeier A, Etayo J, Fernández I, Fiard JP, Fournier J, Fuentes-Aponte S, Ghanbary MAT, Ghorbani G, Giraldo A, Glushakova AM, Gouliamova DE, Guarro J, Halleen F, Hampe F, Hernández-Restrepo M, Iturrieta-González I, Jeppson M, Kachalkin AV, Karimi O, Khalid AN, Khonsanit A, Kim JI, Kim K, Kiran M, Krisai-Greilhuber I, Kučera V, Kušan I, Langenhoven SD, Lebel T, Lebeuf R, Liimatainen K, Linde C, Lindner DL, Lombard L, Mahamedi AE, Matočec N, Maxwell A, May TW, McTaggart AR, Meijer M, Mešić A, Mileto AJ, Miller AN, Molia A, Mongkolsamrit S, Cortés CM, Muñoz-Mohedano J, Morte A, Morozova OV, Mostert L, Mostowfizadeh-Ghalamfarsa R, Nagy LG, Navarro-Ródenas A, Örstadius L, Overton BE, Papp V, Para R, Peintner U, Pham

THG, Pordel A, Pošta A, Rodríguez A, Romberg M, Sandoval-Denis M, Seifert KA, Semwal KC, Sewall BJ, Shivas RG, Slovák M, Smith K, Spetik M, Spies CFJ, Syme K, Tasanathai K, Thorn RG, Tkalčec Z, Tomashevskaya MA, Torres-Garcia D, Ullah Z, Visagie CM, Voitk A, Winton LM, Groenewald JZ (2020) Fungal planet description sheets: 1112–1181. Persoonia 45: 251–409.

Crous PW, Lombard L, Sandoval-Denis M, Seifert KA, Schroers HJ, Chaverri P, Gené J, Guarro J, Hirooka Y, Bensch K, Kema GHJ, Lamprecht SC, Cai L, Rossman AY, Stadler M, Summerbell RC, Taylor JW, Ploch S, Visagie CM, Yilmaz N, Frisvad JC, Abdel-Azeem AM, Abdollahzadeh J, Abdolrasouli A, Akulov A, Alberts JF, Araújo JPM, Ariyawansa HA, Bakhshi M, Bendiksby M, Ben Hadj Amor A, Bezerra JDP, Boekhout T, Câmara MPS, Carbia M, Cardinali G, Castañeda-Ruiz RF, Celis A, Chaturvedi V, Collemare J, Croll D, Damm U, Decock CA, de Vries RP, Ezekiel CN, Fan XL, Fernández NB, Gaya E, González CD, Gramaje D, Groenewald JZ, Grube M, Guevara-Suarez M, Gupta VK, Guarnaccia V, Haddaji A, Hagen F, Haelewaters D, Hansen K, Hashimoto A, Hernández-Restrepo M, Houbraken J, Hubka V, Hyde KD, Iturriaga T, Jeewon R, Johnston PR, Jurjević Ž, Karalti İ, Korsten L, Kuramae EE, Kušan I, Labuda R, Lawrence DP, Lee HB, Lechat C, Li HY, Litovka YA, Maharachchikumbura SSN, Marin-Felix Y, Matio Kemkuignou B, Matočec N, McTaggart AR, Mlčoch P, Mugnai L, Nakashima C, Nilsson RH, Noumeur SR, Pavlov IN, Peralta MP, Phillips AJL, Pitt JI, Polizzi G, Quaedvlieg W, Rajeshkumar KC, Restrepo S, Rhaiem A, Robert J, Robert V, Rodrigues AM, Salgado-Salazar C, Samson RA, Santos ACS, Shivas RG, Souza-Motta CM, Sun GY, Swart WJ, Szoke S, Tan YP, Taylor JE, Taylor PWJ, Tiago PV, Váczy KZ, van de Wiele N, van der Merwe NA, Verkley GJM, Vieira WAS, Vizzini A, Weir BS, Wijayawardene NN, Xia JW, Yáñez-Morales MJ, Yurkov A, Zamora JC, Zare R, Zhang CL, Thines M (2021) *Fusarium*: more than a node or a foot-shaped basal cell. Studies in mycology 98: 1–184.

Danin A, Orshan G (1995) Circular arrangement of *Stipagrostis ciliata* clumps in the Negev, Israel and near Gokaeb, Namibia. Journal of Arid Environments 30: 307–313.

de Hoog GS, van den Ende AHGG (1998) Molecular diagnostics of clinical strains of filamentous Basidiomycetes. Mycoses 41: 183–189.

Deblauwe V, Barbier N, Couteron P, Lejeune O, Bogaert J (2008) The global biogeography of semi-arid periodic vegetation patterns. Global Ecology and Biogeography 17: 715–723.

Dietz RS (1945) The Small Mounds of the Gulf Coastal Plain. Science 102: 596–597.

Dransfield M (1966) The fungal air-spora at Samaru, Northern Nigeria. Transactions of the British Mycological Society 49: 121–132.

Eicker A, Theron G, Grobbelaar N (1982) ’n Mikrobiologiese studie van ‘kaal kolle’in die Giribesvlakte van Kaokoland, SWA-Namibië. South African Journal of Botany 1: 69–74.

Eisenman HC, Casadevall A (2012) Synthesis and assembly of fungal melanin. Applied microbiology and biotechnology 93: 931–940.

Ferdinandez HS, Manamgoda DS, Udayanga D, Deshappriya N, Munasinghe MS, Castlebury LA (2021) Molecular phylogeny and morphology reveal three novel species of *Curvularia* (*Pleosporales*, *Pleosporaceae*) associated with cereal crops and weedy grass hosts. Mycological Progress 20: 431–451.

Fernandez-Oto C, Tlidi M, Escaff D, Clerc MG (2014) Strong interaction between plants induces circular barren patches: fairy circles. Philosophical Transactions of the Royal Society A: Mathematical, Physical and Engineering Sciences 372: 1–5.

Fraley L (1987) Response of shortgrass plains vegetation to gamma radiation—III. Nine years of chronic irradiation. Environmental and Experimental Botany 27: 193–201.

Gessler NN, Egorova AS, Belozerskaya TA (2014) Melanin pigments of fungi under extreme environmental conditions (Review). Applied Biochemistry and Microbiology 50: 105–113.

Getzin S, Erickson TE, Yizhaq H, Muñoz-Rojas M, Huth A, Wiegand K (2020) Bridging ecology and physics: Australian fairy circles regenerate following model assumptions on ecohydrological feedbacks. Journal of Ecology n/a: 1–18.

Getzin S, Nambwandja A, Holch S, Wiegand K (2021a) Revisiting Theron's hypothesis on the origin of fairy circles after four decades: *Euphorbia'*s are not the cause. BMC Ecology and Evolution 21: 1–23.

Getzin S, Wiegand K, Wiegand T, Yizhaq H, von Hardenberg J, Meron E (2015a) Adopting a spatially explicit perspective to study the mysterious fairy circles of Namibia. Ecography 38: 1–11.

Getzin S, Wiegand K, Wiegand T, Yizhaq H, Von Hardenberg J, Meron E (2015b) Clarifying misunderstandings regarding vegetation self-organisation and spatial patterns of fairy circles in Namibia: a response to recent termite hypotheses. 40: 669–675.

Getzin S, Yizhaq H (2019) Unusual Namibian fairy circle patterns in heterogeneous and atypical environments. Journal of Arid Environments 164: 85–89.

Getzin S, Yizhaq H, Bell B, Erickson TE, Postle AC, Katra I, Tzuk O, Zelnik YR, Wiegand K, Wiegand T, Meron E (2016) Discovery of fairy circles in Australia supports self-organization theory. Proceedings of the National Academy of Sciences 113: 3551–3556.

Getzin S, Yizhaq H, Muñoz-Rojas M, Wiegand K, Erickson TE (2019) A multi-scale study of Australian fairy circles using soil excavations and drone-based image analysis. Ecosphere 10: e02620.

Getzin S, Yizhaq H, Tschinkel WR (2021b) Definition of "fairy circles" and how they differ from other common vegetation gaps and plant rings. Journal of Vegetation Science 32: e13092.

Glass NL, Donaldson GC (1995) Development of primer sets designed for use with the PCR to amplify conserved genes from filamentous ascomycetes. Applied and Environmental Microbiology 61: 1323–1330.

Grabovsky VI (2018) A model of vegetation cover in conditions of resource scarcity: Fairy rings in Namibia. Biology Bulletin Reviews 8: 169–180.

Grossi V, Cravo-Laureau C, Guyoneaud R, Ranchou-Peyruse A, Hirschler-Réa A (2008) Metabolism of n-alkanes and n-alkenes by anaerobic bacteria: A summary. Organic Geochemistry 39: 1197–1203.

Grube S (2002) The fairy circles of Kaokoland (Northwest Namibia) – is the harvester termite *Hodotermes mossambicus* the prime causal factor in circle formation? Basic and Applied Ecology 3: 367–370.

Herman RP, Provencio KR, Herrera-Matos J, Torrez RJ (1995) Resource islands predict the distribution of heterotrophic bacteria in chihuahuan desert soils. Applied and Environmental Microbiology 61: 1816–1821.

Hernández-Restrepo M, Madrid H, Tan YP, da Cunha KC, Gené J, Guarro J, Crous PW (2018) Multi-locus phylogeny and taxonomy of *Exserohilum*. Persoonia 41: 71–108.

Herrera J, Khidir HH, Eudy DM, Porras-Alfaro A, Natvig DO, Sinsabaugh RL (2010) Shifting fungal endophyte communities colonize *Bouteloua gracilis*: effect of host tissue and geographical distribution. Mycologia 102: 1012–1026.

Hoang DT, Chernomor O, von Haeseler A, Minh BQ, Vinh LS (2017) UFBoot2: improving the ultrafast bootstrap approximation. Molecular Biology and Evolution 35: 518–522.

Hong S-B, Go S-J, Shin H-D, Frisvad JC, Samson RA (2005) Polyphasic Taxonomy of *Aspergillus fumigatus* and Related Species. Mycologia 97: 1316–1329.

Hou LW, Groenewald JZ, Pfenning LH, Yarden O, Crous PW, Cai L (2020) The phoma-like dilemma. Studies in mycology 96: 309–396.

Iturrieta-González I, Gené J, Wiederhold N, García D (2020) Three new *Curvularia* species from clinical and environmental sources. MycoKeys 68: 1–21.

Jacobson K, van Diepeningen A, Evans S, Fritts R, Gemmel P, Marsho C, Seely M, Wenndt A, Yang X, Jacobson P (2015) Non-rainfall moisture activates fungal decomposition of surface litter in the Namib Sand Sea. PLOS ONE 10: e0126977.

Jankowitz WJ, Rooyen MWV, Shaw D, Kaumba JS, Rooyen NV (2008) Mysterious circles in the Namib Desert. South African Journal of Botany 74: 332–334.

Johnson RM, Ramond J-B, Gunnigle E, Seely M, Cowan DA (2017) Namib Desert edaphic bacterial, fungal and archaeal communities assemble through deterministic processes but are influenced by different abiotic parameters. Extremophiles 21: 381–392.

Juergens N (2013) The biological underpinnings of Namib Desert fairy circles. Science 339: 1618–1621.

Juergens N (2015) Exploring common ground for different hypotheses on Namib fairy circles. Ecography 38: 12–14.

Jüergens N, Vlieghe KEP, Bohn C, Erni B, Gunter F, Oldeland J, Rudolph B, Picker MD (2015) Weaknesses in the plant competition hypothesis for fairy circle formation and evidence supporting the sand termite hypothesis. Ecological Entomology 40: 661–668.

Jürgens N, Gunter F, Oldeland J, Groengroeft A, Henschel JR, Oncken I, Picker MD (2020) Largest on earth: Discovery of a new type of fairy circle in Angola supports a termite origin. Ecological Entomology n/a: 1–13.

Kalyaanamoorthy S, Minh BQ, Wong TKF, Von Haeseler A, Jermiin LS (2017) ModelFinder: fast model selection for accurate phylogenetic estimates. Nature Methods 14: 587–589.

Kappel C, Illing N, Huu CN, Barger NN, Cramer MD, Lenhard M, Midgley JJ (2020) Fairy circles in Namibia are assembled from genetically distinct grasses. Communications Biology 3: 1–8.

Katoh K, Standley DM (2013) MAFFT multiple sequence alignment software version 7: Improvements in performance and usability. Molecular Biology and Evolution 30: 772–780.

Kinast S, Zelnik YR, Bel G, Meron E (2014) Interplay between turing mechanisms can increase pattern diversity. Physical Review Letters 112: 078701.

Kiss N, Homa M, Manikandan P, Mythili A, Krizsán K, Revathi R, Varga M, Papp T, Vágvölgyi C, Kredics L, Kocsubé S (2020) New species of the genus *Curvularia*: *C. tamilnaduensis* and *C. coimbatorensis* from fungal keratitis cases in South India. Pathogens 9: 439–451.

Kõljalg U, Nilsson RH, Abarenkov K, Tedersoo L, Taylor AFS, Bahram M, Bates ST, Bruns TD, Bengtsson-Palme J, Callaghan TM, Douglas B, Drenkhan T, Eberhardt U, Dueñas M, Grebenc T, Griffith GW, Hartmann M, Kirk PM, Kohout P, Larsson E, Lindahl BD, Lücking R, Martín MP, Matheny PB, Nguyen NH, Niskanen T, Oja J, Peay KG, Peintner U, Peterson M, Põldmaa K, Saag L, Saar I, Schüßler A, Scott JA, Senés C, Smith ME, Suija A, Taylor DL, Telleria MT, Weiss M, Larsson K-H (2013) Towards a unified paradigm for sequence-based identification of fungi. Molecular Ecology 22: 5271–5277.

Kornerup A, Wanscher JH (1978) Methuen handbook of colour. E. Methuen, London,

Lefever R, Lejeune O (1997) On the origin of tiger bush. Bulletin of Mathematical Biology 59: 263–294.

Lejeune O, Tlidi M (1999) A model for the explanation of vegetation stripes (tiger bush). Journal of Vegetation Science 10: 201–208.

Leslie JF, Summerell BA (2006a) *Fusarium*-laboratory manual. Blackwell Publishing, Ames, Iowa, 387 pp.

Leslie JF, Summerell BA (2006b) Species concepts in *Fusarium*. The *Fusarium* Laboratory Manual, 87–96.

Letunic I, Bork P (2021) Interactive tree of life (iTOL) v5: an online tool for phylogenetic tree display and annotation. Nucleic Acids Research 49: W293–W296.

Lovegrove B, Siegfried W (1986) Distribution and formation of Mima-like earth mounds in the western Cape Province of South Africa. South African Journal of Science 82: 432–436.

Makhalanyane TP, Valverde A, Gunnigle E, Frossard A, Ramond J-B, Cowan DA (2015) Microbial ecology of hot desert edaphic systems. FEMS Microbiology Reviews 39: 203–221.

Manamgoda DS, Cai L, Bahkali AH, Chukeatirote E, Hyde KD (2011) *Cochliobolus*: an overview and current status of species. Fungal Diversity 51: 3–42.

Manamgoda DS, Cai L, McKenzie EHC, Crous PW, Madrid H, Chukeatirote E, Shivas RG, Tan YP, Hyde KD (2012) A phylogenetic and taxonomic re-evaluation of the *Bipolaris* - *Cochliobolus* - *Curvularia* Complex. Fungal Diversity 56: 131–144.

Manamgoda DS, Rossman AY, Castlebury LA, Chukeatirote E, Hyde KD (2015) A taxonomic and phylogenetic re-appraisal of the genus *Curvularia* (*Pleosporaceae*): human and plant pathogens. Phytotaxa 212: 175–198.

Manamgoda DS, Rossman AY, Castlebury LA, Crous PW, Madrid H, Chukeatirote E, Hyde KD (2014) The genus *Bipolaris*. Studies in mycology 79: 221–288.

Marin-Felix Y, Groenewald JZ, Cai L, Chen Q, Marincowitz S, Barnes I, Bensch K, Braun U, Camporesi E, Damm U, de Beer ZW, Dissanayake A, Edwards J, Giraldo A, Hernández-Restrepo M, Hyde KD, Jayawardena RS, Lombard L, Luangsa-Ard J, McTaggart AR, Rossman AY, Sandoval-Denis M, Shen M, Shivas RG, Tan YP, van der Linde EJ, Wingfield MJ, Wood AR, Zhang JQ, Zhang Y, Crous PW (2017) Genera of phytopathogenic fungi: GOPHY 1. Studies in mycology 86: 99–216.

Marin-Felix Y, Hernández-Restrepo M, Crous PW (2020) Multi-locus phylogeny of the genus *Curvularia* and description of ten new species. Mycological Progress 19: 559–588.

Martyn RD, Miller ME (1996) *Monosporascus* root rot and vine decline: an emerging disease of melons woldwide. Plant Disease 80: 716–725.

Masclaux F, Guého E, de Hoog GS, Christen R (1995) Phylogenetic relationships of human-pathogenic *Cladosporium* (*Xylohypha*) species inferred from partial LS rRNA sequences. Journal of Medical and Veterinary Mycology 33: 327–338.

Mehrabi-Koushki M, Pooladi P, Eisvand P, Babaahmadi G (2018) *Curvularia ahvazensis* and *C. rouhanii* spp. nov. from Iran. Mycosphere 9: 1173–1186.

Meron E, Yizhaq H, Gilad E (2007) Localized structures in dryland vegetation: Forms and functions. Chaos: An Interdisciplinary Journal of Nonlinear Science 17: 037109.

Meyer J, Schutte C, Hurter J, Galt N, Degashu P, Breetzke G, Baranenko D, Meyer N (2020) The allelopathic, adhesive, hydrophobic and toxic latex of Euphorbia

species is the cause of fairy circles investigated at several locations in Namibia. BMC Ecology 20: 1–23.

Meyer JJM, Schutte CS, Galt N, Hurter JW, Meyer NL (2021) The fairy circles (circular barren patches) of the Namib Desert - What do we know about their cause 50 years after their first description? South African Journal of Botany 140: 226–239.

Meyer JJM, Senejoux F, Heyman HM, Meyer NL, Meyer MA (2015) The occurrence of triterpenoids from *Euphorbia gummifera* inside the fairy circles of Garub in the southern Namibian pro-desert. South African Journal of Botany 98: 10–15.

Moll E (1994) The origin and distribution of fairy rings in Namibia, 1203–1209 pp.

Moore JM, Picker MD (1991) Heuweltjies (earth mounds) in the Clanwilliam district, Cape Province, South Africa: 4000-year-old termite nests. Oecologia 86: 424–432.

Nash SN, Snyder WC (1962) Quantitative estimations by plate counts of propagules of the bean rot *Fusarium* in field soils. Phytopathology 73: 458–462.

Naudé Y, van Rooyen MW, Rohwer ER (2011) Evidence for a geochemical origin of the mysterious circles in the Pro-Namib desert. Journal of Arid Environments 75: 446–456.

Newsham KK (2011) A meta-analysis of plant responses to dark septate root endophytes. New Phytologist 190: 783–793.

Nguyen BT, Shuval K, Yaroch AL (2015) Nguyen *et al.* Respond. American journal of public health 105: e2–e2.

Nilsson RH, Tedersoo L, Ryberg M, Kristiansson E, Hartmann M, Unterseher M, Porter TM, Bengtsson-Palme J, Walker DM, de Sousa F, Gamper HA, Larsson E, Larsson K-H, Kõljalg U, Edgar RC, Abarenkov K (2015) A comprehensive, automatically updated fungal ITS sequence dataset for reference-based chimera control in environmental sequencing efforts. Microbes and Environments 30: 145–150.

O'Donnell K, Kistler HC, Cigelnik E, Ploetz RC (1998) Multiple evolutionary origins of the fungus causing Panama disease of banana: concordant evidence from nuclear and mitochondrial gene genealogies. Proceedings of the National Academy of Sciences of the United States of America 95: 2044–2049.

O'Donnell K, Ward TJ, Robert VARG, Crous PW, Geiser DM, Kang S (2015) DNA sequence-based identification of *Fusarium*: Current status and future directions. Phytoparasitica 43: 583–595.

Picker MD, Ross-Gillespie V, Vlieghe K, Moll E (2012) Ants and the enigmatic Namibian fairy circles – cause and effect? Ecological Entomology 37: 33–42.

Porras-Alfaro A, Bayman P (2011) Hidden Fungi, Emergent Properties: Endophytes and Microbiomes. Annual Review of Phytopathology 49: 291–315.

Porras-Alfaro A, Herrera J, Sinsabaugh RL, Odenbach KJ, Lowrey T, Natvig DO (2008) Novel root fungal consortium associated with a dominant desert grass. Applied and Environmental Microbiology 74: 2805–2813.

Rai M, Ingle AP, Ingle P, Gupta I, Mobin M, Bonifaz A, Alves M (2021) Recent advances on mycotic keratitis caused by dematiaceous hyphomycetes. Journal of Applied Microbiology 131: 1652–1667.

Ramond J-B, Pienaar A, Armstrong A, Seely M, Cowan DA (2014) Niche-partitioning of edaphic microbial communities in the Namib Desert gravel plain fairy circles. PLOS ONE 9: e109539.

Ramos S, García Acha I (1975) A vegetative cycle of *Pullularia pullulans*. Transactions of the British Mycological Society 64: 129–135.

Ravi S, Wang L, Kaseke KF, Buynevich IV, Marais E (2017) Ecohydrological interactions within “fairy circles” in the Namib Desert: Revisiting the self-organization hypothesis. Journal of Geophysical Research: Biogeosciences 122: 405–414.

Rietkerk M, Koppel Jvd (2008) Regular pattern formation in real ecosystems. Trends in Ecology and Evolution 23: 169–175.

Rinaldi M, Phillips P, Schwartz J, Winn R, Holt G, Shagets F, Elrod J, Nishioka G, Aufdemorte T (1987) Human *Curvularia* infections: report of five cases and review of the literature. Diagnostic microbiology and infectious disease 6: 27–39.

Sahagian D (2017) The magic of fairy circles: Built or created? Journal of Geophysical Research: Biogeosciences 122: 1294–1295.

Samson RA, Visagie CM, Houbraken J, Hong SB, Hubka V, Klaassen CHW, Perrone G, Seifert KA, Susca A, Tanney JB, Varga J, Kocsubé S, Szigeti G, Yaguchi T, Frisvad JC (2014) Phylogeny, identification and nomenclature of the genus *Aspergillus*. Studies in mycology 78: 141–173.

Sangalang AE, Burgess LW, Backhouse D, Duff J, Wurst M (1995) Mycogeography of *Fusarium* species in soils from tropical, arid and mediterranean regions of Australia. Mycological Research 99: 523–528.

Schoch CL, Crous PW, Groenewald JZ, Boehm EWA, Burgess TI, de Gruyter J, de Hoog GS, Dixon LJ, Grube M, Gueidan C, Harada Y, Hatakeyama S, Hirayama K, Hosoya T, Huhndorf SM, Hyde KD, Jones EBG, Kohlmeyer J, Kruys A, Li YM, Lücking R, Lumbsch HT, Marvanová L, Mbatchou JS, McVay AH, Miller AN, Mugambi GK, Muggia L, Nelsen MP, Nelson P, Owensby CA, Phillips AJL, Phongpaichit S, Pointing SB, Pujade-Renaud V, Raja HA, Plata ER, Robbertse B, Ruibal C, Sakayaroj J, Sano T, Selbmann L, Shearer CA, Shirouzu T, Slippers B, Suetrong S, Tanaka K, Volkmann-Kohlmeyer B, Wingfield MJ, Wood AR, Woudenberg JHC, Yonezawa H, Zhang Y, Spatafora JW (2009) A class-wide phylogenetic assessment of *Dothideomycetes*. Studies in mycology 64: 1–15.

Schoch CL, Seifert KA, Huhndorf S, Robert V, Spouge JL, Levesque CA, Chen W, Consortium FB (2012) Nuclear ribosomal internal transcribed spacer (ITS) region as a universal DNA barcode marker for Fungi. Proceedings of the National Academy of Sciences 109: 6241–6246.

Selbmann L, Stoppiello GA, Onofri S, Stajich JE, Coleine C (2021) Culture-dependent and amplicon sequencing approaches reveal diversity and distribution of black fungi in antarctic cryptoendolithic communities. Journal of Fungi 7: 213–227.

Sivanesan A (1987) Graminicolous species of *Bipolaris*, *Curvularia*, *Exserohilum* and their teleomorphs. 158: 1–261.

Subramanian C (1953) Fungi imperfecti from Madras—*Curvularia*. Springer India, 27–39 pp.

Sung G-H, Sung J-M, Hywel-Jones NL, Spatafora JW (2007) A multi-gene phylogeny of *Clavicipitaceae* (*Ascomycota*, *Fungi*): Identification of localized incongruence using a combinational bootstrap approach. Molecular phylogenetics and evolution 44: 1204–1223.

Tan YP, Crous PW, Shivas RG (2018) Cryptic species of *Curvularia* in the culture collection of the Queensland plant pathology herbarium. MycoKeys 35: 1–25.

Tarnita CE, Bonachela JA, Sheffer E, Guyton JA, Coverdale TC, Long RA, Pringle RM (2017) A theoretical foundation for multi-scale regular vegetation patterns. Nature 541: 398–401.

Theron G (1979) Die verskynsel van kaal kolle in Kaokoland, Suidwes-Afrika. Journal of the South African Biological Society 20: 43–53.

Tinley KL (1971) Etosha and the Kaokoveld. African Wild Life 25: 1–16.

Tlidi M, Lefever R, Vladimirov A (2008) On vegetation clustering, localized bare soil spots and fairy circles. Dissipative Solitons: From Optics to Biology and Medicine. Springer Berlin Heidelberg, Berlin, Heidelberg, 1–22.

Tschinkel WR (2012) The life cycle and life span of Namibian fairy circles. PLOS ONE 7: e38056.

Tschinkel WR (2015) Experiments testing the causes of Namibian fairy circles. PLOS ONE 10: e0140099.

Tsuda M, Ueyama A (1981) *Pseudocochliobolus australiensis*, the ascigerous state of *Bipolaris australiensis*. Mycologia 73: 88–96.

van der Walt AJ, Johnson RM, Cowan DA, Seely M, Ramond J-B (2016) Unique microbial phylotypes in Namib desert dune and gravel plain fairy circle soils. Applied and Environmental Microbiology 82: 4592–4601.

van Rooyen MW, Theron GK, van Rooyen N, Jankowitz WJ, Matthews WS (2004) Mysterious circles in the Namib Desert: Review of hypotheses on their origin. Journal of Arid Environments 57: 467–485.

Verma P, Singh S, Singh R (2013) Seven species of *Curvularia* isolated from three lakes of Bhopal. Advances in Life Science and Technology 8: 13–16.

Vilgalys R, Hester M (1990) Rapid genetic identification and mapping of enzymatically amplified ribosomal DNA from several *Cryptococcus* species. Journal of Bacteriology 172: 4238–4246.

Visagie CM, Houbraken J, Frisvad JC, Hong SB, Klaassen CHW, Perrone G, Seifert KA, Varga J, Yaguchi T, Samson RA (2014) Identification and nomenclature of the genus *Penicillium*. Studies in mycology 78: 343–371.

Vlieghe K, Picker M (2019) Do high soil temperatures on Namibian fairy circle discs explain the absence of vegetation? PloS one 14: e0217153. doi:10.1371/journal.pone.0217153

Vlieghe K, Picker M, Ross-Gillespie V, Erni B (2015) Herbivory by subterranean termite colonies and the development of fairy circles in SW Namibia. Ecological Entomology 40: 42–49.

Walsh B, Ikeda SS, Boland GJ (1999) Biology and management of dollar spot (*Sclerotinia homoeocarpa*): an important disease of turfgrass. HortScience 34: 13–21.

Wenndt AJ, Evans SE, van Diepeningen AD, Logan JR, Jacobson PJ, Seely MK, Jacobson KM (2021) Why plants harbor complex endophytic fungal communities: Insights from perennial bunchgrass *Stipagrostis sabulicola* in the Namib sand sea. Frontiers in microbiology 12: 1–13.

Whitford W, Wade EL (2002) Chapter 3 - Characterization of desert climates. In: Whitford W, Wade EL (Eds) Ecology of Desert Systems. Academic Press, London, 43–63.

Woudenberg JHC, Groenewald JZ, Binder M, Crous PW (2013) *Alternaria* redefined. Studies in mycology 75: 171–212.

Zelnik YR, Meron E, Bel G (2015) Gradual regime shifts in fairy circles. Proceedings of the National Academy of Sciences 112: 12327–12331.

Zhao L-X, Zhang K, Siteur K, Li X-Z, Liu Q-X, van de Koppel J (2021) Fairy circles reveal the resilience of self-organized salt marshes. Science Advances 7: eabe1100.

Tables and figures

Table 1. Primers and PCR conditions for amplification of different loci

Locus	Annealing temp (°C)	Cycles	Primer	Primer Direction	Primer sequence (5'-3')	Reference
Beta-tubulin (*BenA*)	52	35	Bt2a	Forward	GGTAACCAAATCGGTGCTGCTTTC	Glass and Donaldson (1995)
			Bt2b	Reverse	ACCCTCAGTGTAGTGACCCTTGGC	Glass and Donaldson (1995)
Calmodulin (*CaM*)	55	35	Cmd5	Forward	CCGAGTACAAGGARGCCTTC	Hong et al. (2005)
			Cmd6	Reverse	CCGATRGAGGTCATRACGTGG	Hong et al. (2005)
Glyceraldehyde-3-phosphate dehydrogenase (*GAPDH*)	52	30	GDP1	Forward	CAACGGCTTCGGTCGCATTG	Berbee et al. (1999)
			GDP2	Reverse	GCCAAGCAGTTGGTTGTGC	Berbee et al. (1999)

Locus	Annealing temp (°C)	Cycles	Primer	Primer Direction	Primer sequence (5'-3')	Reference
Internal transcribed spacer (ITS)	52	35	V9G	Forward	TTACGTCCCTGCCCTTTGTA	de Hoog and van den Ende (1998)
			LS266	Reverse	GCATTCCCAAACAACTCGACTC	Masclaux et al. (1995)
28S large subunit rDNA (LSU)	52	35	LR5	Forward	TCCTGAGGGAAACTTCG	Vilgalys and Hester (1990)
			LROR	Reverse	ACCCGCTGAACTTAAGC	Vilgalys and Hester (1990)
RNA polymerase II second largest subunit (*RPB2*)	54	35	RPB2-5F2	Forward	GGGGWGAYCAGAAGAAGGC	Sung et al. (2007)
			RPB2-7CR	Reverse	CCCATRGCTTGTYYRCCCAT	Sung et al. (2007)

Locus	Annealing temp (°C)	Cycles	Primer	Primer Direction	Primer sequence (5'-3')	Reference
Translation elongation factor 1-alpha (*TEF1*)	52	35	EF1-728F	Forward	CATCGAGAAGTTCGAGAAGG	Carbone and Kohn (1999)
			EF1-986R	Reverse	TACTTGAAGGAACCCTTACC	Carbone and Kohn (1999)
Translation elongation factor 1-alpha (*TEF1*) (*Fusarium*)	52	35	EF1	Forward	ATGGGTAAGGARGACAAGAC	O'Donnell et al. (1998)
			EF2	Reverse	GGARGTACCAGTSATCATG	O'Donnell et al. (1998)

Table 2. Gene regions sequenced of strains isolated from Namib desert fairy circles

Species	Strains	Locality	Gene regions							
			BenA	*CaM*	*GAPDH*	ITS	LSU	*RPB1*	*RPB2*	*TEF1*
Achaetomium cristalliferum	CN044F9=CMW58162, CN059F9	Far East				x				
Achaetomium globosum	CN020H5, CN044E6	Mirabib & Far East							x	
Achroiostachys aurantispora	CN026F8=CMW58163, CN026F9	Mirabib								x
Acremonium persicinum	CN018H9=CMW58164, CN018I3	Mirabib				x				
Acrophialophora fusispora	CN017A5=CMW58165, CN017A8, CN017C7, CN021G4	Mirabib				x				
Allocanariomyces tritici	CN021G4	Far East							x	
Allocryptovalsa rabenhorstii	CN043B9=CMW58167	Far East				x				
Alternaria alternata	CN011C6, CN013D1, CN015H9, CN016G1, CN016H4, CN016H5, CN022A4, CN023B5=CMW58168, CN024F5, CN025A5, CN025H4, CN025H7, CN043D2, CN043F8	Mirabib & Far East			x	x			x	

Species	Strains	Locality	Gene regions							
			BenA	*CaM*	*GAPDH*	ITS	LSU	*RPB1*	*RPB2*	*TEF1*
Alternaria infectoria	CN011A1, CN011A5, CN011F5, CN012E7, CN012E8, CN013A9, CN013F3, CN024A1, CN025F7	Mirabib & Far East				x				
Alternaria longipes	CN023C2, CN023I5, CN024B5, CN044C5	Far East			x					
Alternaria species	CN027G3	Far East				x				
Alternaria tenuissima	CN012E6	Mirabib							x	
Amesia atrobrunnea	CN019I3=CMW58169	Mirabib				x				
Ascotricha chartarum	CN010G5=CMW58170	Mirabib				x				
Aspergillus aureoterreus	CN018G1=CMW58171, CN019D3, CN019D4	Mirabib		x						
Aspergillus fumigatiaffinis	CN018C5, CN018D8	Mirabib		x						
Aspergillus fumigatus	CN018D7	Mirabib		x						
Aspergillus lentulus	CN018C4	Mirabib		x		x				
Aureobasidium melanogenum	CN010G4, CN012D8, CN023A5=CMW58172, CN023D2,	Mirabib & Far East				x				

Species	Strains	Locality	Gene regions							
			BenA	*CaM*	*GAPDH*	ITS	LSU	*RPB1*	*RPB2*	*TEF1*
	CN027E6, CN027F5, CN027F7, CN044A2									
Aureobasidium pullulans	CN010G3, CN013G1, CN013G2, CN017C5, CN018E2, CN018I8, CN022E5, CN024C9, CN027F2, CN027F3, CN027F4, CN027F6, CN027F8, CN027F9, CN027H7, CN043D5, CN043I6, CN043I8, CN044A1, CN044A7, CN023I2, CN023I3, CN027C6	Mirabib & Far East				x				
Bipolaris maydis	CN021H8=CMW58173	Far East				x				
Bipolaris variabilis	CN024E5	Far East				x				
Bipolaris zeae	CN021F6, CN021F7, CN043D7	Far East			x	x				
Camillea tinctor	CN028G1, CMW58174	Far East							x	
Canariomyces arenarius	CN015B5, CN022H7=CMW58175, CN043C7	Mirabib & Far East				x			x	
Canariomyces microspores	CN021A2, CN022E9, CN022F1, CN022G6, CN023D9, CN043I1, CN043I9	Mirabib & Far East				x				

Species	Strains	Locality	Gene regions							
			BenA	*CaM*	*GAPDH*	ITS	LSU	*RPB1*	*RPB2*	*TEF1*
Canariomyces notabilis	CN044D5	Far East				x				
Canariomyces subthermophilus	CN022E7, CN022F7, CN043G3	Far East				x				
Chaetomium cochliodes	CN028A2	Far East				x				
Chaetomium madrasense	CN016H1, CN027H5, CN027H8	Mirabib & Far East				x				
Chaetomium strumarium	CN016H7	Mirabib				x				
Chaetomium tenue	CN017C6	Mirabib				x				
Chrysocorona lucknowensis	CN013C6, CN015B1, CN015B2, CN015B3, CN042I5=CMW58176	Mirabib & Far East				x				
Clypeosphaeria mamillana	CN026A6	Mirabib								x
Coniochaeta hoffmannii	CN043H7=CMW58178	Far East				x				
Corynascella humicola	CN010G8=CMW58179, CN016B3, CN016B6, CN021C7	Mirabib							x	

Species	Strains	Locality	Gene regions							
			BenA	*CaM*	*GAPDH*	ITS	LSU	*RPB1*	*RPB2*	*TEF1*
Curvularia bannonii	CN021G8=CMW58180, CN024C4, CN043D8	Far East			x	x				
Curvularia prasadii	CN011B8, CN011G6, CN011G7, CN012B3, CN012D4, CN012F2, CN013C9	Mirabib			x	x				
Curvularia eragrosticola	CN011H1, CN010F8=CMW58182	Mirabib				x				
Curvularia geniculata	CN013F5	Mirabib				x				
Curvularia kusanoi	CN011F6, CN015B6	Mirabib				x				
Curvularia lamingtonensis	CN011C4	Mirabib				x				
Curvularia manamgodae	CN043A5=CMW58184	Far East			x	x				
Curvularia moringae	CN011E9, CN010G2, CN010G6, CN010H3, CN010H5, CN011F2=CMW58186, CN011H6, CN011I1, CN012B1, CN012F6, CN013B5, CN013E1, CN013E2, CN013F7, CN015D4, CN015E2, CN015E4, CN015E7, CN016A3, CN016F2, CN021E8, CN022A3, CN022G5, CN022I7, CN022I8,	Mirabib & Far East			x	x				x

Species	Strains	Locality	Gene regions							
			BenA	*CaM*	*GAPDH*	ITS	LSU	*RPB1*	*RPB2*	*TEF1*
	CN024B8, CN024E8, CN027D2, CN043B8, CN044A3									
Curvularia papendorfii	CN013H2=CMW58187, CN025F4	Mirabib & Far East				x				
Curvularia rouhanii	CN022H5, CN010F6=CMW58189, CN010I9, CN025B3, CN028H7	Mirabib & Far East			x	x				x
***Curvularia* sp. nov. 1**	CN013C4=CMW58192, CN010F9=CMW58191, CN013F6=CMW58193	Mirabib			x	x				x
***Curvularia* sp. nov. 2**	CN021G3=CMW58194	Far East			x	x				x
***Curvularia* sp. nov. 3**	CN015H8=CMW58196, CN023D3=CMW58197, CN024D2=CMW58198, CN027A9=CMW58199, CN027C4=CMW58200, CN044C8=CMW58211	Mirabib & Far East			x	x				x
***Curvularia* sp. nov. 4**	CN044D1=CMW58216, CN011D7=CMW58213	Mirabib & Far East			x	x				x
Curvularia sporobolicola	CN011D5=CMW58220, CN011D8=CMW58219	Mirabib			x	x				

Species	Strains	Locality	Gene regions							
			BenA	*CaM*	*GAPDH*	ITS	LSU	*RPB1*	*RPB2*	*TEF1*
Curvularia tribuli	CN024H6, CN024I3, CN027E2=CMW58221, CN043E2, CN043E6	Far East			x	x				
Cyclaneusma minus	CN016D8=CMW58223	Mirabib							x	
Daldinia bambusicola	CN022H6, CN027A3, CN027H1, CN027H4, CN028E2, CN028E4, CN028E5	Far East				x				
Darksidea alpha	CN011I4, CN011I5, CN011I6, CN011I9, CN012B7, CN012E1, CN015C1, CN015I2, CN027I2=CMW58224, CN043C8, CN043C9, CN044A4	Mirabib & Far East				x				
Darksidea species	CN012D5	Mirabib				x				
Diatrypella elaeidis	CN016I1=CMW58225	Mirabib							x	
Didymella dimorpha	CN010H4, CN011C3, CN012A1, CN013D4, CN013G3, CN015G1, CN015I5, CN016B8, CN016C5, CN016D4, CN016G6, CN016G7, CN024A2, CN024G9	Mirabib & Far East	x				x		x	

Species	Strains	Locality	Gene regions							
			BenA	***CaM***	***GAPDH***	**ITS**	**LSU**	***RPB1***	***RPB2***	***TEF1***
Didymella gardeniae	CN019H2, CN027B1	Mirabib & Far East							x	
Didymella pinodella	CN011G1	Mirabib							x	
Didymella prolaticolla	CN011C5, CN012G7, CN012H1, CN013C8, CN022B9, CN023A8, CN025A3, CN025A7, CN026I5, CN027B4	Mirabib & Far East	x				x		x	
Bipolaris yamadae	CN043E5=CMW58227	Far East				x				
Eutypa species	CN018B2, CN018B3, CN018B8=CMW58228, CN018H2, CN019G2, CN019G5, CN019I1, CN020C5, CN020C6, CN020C8, CN020D1, CN021E1, CN021E2, CN021G1, CN021H1, CN026H7, CN027G2, CN027G4, CN027G5, CN027G6, CN027G7, CN027H9, CN028I3, CN029A3, CN042I6, CN042I7, CN043A2, CN043E7, CN044B4	Mirabib & Far East				x				
Eutypella quaternata	CN012C9, CN020E8=CMW58229	Mirabib							x	

Species	Strains	Locality	Gene regions							
			BenA	*CaM*	*GAPDH*	ITS	LSU	*RPB1*	*RPB2*	*TEF1*
Exserohilum rostratum	CN011B6, CN012A5, CN012A8, CN012A9, CN013A1, CN013A8, CN013H3, CN015D3, CN025G2=CMW58230, CN027A7, CN027D3, CN027D4	Mirabib & Far East			x					
Fusarium aethiopicum	CN026E7	Mirabib								x
Fusarium burgessii	CN026D9, CN026F1, CN026H1	Mirabib								x
Fusarium chlamydosporum	CN018E4, CN018E8, CN026A4, CN026A9, CN026B1, CN026B2, CN026B3, CN026B4, CN026B7, CN026B8=CMW58231, CN026B9, CN026C1, CN026C2, CN026C4, CN026C5, CN026C6, CN026C7, CN026C8, CN026C9, CN026D1, CN026D3, CN026D4, CN026D5, CN026D6, CN026D7, CN026E2, CN026E3, CN026E4, CN026E5, CN026E6, CN026E8, CN026E9, CN026F2, CN026F6, CN026G2, CN026G5, CN026G6, CN026G7, CN047H6, CN047H7, CN047H9, CN047I1, CN047I2, CN047I3, CN047I4, CN047I5, CN047I6, CN047I7, CN047I8, CN048A1, CN048A2, CN048A3, CN048A4,	Mirabib & Far East		x				x	x	x

Species	Strains	Locality	Gene regions							
			BenA	*CaM*	*GAPDH*	ITS	LSU	*RPB1*	*RPB2*	*TEF1*
	CN048A5, CN048A6, CN048A7, CN048A8, CN048A9, CN048B1, CN048B2, CN059G1, CN059G6									
Fusarium microconidium	CN047H8	Far East								x
Fusarium oxysporum	CN026A5, CN026H2	Mirabib								x
Fusarium sporodochiale	CN026A2	Mirabib		x				x	x	x
Fusarium udum	CN026B5, CN026B6, CN026D8	Mirabib								x
Hypocorpra rostrata	CN028I1=CMW58232	Far East				x				
Lentithecium aquaticum	CN011I7, CN011I8, CN012B9, CN028F8=CMW58233	Mirabib & Far East							x	
Madurella mycetomatis	CN010G1=CMW58234, CN018C1	Mirabib			x					
Microsphaeropsis olivacea	CN027G9=CMW58235	Far East				x				
Monosporascus cannonballus	CN017D8, CN017D9, CN020D2, CN020D8	Mirabib				x				

Species	Strains	Locality	Gene regions							
			BenA	*CaM*	*GAPDH*	ITS	LSU	*RPB1*	*RPB2*	*TEF1*
Monosporascus eutypoides	, CN010H1, CN010H2, CN011A9, CN011C7, CN018I1, CN019D1, CN019H5, CN020I9, CN021A1, CN021A3, CN021B1, CN021B2, CN021E5, CN026F5, CN026G1, CN026G3, CN026G4, CN026H4, CN026H6, CN026H8, CN028A4	Mirabib & Far East				x				
Monosporascus ibericus	CN027E9	Far East				x				
Monosporascus species	CN012C8, CN016B4, CN018B5, CN018E1, CN021A9, CN021G5, CN022A9, CN026F4, CN028D4, CN029A5, CN029A6, CN043A4, CN044B8, CN044D6, CN044D7	Mirabib & Far East				x				
Naganishia albida	CN027I7=CMW58237, CN027I8	Far East				x				
Neokalmusia brevispora	CN013E5, CN013E6=CMW58238	Mirabib							x	
Nothophoma gossypiicola	CN024E1=CMW58239, CN027B8	Far East							x	
Paraconiothyrium sporulosum	CN011A3=CMW58240, CN011H4, CN013C5	Mirabib			x					

Species	Strains	Locality	Gene regions							
			BenA	*CaM*	*GAPDH*	ITS	LSU	*RPB1*	*RPB2*	*TEF1*
Penicillium citrinum	CN017G3, CN017H1, CN043G9	Mirabib & Far East	x							
Penicillium fellutanum	CN017G1=CMW58241, CN017G9, CN017G4	Mirabib	x							
Penicillium glabrum	CN017H3	Mirabib	x							
Penicillium magnielliptisporum	CN043C3, CN043G5	Far East	x							
Penicillium rubens	CN017F8, CN017H2	Mirabib	x							
Penicillium scabrosum	CN043G4, CN043G6, CN043G7, CN043H2, CN043H3	Far East	x							
Penicillium sumatraense	CN017G2	Mirabib	x							
Peroneutypa scoparia	CN015B7, CN015B8, CN021H6=CMW58242	Mirabib & Far East				x				
Pestalotiopsis microspora	CN027D8=CMW58243	Far East			x					
Phaeodothis winteri	CN013F9, CN027E4=CMW58244	Mirabib & Far East				x				

Species	Strains	Locality	Gene regions							
			BenA	*CaM*	*GAPDH*	ITS	LSU	*RPB1*	*RPB2*	*TEF1*
Phoma herbarum	CN013G4=CMW58245	Mirabib				x				
Phoma species	CN022B4, CN028A1	Far East				x				
Preussia species	CN018G8=CMW58246	Mirabib				x				
Pseudophialophora angusta	CN016D9	Mirabib				x				
Pseudophialophora magnispora	CN017A1	Mirabib				x				
Pseudophialophora species	CN016I4, CN043I3	Mirabib & Far East				x				
Pseudopithomyces atro-olivaceus	CN018D9, CN018F9, CN018G2, CN019A1, CN019B9, CN019C1, CN019C9, CN019G9, CN019I9, CN020I6, CN021D6, CN021D7, CN028A9, CN028B1, CN028B2, CN028B3	Mirabib & Far East			x					
Pseudopithomyces species	CN028C4	Far East			x					
Pseudothielavia terricola	CN011E2=CMW58248	Mirabib							x	

Species	Strains	Locality	Gene regions							
			BenA	*CaM*	*GAPDH*	ITS	LSU	*RPB1*	*RPB2*	*TEF1*
Pyricularia oryzae	CN016E4, CN016I2, CN016I5, CN027H6	Mirabib & Far East				x				
Rosellinia limonispora	CN018B6=CMW58249	Mirabib				x				
Spadicoides xylogena	CN022H4=CMW58250	Far East							x	
Talaromyces malicola	CN017F4, CN017F5, CN017F6, CN017F7, CN017G5, CN017G7, CN017G8, CN018C8=CMW58251	Mirabib	x							
Thielavia basicola	CN019G1=CMW58252	Mirabib				x				
Thielavia species	CN043G2	Far East				x				
Thielavia subthermophila	CN027I6	Far East				x				
Trametes hirsuta	CN019D7=CMW58253	Mirabib				x				
Trametes maxima	CN019D9	Mirabib				x				
Trichoderma koningiopsis	CN018D3=CMW58254	Mirabib				x				

Table 3. Number of strains per species

Genus	Species	Number of strains
Achaetomium	*A. globosum*	2
	A. cristalliferum	2
Achroiostachys	*Ac. aurantispora*	2
Acremonium	*Acr. persicinum*	2
Acrophialophora	*Acro. fusispora*	3
Allocanariomyces	*Al. tritici*	1
Allocryptovalsa	*All. rabenhorstii*	1
Alternaria	*Alt. alternata*	14
	Alt. infectoria	9
	Alt. longipes	4
	Alt. tenuissima	1
	Alternaria species	1
Amesia	*Am. atrobrunnea*	1
Ascotricha	*As. chartarum*	1
Aspergillus	*Asp. aureoterreus*	3
	Asp. fumigatiaffinis	2
	Asp. fumigatus	1
	Asp. lentulus	1
Aureobasidium	*Au. melanogenum*	8
	Au. pullulans	20
	Aureobasidium species	3
Bipolaris	*B. zeae*	3
	B. maydis	1
	B. variabilis	1
	B. yamadae	1
Camillea	*C. tinctor*	1
Canariomyces	*Ca. arenarius*	3
	Ca. microsporus	7
	Ca. notabilis	1
	Ca. subthermophilus	3

Chaetomium	*Ch. cochliodes*	1
	Ch. madrasense	3
	Ch. strumarium	1
	Ch. tenue	1
Chrysocorona	*Chr. lucknowensis*	5
Clypeosphaeria	*Cl. mamillana*	1
Coniochaeta	*Co. hoffmannii*	1
Corynascella	*Cor. humicola*	4
Curvularia	*Cu. bannonii*	3
	Cu. carica-papayae	7
	Cu. eragrosticola	2
	Cu. geniculata	1
	Cu. kusanoi	2
	Cu. lamingtonensis	1
	Cu. manamgodae	1
	Cu. moringae	30
	Cu. papendorfii	2
	Cu. rouhanii	5
	Cu. sp. nov. 1	3
	Cu. sp. nov. 2	1
	Cu. sp. nov. 3	6
	Cu. sp. nov. 4	3
	Cu. sporobolicola	1
	Cu. tribuli	5
Cyclaneusma	*Cy. minus*	1
Daldinia	*D. bambusicola*	7
Darksidea	*Da. alpha*	12
	Darksidea species	1
Diatrypella	*Di. elaeidis*	1
Didymella	*Did. dimorpha*	14
	Did. gardeniae	2
	Did. pinodella	1
	Did. prolaticolla	10
Eutypa	*Eutypa* species	29

Eutypella	*Eu. quaternata*	2
Exserohilum	*Ex. rostratum*	12
Fusarium	*F. aethiopicum*	1
	F. burgessii	3
	F. chlamydosporum	62
	F. microconidium	1
	F. oxysporum	2
	F. sporodochiale	1
	F. udum	3
Hypocorpra	*H. rostrata*	1
Lentithecium	*L. aquaticum*	4
Madurella	*M. mycetomatis*	2
Microsphaeropsis	*Mi. olivacea*	1
Monosporascus	*Mo. cannonballus*	4
	Mo. eutypoides	21
	Mo. ibericus	1
	Monosporascus species	15
Naganishia	*N. albida*	2
Neokalmusia	*Ne. brevispora*	2
Nothophoma	*No. gossypiicola*	2
Paraconiothyrium	*P. sporulosum*	3
Penicillium	*Pe. citrinum*	3
	Pe. fellutanum	3
	Pe. glabrum	1
	Pe. magnielliptisporum	2
	Pe. rubens	2
	Pe. scabrosum	5
	Pe. sumatraense	1
Peroneutypa	*Per. scoparia*	3
Pestalotiopsis	*Pes. microspora*	1
Phaeodothis	*Ph. winteri*	2
Phoma	*Pho. herbarum*	1
	Phoma species	2
Preussia	*Preussia* species	1

Pseudophialophora	*Ps. angusta*	1
	Ps. magnispora	1
	Pseudophialophora species	2
Pseudopithomyces	*Pse. atro-olivaceus*	16
	Pseudopithomyces species	1
Pseudothielavia	*Pseu. terricola*	1
Pyricularia	*Py. oryzae*	4
Rosellinia	*R. limonispora*	1
Spadicoides	*S. xylogena*	1
Talaromyces	*T. malicola*	8
Thielavia	*Th. basicola*	1
	Th. subthermophila	1
	Thielavia species	1
Trametes	*Tr. hirsuta*	1
	Tr. maxima	1
Trichoderma	*Tri. koningiopsis*	1
Total		485

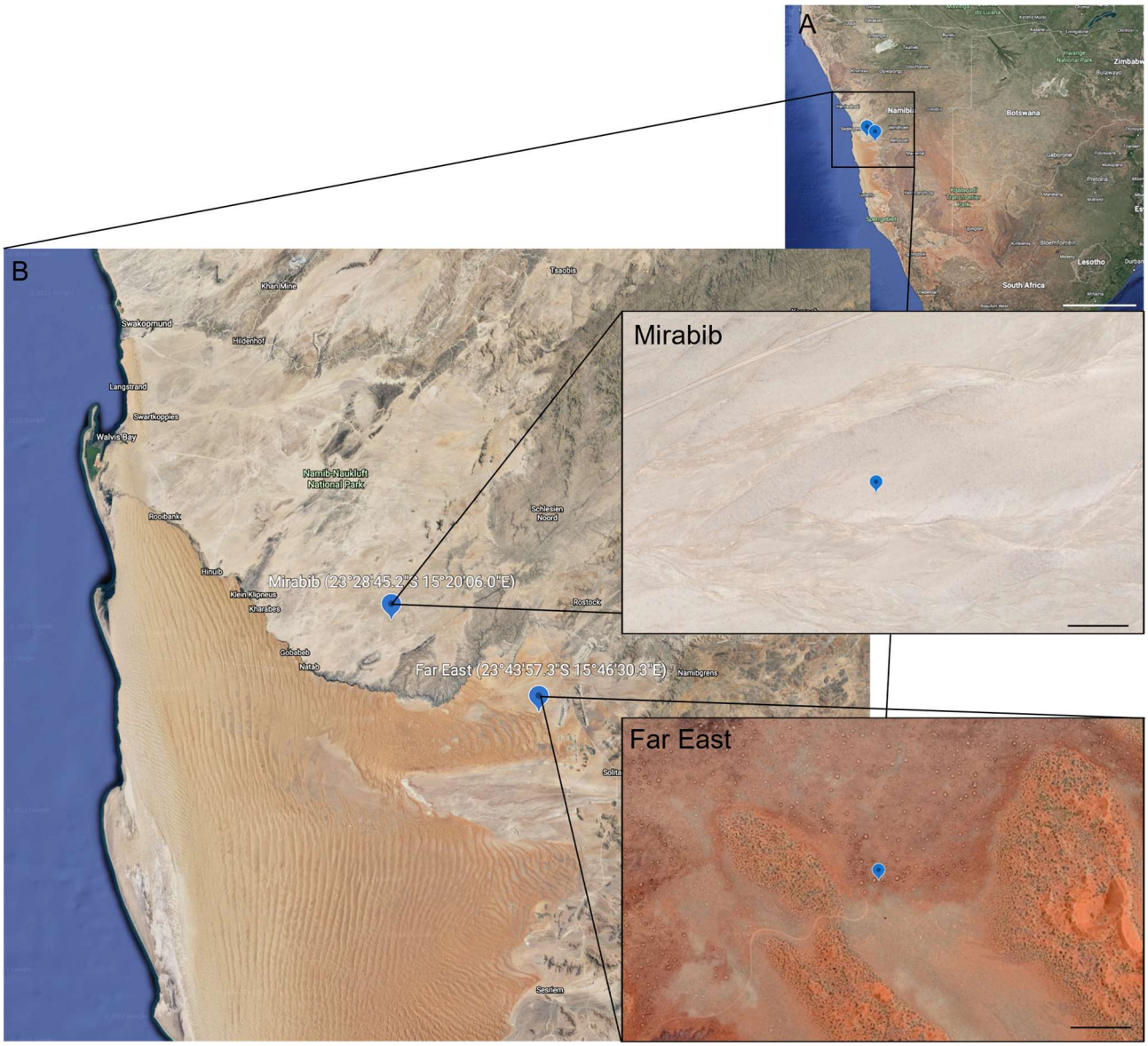

Figure 1. Sampling sites in Namibia. A: Overview of Namibia with pin drops of sampling sites, scale 400 km; B: The Mirabib and Far East sampling sites shown at a higher resolution and bubbles of the sampling sites with scale 100 m (Image generated using Google Earth v. 9.168.0.0 and Affinity Designer).

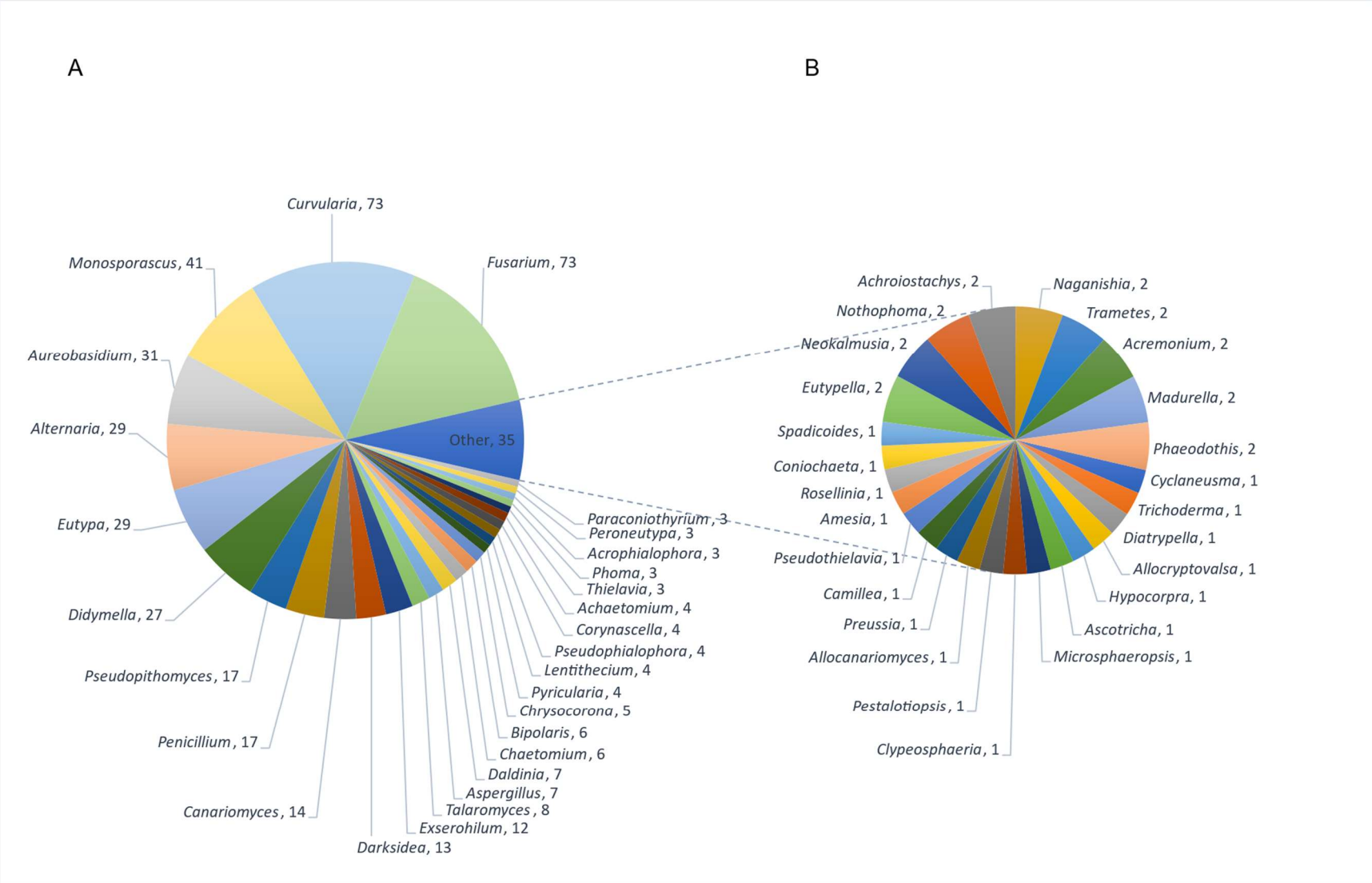

Figure 2. The abundance of fungal genera from Namib desert fairy circles; A: Genera having more than 3 strains; B: Genera having 3 or less strains.

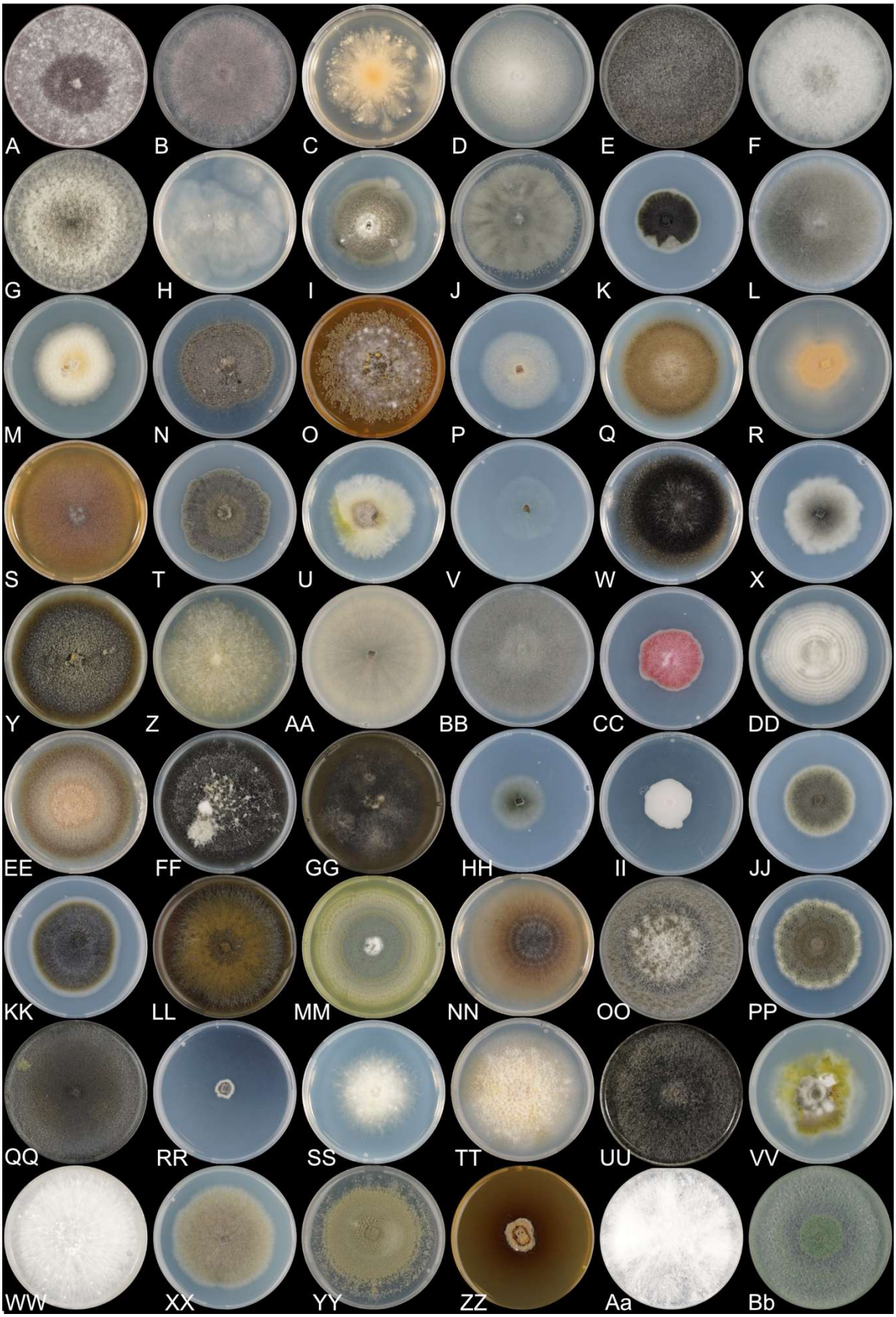

Figure 3. Representative of each fungal genus identified from the Mirabib and Far East sampling regions, on quarter PDA. A: *Achaetomium;* B: *Achroiostachys;* C: *Acremonium;* D: *Acrophialophora;* E: *Allocanariomyces;* F: *Allocryptovalsa;* G: *Alternaria;* H: *Amesia;* I:

Ascotricha; J: *Aspergillus;* K: *Aureobasidium;* L: *Bipolaris;* M: *Camillea;* N: *Canariomyces;* O: *Chaetomium;* P: *Chrysocorona;* Q: *Clypeosphaeria;* R: *Coniochaeta*; S: *Corynascella;* T: *Curvularia;* U: *Cyclaneusma;* V: *Daldinia;* W: *Darksidea;* X: *Diatrypella;* Y: *Didymella;* Z: *Eutypa;* AA: *Eutypella;* BB: *Exserohilum;* CC: *Fusarium;* DD: *Hpocopra;* EE: *Lentithecium;* FF: *Madurella;* GG: *Microsphaeropsis;* HH: *Monosporascus;* II: *Naganishia;* JJ: *Neokalmusia;* KK: *Nothophoma;* LL: *Paraconiothyrium;* MM: *Penicillium;* NN: *Peroneutypa;* OO: *Pestalotiopsis;* PP: *Phaeodothis;* QQ: *Phoma;* RR: *Preussia;* SS: *Pseudophialophora;* TT *Pseudopithomyces;* UU: *Pseudothielavia;* VV: *Pyricularia;* WW: *Rosellinia;* XX: *Spadicoides;* YY: *Talaromyces;* ZZ: *Thielavia;* Aa: *Trametes;* Bb: *Trichoderma.*

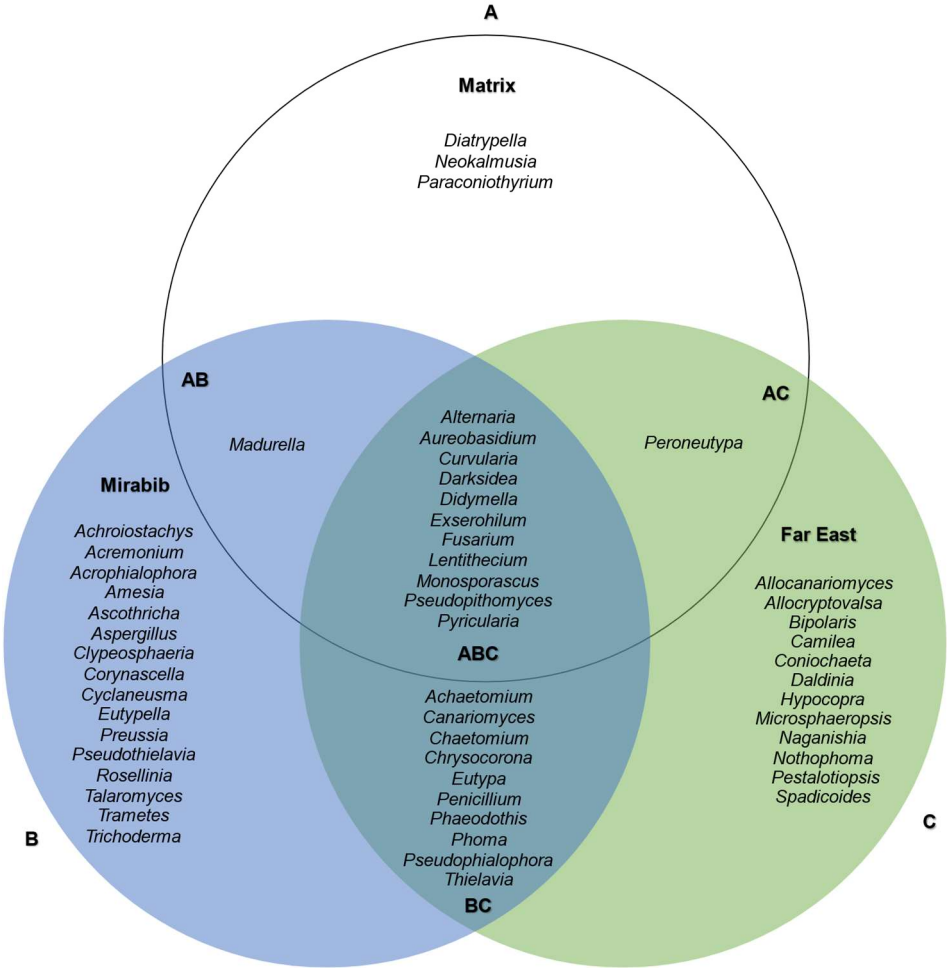

Figure 4. Venn Diagram illustrating community composition of the Namib desert fairy circles and matrix vegetation; A: Genera unique to matrix vegetation in the Mirabib region; AB: Genera from the Mirabib matrix and fairy circle; ABC: Genera shared between all samples; AC: Genera shared between the matrix vegetation and the Far East fairy circles; B: Genera unique to the Mirabib fairy circle; C: Genera unique to the Far East fairy cicle; BC: Genera shared between the Mirabib and Far East fairy circles.

Chapter 3

Four novel *Curvularia* species (*Pleosporaceae, Pleosporales*) isolated from Namib desert 'fairy circles'

Prepared for publication in Mycokeys

Abstract

Curvularia is a cosmopolitan genus of fungi found from a wide range of substrates and geographic localities. A survey of the grass *Stipagrostis ciliata* and associated rhizosphere soils collected from so-called fairy circles in the Namib desert, revealed *Curvularia* as one of the most common genera. A total of 73 *Curvularia* strains were found representing twelve species. Initial sequence-based identifications were not conclusive for several strains. Multi-locus sequence comparisons of the Glyceraldehyde-3-phosphate dehydrogenase (*GAPDH*), internal transcribed spacer rDNA region (ITS), and translation elongation factor 1-alpha (*TEF1*) gene regions, revealed these strains to be of four undescribed taxa. These *Curvularia* species are described here as *C. gobabebensis*, *C. maraisii, C. namibensis,* and *C. stipagrosticola.*

Introduction

The genus *Curvularia* [MB 7847] was described by Boedjin (1933) and is currently classified in the family *Pleosporaceae* (order *Pleosporales*, class *Dothidiomycetes*) (Ferdinandez et al. 2021). *Curvularia* contains more than 200 validly described species (excluding varieties) (https://www.mycobank.org). *Curvularia* species can be saprophytes, endophytes or pathogens, and are found from a wide range of sources including air, indoor environments, soil, water, and plant material (Almaguer et al. 2012; Dransfield 1966; Manamgoda et al. 2015; Marin-Felix et al. 2017; Verma et al. 2013). Some *Curvularia* species such as *C. hominis, C. lunata* and *C. spicifera* can cause infection in human and animal hosts (Barde and Singh 1983; Carter and Boudreaux 2004; Manamgoda et al. 2012; Rai et al. 2021; Rinaldi et al. 1987). And additionally, *Curvularia* accommodates important plant pathogens, particularly on grasses (*Poaceae*) (Marin-Felix et al. 2020) such as *C. lunata*, the causal agent of leaf spot disease on *Zea mays* (Manamgoda et al. 2012).

Curvularia species are dematiaceous and characterized by their curved conidia that result from the unequally enlarged intermediate cells of these distoseptate spores (Marin-Felix et al. 2020). Both *Curvularia* and the closely related genus *Bipolaris* [MB 7375] include species that exhibit conidial characters that range from curved to straight (Manamgoda et al. 2012), thus making it challenging to delimit species using only morphology. The sexual morphs of these genera were previously classified in *Cochliobolus* [MB 1158], but this state is rarely observed in nature and challenging to induce in culture (Manamgoda et al. 2014). Due to the difficulty in distinguishing these fungi using morphological characteristics recent descriptions of *Curvularia* and the related *Bipolaris* species have relied on multi-locus sequence analyses of the partial glyceraldehyde-3-phosphate dehydrogenase (*GAPDH*), internal transcribed spacer rDNA region (ITS), and partial translation elongation factor 1 alpha (*TEF1*) gene regions (Manamgoda et al. 2012; Marin-Felix et al. 2017; Marin-Felix et al. 2020; Tan et al. 2018).

Fairy circles are barren, circular to nearly circular, patches that are surrounded by healthy grass (*Poaceae*) species at their peripheries (Albrecht et al. 2001). These unusual circles in Namibia were first documented by Tinley (1971) have puzzled scientists for over 50 years, with many hypotheses relating to their origin and maintenance being proposed. Such hypotheses range from termite activity to self-organisation of plants (Albrecht et al.

2001; Getzin et al. 2021b). Ramond et al. (2014) proposed that a soil-borne microbial plant pathogen could be the causal agent of these Namib Fairy Circles. Later, van der Walt et al. (2016) followed on the microbial phytopathogen hypotheses by investigating the composition of Namib desert dune and gravel plain fairy circles and adjacent soils by using high-throughput sequencing (HTS), and discovered 57 fairy circle-specific fungal operational taxonomic units (OTUs), which they hypothesised could play a role in formation and maintenance of fairy circles.

The study of van der Walt et al. (2016), which was culture-independent prompted a study of fungi associated with *Stipagrostis ciliata* and associated rhizosphere soils, collected from the Namib fairy circles. *Curvularia* was one of the most commonly isolated fungi in the prompted study, in which 12 species were identified, with four considered to be novel taxa. The aim of this study was thus to formally describe these four new species and compare them morphologically with close relatives as determined by phylogenetic analyses based on *GAPDH,* ITS and *TEF1*.

Materials and Methods

Sampling and fungal isolations

Strains included in this study were isolated from the tissues of *Stipagrostis ciliata* and associated rhizosphere soils collected in Namib desert fairy circles or so-called reverse circles. Three sites were sampled in Namibia, namely “Mirabib” (23°28.75’S; 15°20.1’ E), “Far East” (23°43.95’S; 15°46.50’E) and an area known as the “Reverse” region (23°32.71’S; 15°14.06’E). The Reverse region had patches of vegetation surrounded by bare areas of soil. Grass and associated rhizosphere soils were sampled from within the margin of the fairy circles, from the margin of the circle, and from the areas between circles. Additionally, samples were taken from an area without fairy circles in the Mirabib region.

Stipagrostis ciliata tissues were surface disinfested using 2 % sodium hypochlorite (bleach) for 3 min, 70 % ethanol for 30 sec and rinsed in distilled water for 10 sec and air-dried on sterile paper towel. The surface disinfested material, as well as the soil samples were plated directly onto Malt Extract Agar (MEA) (20 g/L malt extract, 20 g/L Difco agar) supplemented with 0.4 mg 50 ppm Streptomycin as a general selection medium. Plates were maintained for a period between 1–3 wks, at 19–21 °C. Isolates were purified onto

quarter strength Potato Dextrose Agar (12 g/L Difo Agar, 10 g/L Potato Dextrose Agar) supplemented with 2 mL 100 ppm Chloramphenicol. Strains were incubated for a further 1–3 wks as before for DNA extraction and preservation.

Preservation and DNA extraction

Isolates purified on Potato Dextrose Agar were accessioned into the CN collection (working culture collection of the Applied Mycology group) of the Forestry Agriculture and Biotechnology Institute (FABI), as well as the CMW collection in FABI and the CBS-KNAW collection in the Netherlands (Table 1). Preservation methods included cryopreservation, cultures covered with mineral oil, plugs of mycelium stored in sterile water and cultures on agar slants. Genomic DNA was extracted using PrepMan™ Ultra Sample Preparation Reagent Reagent (Applied Biosystems, Foster City, CA, USA) following the manufacturer's instructions and stored at -20 °C until use.

Polymerase chain reaction (PCR) amplification

PCR amplification of the *GAPDH*, ITS, and *TEF1* loci were conducted using primer pairs and thermal cycle conditions as described in Table 2. Reactions were set up in 25 µL volumes as follow: 17.3 µL Milli-Q® water (Millipore Corporation), 2.5 µL 10x FastStart™ Taq PCR reaction buffer with 20 mM $MgCl_2$ (Sigma-Aldrich, Roche Diagnostics), 2.5 µL of 100 mM of each deoxynucleotide (New England Biolabs®, Inc), 0.5 µL forward primer, 0.5 µL reverse primer, 0.5 µL 25 mM $MgCl_2$ (Sigma-Aldrich, Roche Diagnostics), 0.2 µL of 5 U/µL FastStart™ Taq DNA Polymerase (Sigma-Aldrich, Roche Diagnostics) and 1 µL template DNA. Reactions were run on 1 % Agarose (SeaKem® LE Agarose, Lonza Bioscience) gels electrophoresed for 30 min at 80 V. A 0.5 µg/µL GeneRuler 100 bp DNA ladder (Thermo Fisher Scientific) was run alongside to determine the amplicon sizes. Amplicons were stained with GelRed® Nucleic Acid Gel Stain (Biotium, Hayward, CA, USA).

PCR clean-up, sequencing, and precipitation reactions

PCR products were prepared for sequencing using 2 µL ExoSAP-IT™ PCR clean-up reagent (1 U/µL FastAP™ Thermosensitive Alkaline Phosphatase (Thermo Fisher Scientific), 20 U/µL Exonuclease I (Thermo Fisher Scientific)) and 5 µL PCR product.

Reactions were incubated at 37 °C for 15 min, followed by 85 °C for 15 min, and stored at 4 °C until used.

Bidirectional sequencing was conducted in 96 well plates with reactions having a total volume of 13 µL [7.4 µL Milli-Q® water, 2.1 µL 5x BigDye™ Terminator v3.1 Sequencing buffer (Applied Biosystems, Foster City, CA, USA), 0.5 µL BigDye™ Terminator v3.1 Cycle Sequencing Ready Reaction Mix (Applied Biosystems, Foster City, CA, USA), 1 µL forward or reverse primer, and 2 µL ExoSap product]. Plates were sealed and reagents collected at the bottom of the wells by brief centrifugation. Initial denaturation at 94 °C for 5 min was conducted, followed by 40 cycles of denaturation at 96 °C for 30 sec, annealing at 50 °C for 10 sec, and elongation at 60 °C for 4 min. Reactions were protected from light by storing them at 4 °C wrapped in foil until precipitation.

Reactions were prepared for Sanger sequencing by precipitation using sodium acetate. A master mix was prepared [6 000 µL absolute ethanol, 240 µL 3 M sodium acetate (pH 4.6), and 960 µL of Milli-Q®] and 60 µL of this was transferred into each well. Reactions were centrifuged for 30 min at 3 220 x g at 4 °C. The supernatant was discarded, with the residual supernatant removed by centrifugation at 180 x g for 15 sec with the plate in an inverted manner. A volume of 100 µL 70 % ethanol was added to each well, and the plate centrifuged at 3 220 x g for 10 min, to wash the pellet. The wash step was repeated. Excess ethanol was removed by inverting the plate and centrifuging it as before, after which the reactions were air-dried for 5–10 min. Reactions were sealed using plastic film and kept at 4 °C in foil to protect them from light. Sanger sequencing was conducted on an ABI PRISM™ 3500xl Auto-sequencer (Applied Biosystems, Foster City, CA, USA) at the Sanger Sequencing Facility of the University of Pretoria (Bioinformatics and Computational Biology Unit, v 19.8.22).

Phylogenetic analyses

Forward and reverse sequences were obtained from SeqServe (Bioinformatics and Computational Biology Unit, v 19.8.22) hosted by the DNA Sanger Sequencing Facility at the University of Pretoria. Contigs were assembled and manually checked in Geneious Prime® v.2019.2.3 (Biomatters, Ltd., Auckland, New Zealand). A BLASTn analysis was conducted using NCBI GenBank (National Centre for Biotechnology Information, USA) databases to obtain preliminary identifications. Sequences identified as *Curvularia* were

used in phylogenetic analyses. Newly generated sequences were deposited in GenBank (Table 1).

A reference sequence database was compiled for phylogenetic analyses based on recent literature (Crous et al. 2020; Ferdinandez et al. 2021; Iturrieta-González et al. 2020; Kiss et al. 2020; Manamgoda et al. 2012; Marin-Felix et al. 2020) (Table 3). Sequences were aligned in Geneious Prime® 2019 v2.3 using the MAFFT v1.4.0 plugin (Katoh and Standley 2013), after which sequences were manually trimmed. *Exserohilum turcicum* (CBS 690.71^{T}) and *Bipolaris zeae* (BRIP11512^{IsoPT}) were included as outgroups. For multi-gene phylogenies, alignments were concatenated in Geneious Prime. Individual and multi-gene maximum likelihood phylogenies were constructed in IQtree v1.6.12 (Nguyen et al. 2015), the most suitable model selected for each partition using the integrated Modelfinder (Kalyaanamoorthy et al. 2017), and integrated UFBoot2 was used for the ultrafast bootstrapping approximation (Hoang et al. 2017). Phylogenetic trees were viewed in the interactive Tree of Life ((iTOL), v6.5.2) (Letunic and Bork 2021) and visually edited in Affinity Designer v.1.10.4 (Serif (Europe) Ltd, Nottingham, UK).

Morphology

Strains of novel species were inoculated onto 90 mm Petri dishes containing potato dextrose agar (PDA; 39 % (w/v) BD Difco™ Potato Dextrose Agar), 2 % malt extract agar (MEA; 20 % (w/v) Malt Extract, 20 % (w/v) Difco Agar), synthetic nutrient agar (SNA), oatmeal agar (OA; 30 % (v/v) oatmeal extract, 20 % (w/v) Difco Agar) and water agar (WA; 20 % (w/v) Difco Agar) as described by Marin-Felix et al. (2020). A set of plates were incubated at 25 °C in complete darkness, and a duplicate set in a 12-hr UV light and dark diurnal cycle for 7 d (Marin-Felix et al. 2020). Colony diameter measurements were taken in triplicate from colonies incubated in complete darkness. Colony colour and characteristics were described using the colour charts in the Methuen Handbook of Colour (Kornerup and Wanscher 1978), for both colonies incubated in light/dark, and complete darkness.

Micromorphology was studied with a Zeiss AXIO Imager.A2 compound microscope equipped with an AxioCaM 512 color camera driven by Zen Blue v. 3.2 software (Carl Zeiss CMP GmbH, Göttingen, Germany). Specimens from water agar were mounted in water on glass slides. Approximately 25 measurements of characteristic morphological structures were taken for representative strains of each species using NIS-Elements

Basic Research software (Nikon Europe B.V.). The mean and standard deviation values for each structural element were calculated and the ranges expressed as follow: (minimum value-) typical range (-maximum value). Photo plates were made using Affinity Photo v.1.10.4 (Serif (Europe) Ltd, Nottingham, UK).

Results

Phylogenetic analyses

A total of 138 strains were included in the multi-locus sequence analysis. Alignments of the *GAPDH*, ITS, and *TEF1* datasets were manually trimmed to approximately 528 bp, 762 bp, and 863 bp, respectively. The most suitable substitution models were TNe+I+G4 for GAPDH and ITS, and TN+F+I+G4 for *TEF1*. Tree topologies for individual gene phylogenies were congruent (Figures 7, 8 & 9) and a concatenated phylogeny was thus used to display results. Based on this phylogeny, we considered four clades to represent new species.

The strains in this study were resolved into a total of twelve species in the concatenated gene phylogeny (Figure 1), which included four well distinguished clades that are described as novel species below in the Taxonomy section.

Fungal isolations and identifications

This study included 73 *Curvularia* strains for which 138 new DNA sequences were generated (62 *GAPDH,* 53 ITS and 23 *TEF1*) and submitted to GenBank. Strains were identified as twelve species, namely *C. bannonii* (n = 2), *Curvularia moringae* (n = 17), *C. prasadii* (n = 5), *C. rouhanii* (n = 7), *C. tribuli* (n = 8), and single strains of *C. mebaldsii, C. papendorfii,* and *C. pseudolunata*, with four that could not be identified. Strain information and other metadata are summarised in Table 1.

Most strains were identified from the Mirabib region (n = 28), followed by Far East region (n = 27), and finally the Reverse region (n = 18) (Table 1). A total of 20 strains were identified from the rhizosphere samples, and 53 from *Stipagrostis* samples, with no strains unique to the rhizosphere samples. In contrast, *C bannonii, C. gobabebensis* sp. nov., *C. mebaldsii, C. papendorfii,* and *C. pseudolunata* were unique to *Stipagrostis ciliata* samples (Figure 2). Furthermore, some *Curvularia* species were found to be unique to certain sampling regions. These included *C. bannonii* and *C. maraisii* that were were

isolated from the Far East region only. *Curvularia gobabebensis* sp. nov., *C. papendorfii,* and *C. prasadii* were isolated from the Mirabib region only. *Curvularia mebaldsii* and *C. pseudolunata* were only isolated from the Reverse region.

Taxonomy

Curvularia gobabebensis van Vuuren, Visagie, M.J. Wingf. & Yilmaz, **prov. nom.** Fig. 3A–G

Etymology. Named after the Gobabeb research and training Centre in Namibia, in recognition of the contribution that it has made to research in the Namib desert.

Typus. NAMIBIA, Mirabib, from the roots of *Stipagrostis ciliata* in an area where no fairy circles occurred, November 2019, coll. Neriman Yilmaz (ex-type strain CMW58192 = CN013C4)

Asexual morph on PDA. *Hyphae* subhyaline to pale brown, branched, septate, smooth, size (3) 4–5 (8) µm wide. *Conidiophores* single or in small groups, semi-macronematous, septate, straight to flexuous, geniculate towards the upper part, branched, cell walls thicker than those of vegetative hyphae, mononematous, pale brown to brown, not swollen at the base, size (28) 40–108 (316) µm x (3) 4–6 (9) µm. *Conidiogenous cells* smooth-walled, terminal or intercalary, proliferating sympodially, pale brown to brown with dark scars, size (5) 8–12 (18) x (3) 4–6 (8) µm. *Conidia* smooth-walled, ellipsoidal, straight, rarely curved, brown to dark brown, rounded at the apex, 6 distoseptate, sometimes 2 to 7-distoseptate, (13) 34–36 (45) (SD=6.23) x (8) 10–11 (14) (SD=0.95) µm; *hila* slightly protuberant, darkened and thickened, 1–3 µm wide. *Chlamydospores* not observed.

Culture characteristics on PDA. *Cultures incubated in the dark:* Observe greenish grey with a dark green outer, reverse greenish grey to black, does not cover the surface of the petri dish in 7 d, margin greenish grey, moderate aerial mycelium giving the colony a slightly cottony appearance. Colonies reaching 54 mm after 7 d. *Cultures incubated in a 12-hr diurnal UV light cycle:* Observe greenish grey with a dark green outer, reverse greenish grey to black, does not cover the surface of the petri dish in 7 d, margin greenish grey, moderate aerial mycelium giving the colony a slightly cottony appearance.

Aditional material examined. NAMIBIA, Erongo region, from *Stipagrotis ciliate* tissues and surrounding rhizosphere, *C. bannonii* (CN021G8=CMW58180, CN024C4), *C. maraisii* sp. nov. (CN021G3=CMW58194=CBS149142, CN037F7=CMW58195=CBS149143), *C. mebaldsii* (CN060G8=CMW58185), *C. moringae* (CN010G6, CN010H3, CN010H5, CN011E9, CN011F2=CMW58186, CN011H6, CN012B1, CN013B5, CN013E2, CN022A3, CN024B8, CN034A3, CN038C9, CN059H1, CN060H6, CN060I1, CN060I4), *C. namibensis* sp. nov. (CN015H8=CMW58196=CBS149144, CN023D3=CMW58197, CN024D2=CMW58198=CBS149145, CN027A9=CMW58199, CN027C4=CMW58200, CN034A7, CN036F1=CMW58202, CN036F6=CMW58203, CN036G9=CMW58204, CN036I5=CMW58205=CBS149146, CN037D8=CMW58206, CN037F2=CMW58207, CN037F3=CMW58208, CN037F5=CMW58209, CN037F6=CMW58210, CN044C8=CMW58211=CBS149147, CN060F9=CMW58212), *C. papendorfii* (CN011B8, CN011G7, CN012B3, CN012D4, CN036F4), *C. prasadii* (CN011B8, CN011G7, CN012B3, CN012D4, CN036F4) *C. pseudolunata* (CN061A4=CMW58188), *C. rouhanii* (CN010F6=CMW58189, CN010I9, CN022H5, CN025B3, CN028H7, CN034A6, CN061A5), *C. stipagrosticola* sp. nov. (CN011D7=CMW58213, CN011D8=CMW58219, CN034B7, CN034B8=CMW58214=CBS149148, CN034H8=CMW58215, CN044D1=CMW58216, CN060G3=CMW58217=CBS149149, CN060G4, CN060H5=CMW58218=CBS149150), *C. tribuli* (CN024H6, CN024I3, CN027E2=CMW58221, CN036G4, CN038E7, CN043E2, CN043E6, CN059G9).

Notes. *Curvularia gobabebensis* is phylogenetically closely related to *C. australiensis* (Figure 1). *Curvularia australiensis* has smaller conidia (14–40 µm x 6–11 µm), longer conidiophores (up to 150 µm x 3–7 µm), and mostly 3-distoseptate conidia when compared to *Curvularia gobabebensis* (conidia dimensions; conidiophore length; 6-distoseptate) (Tsuda and Ueyama 1981). *Curvularia gobabebensis* has a pairwise identity of 97.9% (*GAPDH*) (Alignment differs at bps 26 (C), 34–35 (G,T), 49 (T), 225 (T), 230 (T), 243–245 (CGA), 247–248 (AT), 298 (C), 328 (C), 367 (T), & 418 (C)), 99.6% (*TEF1*) (Differs at bps 258 (G), 264 (A), 354 (G), 386 (C), 431 (C), & 593 (C)) and 99.9% (ITS) (differs at bp 586 (G)) with *C. australiensis. Curvularia australiensis* was described to be grey to blackish brown on PDA whereas *C. gobabebensis* is greenish grey. *Curvulaira australiensis* has been noted from *Chloris gayana,* a member of the *Poaceae* (Tsuda and Ueyama 1981).

Curvularia maraisii van Vuuren, Visagie, M.J. Wingf. & Yilmaz, **prov. nom.** Fig. 4A–H

Etymology. Named for Dr Eugene Mairais, an exceptional scientist based at the Gobabeb Reserch Centre.

Typus. NAMIBIA, from soil surrounding fairy circles in the Far East region of the Namib desert, November 2019, coll. Neriman Yilmaz (ex-type strain CMW58195 = CN037F7)

Asexual morph on PDA. *Hyphae* hyaline to pale brown, branched, septate, smooth, (2) 4–5 (7) µm. *Conidiophores* single or in small groups, macronematous, septate, straight to flexuous, geniculate towards the upper part, sometimes branched, cell walls thicker than those of vegetative hyphae, mononematous, pale brown to brown, tapers towards the base, apex often darker than base, (15) 71–88 (254) µm x (3) 4–5 (7) µm. *Conidiogenous cells* smooth-walled, terminal or intercalary, proliferating sympodially, pale brown to brown with dark scars (3) 7–9 (16) µm x (4) 5–6 (18) µm. *Conidia* ellipsoidal to curved, sometimes atypical and bifurcate (forking at the apex), the third cell from the base is often swollen unequally, asymmetrical, pale brown to dark brown, base and apex often paler, rounded at the apex, 4-distoseptate, sometimes 1 to 6-distoseptate, (12) 24–29 (45) (SD=5.90) µm x (6) 10–12 (19) (SD=2.51) µm; *hila* slightly protuberant, darkened and thickened, (2) 3–4 µm. *Chlamydospores* (9) 10–14 (16) µm x (8) 9–12 (15) µm.

Culture characteristics on PDA. *Cultures incubated in the dark:* Observe dark green, reverse greenish grey to black, does not cover the surface of the petri dish in 7 d, margin hyaline and fimbriate, powdery, abundant sporulation. Colonies reaching 67 mm in 7 d. *Cultures incubated in a 12-hr diurnal UV light cycle:* Observe dark green, reverse greenish grey to black, does not cover the surface of the petri dish in 7 d, margin hyaline and fimbriate, powdery, abundant sporulation.

Aditional material examined. NAMIBIA, Erongo region, from *Stipagrotis ciliate* tissues and surrounding rhizosphere, *C. bannonii* (CN021G8=CMW58180, CN024C4), *C. gobabebensis* sp. nov. (CN010F9=CMW58191=CBS149139, CN013C4=CMW58192=CBS149140, CN013F6=CMW58193=CBS149141), *C. mebaldsii* (CN060G8=CMW58185), *C. moringae* (CN010G6, CN010H3, CN010H5, CN011E9, CN011F2=CMW58186, CN011H6, CN012B1, CN013B5, CN013E2, CN022A3, CN024B8, CN034A3, CN038C9, CN059H1, CN060H6, CN060I1, CN060I4),

C. namibensis sp. nov. (CN015H8=CMW58196=CBS149144, CN023D3=CMW58197, CN024D2=CMW58198=CBS149145, CN027A9=CMW58199, CN027C4=CMW58200, CN034A7, CN036F1=CMW58202, CN036F6=CMW58203, CN036G9=CMW58204, CN036I5=CMW58205=CBS149146, CN037D8=CMW58206, CN037F2=CMW58207, CN037F3=CMW58208, CN037F5=CMW58209, CN037F6=CMW58210, CN044C8=CMW58211=CBS149147, CN060F9=CMW58212), *C. papendorfii* (CN011B8, CN011G7, CN012B3, CN012D4, CN036F4), *C. prasadii* (CN011B8, CN011G7, CN012B3, CN012D4, CN036F4) *C. pseudolunata* (CN061A4=CMW58188), *C. rouhanii* (CN010F6=CMW58189, CN010I9, CN022H5, CN025B3, CN028H7, CN034A6, CN061A5), *C. stipagrosticola* sp. nov. (CN011D7=CMW58213, CN011D8=CMW58219, CN034B7, CN034B8=CMW58214=CBS149148, CN034H8=CMW58215, CN044D1=CMW58216, CN060G3=CMW58217=CBS149149, CN060G4, CN060H5=CMW58218=CBS149150), *C. tribuli* (CN024H6, CN024I3).

Notes. *Curvularia maraisii* is phylogenetically closely related to *C. indica* (Figure 1). The latter species produces mostly straight, rarely curved, 3-distoseptate conidia (Subramanian 1953) as opposed to the typically curved 4-distoseptate conidia of *C. maraisii*. *Curvularia maraisii* has a pairwise identity of 98.6% (*GAPDH*) (Alignment differs at bp 33 (A), 51 (T), 147 (A), 155 (A), 242 (T), 248 (C), 436 (T), & 496 (T)) shared with *C. indica. Curvularia indica* was described from dead culms of *Scirpus,* a grass-like plant that falls within the family *Cyperaceae* (Subramanian 1953).

Curvularia namibensis van Vuuren, Visagie, M.J. Wingf. & Yilmaz, **prov. nom.** Fig. 5A–I

Etymology. Name reflects the Namib desert and the locality where the sample was collected from which the holotype was isolated.

Typus. NAMIBIA, Mirabib, from the roots of *Stipagrostis ciliata* in an area with no fairy circles present, November 2019, coll. Neriman Yilmaz (ex-type strain. CMW58196 = CN015H8)

Asexual morph on PDA. *Hyphae* hyaline to pale brown, branched, septate, smooth walled, (1) 4–5 (8) µm. *Conidiophores* single or in small groups, macronematous, septate, straight to flexuous, geniculate at the upper part, sometimes branched, cell walls thicker than those of vegetative hyphae, mononematous, pale brown to brown, (13) 51–88 (284)

µm x (2) 4–5 (7) µm. *Conidiogenous cells* smooth-walled, terminal or intercalary, proliferating sympodially, sometimes swollen, (5) 7–10 (25) µm x (3) 4–5 (9) µm. *Conidia* ellipsoidal to curved, the third cell from the base is often swollen unequally, asymmetrical, pale brown to dark brown, base and apex often paler, rounded at the apex, 4-distoseptate, sometimes 2-distoseptate, (12) 20–24 (29) (SD=3.23) µm x (8) 10–12 (17) (SD=1.53) µm; *hila* flat, darkened and thickened, 2–3 µm. *Chlamydospores* (3) 6–12 (24) µm x (3) 8–11 (28) µm.

Culture characteristics on PDA. *Cultures incubated in the dark:* Observe nickel green to dull green, reverse greenish grey to black, does not cover the surface of the petri dish in 7 d, moderate aerial mycelia giving the colony a cottony appearance in the center, margin fimbriate and hyaline to white in colour. Colonies reaching 77 mm in 7 d. *Cultures incubated in a 12-hr diurnal UV light cycle:* Observe olive green to ivy green, reverse greenish grey, grey or black, does not cover the surface of the petri dish in 7 d, moderate aerial mycelia giving the colony a cottony appearance in the center, margin fimbriate and hyaline to brown in colour.

Aditional material examined. NAMIBIA, Erongo region, from *Stipagrotis ciliate* tissues and surrounding rhizosphere, *C. bannonii* (CN021G8=CMW58180, CN024C4), *C. gobabebensis* sp. nov. (CN010F9=CMW58191=CBS149139, CN013C4=CMW58192=CBS149140, CN013F6=CMW58193=CBS149141), *C. mebaldsii* (CN060G8=CMW58185), *C. maraisii* sp. nov. (CN021G3=CMW58194=CBS149142, CN037F7=CMW58195=CBS149143), *C. mebaldsii* (CN060G8=CMW58185), *C. moringae* (CN010G6, CN010H3, CN010H5, CN011E9, CN011F2=CMW58186, CN011H6, CN012B1, CN013B5, CN013E2, CN022A3, CN024B8, CN034A3, CN038C9, CN059H1, CN060H6, CN060I1, CN060I4), *C. papendorfii* (CN011B8, CN011G7, CN012B3, CN012D4, CN036F4), *C. prasadii* (CN011B8, CN011G7, CN012B3, CN012D4, CN036F4) *C. pseudolunata* (CN061A4=CMW58188), *C. rouhanii* (CN010F6=CMW58189, CN010I9, CN022H5, CN025B3, CN028H7, CN034A6, CN061A5), *C. stipagrosticola* sp. nov. (CN011D7=CMW58213, CN011D8=CMW58219, CN034B7, CN034B8=CMW58214=CBS149148, CN034H8=CMW58215, CN044D1=CMW58216, CN060G3=CMW58217=CBS149149, CN060G4, CN060H5=CMW58218=CBS149150), *C. tribuli* (CN024H6, CN024I3, CN027E2=CMW58221, CN036G4, CN038E7, CN043E2, CN043E6, CN059G9).

Notes. *Curvularia namibensis* is closely related to *C. warrabarensis, C. carica-papayae, C. ovoidea* and *C. prasadii* (Figure 1). *Curvularia warrabarensis* displays differences from *Curvularia namibensis* in the conidia, which are mostly 3 distoseptate in contrast to that of *Curvularia namibensis*, which is mostly 4 distoseptate. Additionally, *Curvularia namibensis* had chlamydospores, a feature not mentioned in the original description of *C. warrabarensis* (Tan et al. 2018). Lastly, the colony diameter of *C. warrabarensis* after 7 d of incubation was smaller (6–7 mm) than that of *Curvularia namibensis* (77 mm) (Tan et al. 2018). *Curvularia namibensis* has a pairwise identity of 99.5% (*GAPDH*) (Alignment differs at bps 20 (C), 55 (T), 132 (T), 173 (A), 253 (A), 256 (A), & 344 (C)), 99.99% (ITS) 99.8% (*TEF1*) (Alignment differs at bps 215 (C), 338 (C), 344 (T), 686 (C)), to *C. warraberensis.* Furthermore, *Curvularia namibensis* displays a pairwise identity against *C. carica-papayae* of 99.6% (*GAPDH*) (Alignment differs at bps 70 (C) & 173 (A)) and 99.99% (ITS), and a pairwise identity 99.6% (*GAPDH*) (Alignment differs at bp 173 (A)), 99.8% (ITS) (Alignment differs at bp 656), and 99.8% (*TEF1*) (Alignment differs at bps 344 (T) & 543–544 (AC)) with *C. prasadii*. *Curvularia warrabarensis* was also described from a member of the *Poaceae, Dactyloctenium aegyptium*, however, *C. carica-papayae* was described from a *Carica papaya* leaf, and *C. ovoidea* was originally described from *Capsicum annuum* (Fernandez-Oto et al. 2014; Iturrieta-González et al. 2020; Tan et al. 2018).

Curvularia stipagrosticola van Vuuren, Visagie, M.J. Wingf. & Yilmaz, **prov. nom.** Fig. 6A–H

Etymology. Name refers to *Stipagrostis*, the genus of grass from which the holotype was collected.

Typus. NAMIBIA, from shoots of *Stipagrostis ciliata* on the margin of a vegetation patch, November 2019, coll. Neriman Yilmaz (ex-type strain. CMW58217=CN060G3)

Asexual morph on PDA. *Hyphae* hyaline to pale brown, branched, septate, smooth walled (3) 5–7 (8) µm. *Conidiophores* single or in small groups, semi-maronematous, septate, straight to flexous, geniculate towards upper part, sometimes branched, cell walls thicker than those of vegetative hyphae, mononematous, uniformly brown (30) 62–97 (226) µm x (4) 5–7 (9) µm. *Conidiogenous cells* smooth-walled, terminal or intercalary,

proliferating sympodially, 4–11 (31) µm x (4) 6–8 (13) µm. *Conidia* curved, uniformly pale brown to dark brown, 4-distoseptate, sometimes 1 to 5-distoseptate (27) 30–35 (37) (SD=2.51) µm x (12) 13–16 (18) (SD=1.11) µm; *hila* flat, thickened and darkened 2–4 µm. *Chlamydospores* not observed.

Culture characteristics on PDA. *Cultures incubated in the dark:* Observe greenish grey to olive, reverse coal to black, does not cover the surface of the petri dish in 7 d, little to moderate aerial mycelia giving the colony a cottony appearance, margin hyaline to white and lobate, groves present. Colonies reaching 32 mm in 7 d. *Cultures incubated in a12-hr diurnal UV light cycle:* Observe greenish grey to olive, reverse coal to black, does not cover the surface of the petri dish in 7 d, little to moderate aerial mycelia giving the colony a cottony appearance, margin hyaline to white and lobate.

Aditional material examined. NAMIBIA, Erongo region, from *Stipagrotis ciliate* tissues and surrounding rhizosphere, *C. bannonii* (CN021G8=CMW58180, CN024C4), *C. gobabebensis* sp. nov. (CN010F9=CMW58191=CBS149139, CN013C4=CMW58192=CBS149140, CN013F6=CMW58193=CBS149141), *C. mebaldsii* (CN060G8=CMW58185), *C. maraisii* sp. nov. (CN021G3=CMW58194=CBS149142, CN037F7=CMW58195=CBS149143), *C. mebaldsii* (CN060G8=CMW58185), *C. moringae* (CN010G6, CN010H3, CN010H5, CN011E9, CN011F2=CMW58186, CN011H6, CN012B1, CN013B5, CN013E2, CN022A3, CN024B8, CN034A3, CN038C9, CN059H1, CN060H6, CN060I1, CN060I4), *C. namibensis* sp. nov. (CN015H8=CMW58196=CBS149144, CN023D3=CMW58197, CN024D2=CMW58198=CBS149145, CN027A9=CMW58199, CN027C4=CMW58200, CN034A7, CN036F1=CMW58202, CN036F6=CMW58203, CN036G9=CMW58204, CN036I5=CMW58205=CBS149146, CN037D8=CMW58206, CN037F2=CMW58207, CN037F3=CMW58208, CN037F5=CMW58209, CN037F6=CMW58210, CN044C8=CMW58211=CBS149147, CN060F9=CMW58212), *C. papendorfii* (CN011B8, CN011G7, CN012B3, CN012D4, CN036F4), *C. prasadii* (CN011B8, CN011G7, CN012B3, CN012D4, CN036F4) *C. pseudolunata* (CN061A4=CMW58188), *C. rouhanii* (CN010F6=CMW58189, CN010I9, CN022H5, CN025B3, CN028H7, CN034A6, CN061A5).

Notes. *Curvularia stipagrosticola* is closely related to *C. eragrostidicola* (Figure 1) which differs from *Curvularia stipagrosticola* in the smaller colony size after incubation after 7 d (2 cm), the paler colour of the conidia towards the apex, and the 3-distoseptate nature of the conidia (Tan et al. 2018). *Curvularia eragrostidicola* and *Curvularia stipagrosticola* share a pairwise identity of 98.4% (*GAPDH*) (Alignment differs at bp 35 (C), 53 (G), 58 (C), 118 (C), 137 (G), 151 (C), 155 (A), 173 (C), 174 (G), 188 (A), 191 (T), 198 (A), 206 (T), 210 (A), 216 (T), 229 (G), 232 (T), 358 (A), 367 (T), 469 (T), 484 (T), & 514 (T)), 99.6% (ITS) (Alignment differs at bps 170–171 (T), 175 (T) & 583 (A)), and 99.7% (*TEF1*) (Alignment differs a bps 2 (C), 53 (C), 344 (T), 368 (C), 392 (T), 343 (C), 623 (T), & 752 (C)). *Curvularia eragrostidicola,* which was similarly described from a member of the *Poaceae, Eragrostis pilosa* (Tan et al. 2018).

Discussion

This study represents the most extensive collections of *Curvularia* spp. from Africa and specifically from Namibia. In total, 73 *Curvularia* isolates were characterized from *Stipagrostis ciliata* and associated rhizosphere soil. Based on a multi-gene phylogenetic analysis and morphological characteristics, 12 species were identified. These include the four novel species described here as *C. gobabebensis, C. maraisii, C. namibensis*, *and C. stipagrosticola*.

Previous studies in the Namib desert have included records of *Curvularia* spp. For example, Eicker et al. (1982) surveyed rhizosphere soils associated with fairy circles in the Giribes plain and reported the isolation of *Curvularia,* but these were not identified to a species level. Crous et al. (2020), described *Curvularia moringae* from *Moringa ovalifolia* (*Moringaceae*). Furthermore, *C. eragrostidis and C. carica-papayae* were identified in a culture-dependent and -independent approach of standing *Stipagrostis sabulicola* plant litter in the Namib Sand Sea (Wenndt et al. 2021). It is thus, not surprising to find *Curvularia* in the Namib desert, particularly in *Stipagrostis*, as *Curvularia* is a well-known endophyte of *Poaceae* (Manamgoda et al. 2011; Manamgoda et al. 2012; Sivanesan 1987).

Members of the genus *Curvularia* cannot be accurately distinguished from the genus *Bipolaris* ultilising morphological characteristics alone (Marin-Felix et al. 2017; Marin-Felix et al. 2020; Tan et al. 2018). This is due to the many overlapping morphological characteristics, and consequently, phylogenetic inference based on DNA sequence data

is essential (Manamgoda et al. 2014). Because sequence data for the ITS gene region fails to provide the accurate delineation of species, sequences of the *GAPDH*, ITS and *TEF1* gene regions have been included in recent phylogenetic studies of the genus *Curvularia*, (Manamgoda et al. 2015).

Curvularia moringae and *C. namibensis,* were the most commony species identified in this study, each representing 17 strains. *Curvularia moringae* has not previously been documented from grasses or soil. *Curvularia tribuli*, described by Marin-Felix et al. (2020) from puncturevine *Tribulus terrestris* leaves represented eight of the strains isolated and has also not yet been noted from grasses or soil. *Curvularia rouhanii*, representing 7 strains, was described in 2018 from leaves of American Evergreen (*Syngonium vellozianum*) and *Eucalyptus* (Mehrabi-Koushki et al. 2018) and was found in the present study on *Stipagrostis ciliata* and in the associated rhizosphere.

Three strains of *Curvularia gobabebensis* were collected in this study and they were all isolated from the tissues of *S. cilliata*. *Curvularia maraisii* was described based on two strains isolated from *S. ciliata* tissues as well as rhizosphere samples associated with fairy circles in the Far East region. It was found to be fairy circle specific in this study. In contrast, *Curvularia namibensis* and *C. stipagrosticola* included 17 and 9 strains respectively that were found in all the sampled regions and from soil as well as plant tissues.

Desert environments such as those of the Namib, present a harsh environment often subject to high levels of UV-irradiation, radically fluctuating temperatures which are often very high, low precipitation and the soils are often highly saline and acidic (Makhalanyane et al. 2015; Porras-Alfaro et al. 2008; Whitford and Wade 2002). It is now becoming more apparent that fungi are well adapted to live in extreme environments (Coleine et al. 2022). To inhabit these harsh environments, microorganisms typically have resistance mechanisms (Porras-Alfaro et al. 2008; Selbmann et al. 2021). One of these mechanisms is the production of melanin, which protects microorganisms against harmful UV irradiation (Eisenman and Casadevall 2012; Gessler et al. 2014; Newsham 2011). The genus *Curvularia* produce such melanin pigments and it is not surprising that these fungi were commonly found in our surveys of the harsh Namibian desert environment.

The identification of 12 species of *Curvularia* including four novel *Curvularia* species through multi-locus sequence analysis contributes to the current sequence databases available for the genus *Curvularia*. The results of this study also add to our knowledge of the diversity of fungi in the Namib desert. While *Curvularia* species are known to occur in a wide variety of different niches and some include plant pathogens (Marin-Felix et al. 2017), the role in the Namib desert of the *Curvularia* strains isolated in this study remain to be understood.

References

Albrecht C, Joubert JJ, Rycke P (2001) Origin of the enigmatic, circular, barren patches ('Fairy Rings') of the pro-Namib. South African Journal of Science 97: 23–27.

Almaguer M, Rojas TI, Rodríguez-Rajo FJ, Aira MJ (2012) Airborne fungal succession in a rice field of Cuba. European Journal of Plant Pathology 133: 473–482.

Barde AK, Singh SM (1983) A Case of Onychomycosis caused by *Curvularia lunata* (Wakker) Boedijn/ Ein Fall einer onychomykose durch *Curvularia lunata* (Wakker) Boedijn. Mycoses 26: 311–316.

Boedjin K (1933) Ueber einige phragmospren Dematiazeen. Bulletin du Jardin botanique de Buitenzord 13: 120–134.

Carter E, Boudreaux C (2004) Fatal cerebral phaeohyphomycosis due to *Curvularia lunata* in an immunocompetent patient. Journal of Clinical Microbiology 42: 5419–5423.

Coleine C, Stajich JE, Selbmann L (2022) Fungi are key players in extreme ecosystems. Trends in Ecology & Evolution 37: 517–528.

Crous PW, Cowan DA, Maggs-Kölling G, Yilmaz N, Larsson E, Angelini C, Brandrud TE, Dearnaley JDW, Dima B, Dovana F, Fechner N, García D, Gené J, Halling RE, Houbraken J, Leonard P, Luangsa-Ard JJ, Noisripoom W, Rea-Ireland AE, Ševčíková H, Smyth CW, Vizzini A, Adam JD, Adams GC, Alexandrova AV, Alizadeh A, Duarte E, Andjic V, Antonín V, Arenas F, Assabgui R, Ballarà J, Banwell A, Berraf-Tebbal A, Bhatt VK, Bonito G, Botha W, Burgess TI, Caboň M, Calvert J, Carvalhais LC, Courtecuisse R, Cullington P, Davoodian N, Decock CA, Dimitrov R, Di Piazza S, Drenth A, Dumez S, Eichmeier A, Etayo J, Fernández I, Fiard JP, Fournier J, Fuentes-Aponte S, Ghanbary MAT, Ghorbani G, Giraldo A, Glushakova AM, Gouliamova DE, Guarro J, Halleen F, Hampe F, Hernández-Restrepo M, Iturrieta-González I, Jeppson M, Kachalkin AV, Karimi O, Khalid AN, Khonsanit A, Kim JI, Kim K, Kiran M, Krisai-Greilhuber I, Kučera V, Kušan I, Langenhoven SD, Lebel T, Lebeuf R, Liimatainen K, Linde C, Lindner DL, Lombard L, Mahamedi AE, Matočec N, Maxwell A, May TW, McTaggart AR, Meijer M, Mešić A, Mileto AJ, Miller AN, Molia A, Mongkolsamrit S, Cortés CM, Muñoz-Mohedano

J, Morte A, Morozova OV, Mostert L, Mostowfizadeh-Ghalamfarsa R, Nagy LG, Navarro-Ródenas A, Örstadius L, Overton BE, Papp V, Para R, Peintner U, Pham THG, Pordel A, Pošta A, Rodríguez A, Romberg M, Sandoval-Denis M, Seifert KA, Semwal KC, Sewall BJ, Shivas RG, Slovák M, Smith K, Spetik M, Spies CFJ, Syme K, Tasanathai K, Thorn RG, Tkalčec Z, Tomashevskaya MA, Torres-Garcia D, Ullah Z, Visagie CM, Voitk A, Winton LM, Groenewald JZ (2020) Fungal Planet description sheets: 1112–1181. Persoonia 45: 251–409.

Dransfield M (1966) The fungal air-spora at Samaru, Northern Nigeria. Transactions of the British Mycological Society 49: 121–132.

Eicker A, Theron G, Grobbelaar N (1982) ’n Mikrobiologiese studie van ‘kaal kolle’in die Giribesvlakte van Kaokoland, SWA-Namibië. South African Journal of Botany 1: 69–74.

Eisenman HC, Casadevall A (2012) Synthesis and assembly of fungal melanin. Applied microbiology and biotechnology 93: 931–940.

Ferdinandez HS, Manamgoda DS, Udayanga D, Deshappriya N, Munasinghe MS, Castlebury LA (2021) Molecular phylogeny and morphology reveal three novel species of *Curvularia* (*Pleosporales*, *Pleosporaceae*) associated with cereal crops and weedy grass hosts. Mycological Progress 20: 431–451.

Fernandez-Oto C, Tlidi M, Escaff D, Clerc MG (2014) Strong interaction between plants induces circular barren patches: fairy circles. Philosophical Transactions of the Royal Society A: Mathematical, Physical and Engineering Sciences 372: 1–5.

Gessler NN, Egorova AS, Belozerskaya TA (2014) Melanin pigments of fungi under extreme environmental conditions (Review). Applied Biochemistry and Microbiology 50: 105–113.

Getzin S, Yizhaq H, Tschinkel WR (2021) Definition of “fairy circles” and how they differ from other common vegetation gaps and plant rings. Journal of Vegetation Science 32: e13092.

Hoang DT, Chernomor O, von Haeseler A, Minh BQ, Vinh LS (2017) UFBoot2: Improving the ultrafast bootstrap approximation. Molecular Biology and Evolution 35: 518–522.

Iturrieta-González I, Gené J, Wiederhold N, García D (2020) Three new *Curvularia* species from clinical and environmental sources. MycoKeys 68: 1–21.

Kalyaanamoorthy S, Minh BQ, Wong TKF, Von Haeseler A, Jermiin LS (2017) ModelFinder: fast model selection for accurate phylogenetic estimates. Nature Methods 14: 587–589.

Katoh K, Standley DM (2013) MAFFT multiple sequence alignment software Version 7: Improvements in Performance and Usability. Molecular Biology and Evolution 30: 772–780.

Kiss N, Homa M, Manikandan P, Mythili A, Krizsán K, Revathi R, Varga M, Papp T, Vágvölgyi C, Kredics L, Kocsubé S (2020) New species of the genus *Curvularia*: *C. tamilnaduensis* and *C. coimbatorensis* from fungal keratitis cases in South India. Pathogens 9: 439–451.

Kornerup A, Wanscher JH (1978) Methuen handbook of colour. E. Methuen, London,

Leslie JF, Summerell BA (2006) *Fusarium*-laboratory manual. Blackwell Publishing, Ames, Iowa, 387 pp.

Letunic I, Bork P (2021) Interactive Tree Of Life (iTOL) v5: an online tool for phylogenetic tree display and annotation. Nucleic Acids Research 49: W293–W296.

Makhalanyane TP, Valverde A, Gunnigle E, Frossard A, Ramond J-B, Cowan DA (2015) Microbial ecology of hot desert edaphic systems. FEMS Microbiology Reviews 39: 203–221.

Manamgoda DS, Cai L, Bahkali AH, Chukeatirote E, Hyde KD (2011) *Cochliobolus*: an overview and current status of species. Fungal Diversity 51: 3–42.

Manamgoda DS, Cai L, McKenzie EHC, Crous PW, Madrid H, Chukeatirote E, Shivas RG, Tan YP, Hyde KD (2012) A phylogenetic and taxonomic re-evaluation of the *Bipolaris* - *Cochliobolus* - *Curvularia* Complex. Fungal Diversity 56: 131–144.

Manamgoda DS, Rossman AY, Castlebury LA, Chukeatirote E, Hyde KD (2015) A taxonomic and phylogenetic re-appraisal of the genus *Curvularia* (*Pleosporaceae*): human and plant pathogens. Phytotaxa 212: 175–198.

Manamgoda DS, Rossman AY, Castlebury LA, Crous PW, Madrid H, Chukeatirote E, Hyde KD (2014) The genus *Bipolaris*. Studies in mycology 79: 221–288.

Marin-Felix Y, Groenewald JZ, Cai L, Chen Q, Marincowitz S, Barnes I, Bensch K, Braun U, Camporesi E, Damm U, de Beer ZW, Dissanayake A, Edwards J, Giraldo A, Hernández-Restrepo M, Hyde KD, Jayawardena RS, Lombard L, Luangsa-Ard J, McTaggart AR, Rossman AY, Sandoval-Denis M, Shen M, Shivas RG, Tan YP, van der Linde EJ, Wingfield MJ, Wood AR, Zhang JQ, Zhang Y, Crous PW (2017) Genera of phytopathogenic fungi: GOPHY 1. Studies in mycology 86: 99–216.

Marin-Felix Y, Hernández-Restrepo M, Crous PW (2020) Multi-locus phylogeny of the genus *Curvularia* and description of ten new species. Mycological Progress 19: 559–588.

Mehrabi-Koushki M, Pooladi P, Eisvand P, Babaahmadi G (2018) *Curvularia ahvazensis* and *C. rouhanii* spp. nov. from Iran. Mycosphere 9: 1173–1186.

Nash SN, Snyder WC (1962) Quantitative estimations by plate counts of propagules of the bean rot *Fusarium* in field soils. Phytopathology 73: 458–462.

Newsham KK (2011) A meta-analysis of plant responses to dark septate root endophytes. New Phytologist 190: 783–793.

Nguyen BT, Shuval K, Yaroch AL (2015) Nguyen *et al.* Respond. American journal of public health 105: e2–e2.

Porras-Alfaro A, Herrera J, Sinsabaugh RL, Odenbach KJ, Lowrey T, Natvig DO (2008) Novel root fungal consortium associated with a dominant desert grass. Applied and Environmental Microbiology 74: 2805–2813.

Rai M, Ingle AP, Ingle P, Gupta I, Mobin M, Bonifaz A, Alves M (2021) Recent advances on mycotic keratitis caused by dematiaceous hyphomycetes. Journal of Applied Microbiology 131: 1652–1667.

Ramond J-B, Pienaar A, Armstrong A, Seely M, Cowan DA (2014) Niche-partitioning of edaphic microbial communities in the Namib Desert gravel plain fairy circles. PLOS ONE 9: e109539.

Rinaldi M, Phillips P, Schwartz J, Winn R, Holt G, Shagets F, Elrod J, Nishioka G, Aufdemorte T (1987) Human *Curvularia* infections: report of five cases and review of the literature. Diagnostic microbiology and infectious disease 6: 27–39.

Selbmann L, Stoppiello GA, Onofri S, Stajich JE, Coleine C (2021) Culture-dependent and amplicon sequencing approaches reveal diversity and distribution of black fungi in Antarctic cryptoendolithic communities. Journal of Fungi 7: 213–227.

Sivanesan A (1987) Graminicolous species of *Bipolaris*, *Curvularia*, *Exserohilum* and their teleomorphs. 158: 1–261.

Subramanian C (1953) Fungi imperfecti from Madras–*Curvularia*. Springer India, 27–39 pp.

Tan YP, Crous PW, Shivas RG (2018) Cryptic species of *Curvularia* in the culture collection of the Queensland plant pathology herbarium. MycoKeys 35: 1–25.

Tinley KL (1971) Etosha and the Kaokoveld. African Wild Life 25: 1–16.

Tsuda M, Ueyama A (1981) *Pseudocochliobolus australiensis*, the ascigerous state of *Bipolaris australiensis*. Mycologia 73: 88–96.

van der Walt AJ, Johnson RM, Cowan DA, Seely M, Ramond J-B (2016) Unique microbial phylotypes in Namib desert dune and gravel plain fairy circle soils. Applied and Environmental Microbiology 82: 4592–4601.

Verma P, Singh S, Singh R (2013) Seven species of *Curvularia* isolated from three lakes of Bhopal. Advances in Life Science and Technology 8: 13–16.

Wenndt AJ, Evans SE, van Diepeningen AD, Logan JR, Jacobson PJ, Seely MK, Jacobson KM (2021) Why plants harbor complex endophytic fungal communities: Insights from perennial bunchgrass *Stipagrostis sabulicola* in the Namib sand sea. Frontiers in microbiology 12: 1–13.

Whitford W, Wade EL (2002) Chapter 3 - Characterization of desert climates. In: Whitford W, Wade EL (Eds) Ecology of Desert Systems. Academic Press, London, 43–63.

Tables and figures

Table 1. Strains included in this study including their location and GenBank accession numbers

Fungus species	Collection number	Sampling location	Substrate	*GAPDH*	ITS	*TEF1*
C. bannonii	CN021G8=CMW58180, CN024C4	Far East	*Stipagrostis cilliate*	ON355386, ON355392	ON074888, ON074977	–
***C. gobabebensis* sp. nov.**	CN010F9=CMW58191=CBS149139, CN013C4=CMW58192=CBS149140, CN013F6=CMW58193=CBS149141	Mirabib	*Stipagrostis cilliate*	ON355373, ON355381, ON355383	ON332848, ON074797, ON074805	ON355344, ON355347, ON355349
***C. maraisii* sp. nov.**	CN021G3=CMW58194=CBS149142, CN037F7=CMW58195=CBS149143	Far East	*Stipagrostis cilliate* & rhizosphere	ON355385, ON355439	ON074886	ON355351
C. mebaldsii	CN060G8=CMW58185	Reverse		ON661549	ON644443	
C. moringae	CN010G6, CN010H3, CN010H5, CN011E9, CN011F2=CMW58186, CN011H6, CN012B1, CN013B5, CN013E2, CN022A3, CN024B8, CN034A3, CN038C9, CN059H1, CN060H6, CN060I1, CN060I4	Mirabib, Far East & Reverse	*Stipagrostis cilliate* & rhizosphere	ON355378, ON355382, ON355387, ON355391, ON355421, ON355411, ON355416, ON355417, ON355418	OM759877, ON074750, ON074752, ON074770, ON074771, ON074777, ON074784, ON074796, ON074802, ON074957, ON074976, ON332845, ON332834, ON332839, ON332840, ON332841	ON355346, ON355348, ON355352, ON355355, ON355366, ON355369, ON355370

***C. namibensis* sp. nov.**	CN015H8=CMW58196=CBS149144, CN023D3=CMW58197, CN024D2=CMW58198=CBS149145, CN027A9=CMW58199, CN027C4=CMW58200, CN034A7, CN036F1=CMW58202, CN036F6=CMW58203, CN036G9=CMW58204, CN036I5=CMW58205=CBS149146, CN037D8=CMW58206, CN037F2=CMW58207, CN037F3=CMW58208, CN037F5=CMW58209, CN037F6=CMW58210, CN044C8=CMW58211=CBS149147, CN060F9=CMW58212	Mirabib, Far East & Reverse	*Stipagrostis cilliate* & rhizosphere	ON355384, ON355390, ON355393, ON355401, ON355402, ON355424, ON355428, ON355430, ON355432, ON355433, ON355435, ON355436, ON355437, ON355438, ON355408, ON355412	ON074819, ON074972, ON074978, ON075009, ON075010, ON332844, ON074947, ON332835	ON355350, ON355354, ON355356, ON355362, ON355363, ON355365
C. papendorfii	CN013H2=CMW58187	Mirabib	*Stipagrostis cilliate*	–	ON074810	–
C. prasadii	CN011B8, CN011G7, CN012B3, CN012D4, CN036F4	Mirabib	*Stipagrostis cilliate* & rhizosphere	ON355375, ON355379, ON355380, ON355429	ON074762, ON074776, ON332852, ON332830	–
C. pseudolunata	CN061A4=CMW58188	Reverse	*Stipagrostis cilliate*	ON355419	ON332842	–
C. rouhanii	CN010F6=CMW58189, CN010I9, CN022H5, CN025B3, CN028H7, CN034A6, CN061A5	Mirabib, Far East & Reverse	*Stipagrostis cilliate* & rhizosphere	ON355372, ON355374, ON355388, ON355396, ON355404, ON355423, ON355420	OM759872, ON074755, ON074966, ON074981, ON074910, ON332843	ON355353, ON355357, ON355371

***C. stipagrosticola* sp. nov.**	CN011D7=CMW58213, CN011D8=CMW58219, CN034B7, CN034B8=CMW58214=CBS149148, CN034H8=CMW58215, CN044D1=CMW58216, CN060G3=CMW58217=CBS149149, CN060G4, CN060H5=CMW58218=CBS149150	Mirabib, Far East & Reverse	*Stipagrostis cilliate* & rhizosphere	ON355376, ON355377, ON355425, ON355426, ON355427, ON355409, ON355413, ON355414, ON355415	ON074769, ON332836, ON332837, ON332838	ON355345, ON355367, ON355368
C. tribuli	CN024H6, CN024I3, CN027E2=CMW58221, CN036G4, CN038E7, CN043E2, CN043E6, CN059G9	Mirabib, Far East & Reverse	*Stipagrostis cilliate* & rhizosphere	ON355394, ON355395, ON355403, ON355431, ON355440, ON355406, ON355407, ON355410	ON075013, ON332831, ON332832, ON074929, ON074931, ON332833	–

Table 2. PCR reactions and primer details for loci

Locus	Annealing temp (°C)	Cycles	Primer	Primer Direction	Primer sequence (5'-3')	Reference
Glyceraldehyde-3-phosphate dehydrogenase (*GAPDH*)	52	30	GDP1	Forward	CAACGGCTTCGGTCGCATTG	(Berbee et al. 1999)
			GDP2	Reverse	GCCAAGCAGTTGGTTGTGC	(Berbee et al. 1999)
Internal transcribed spacer (ITS)	52	35	V9G	Forward	TTACGTCCCTGCCCTTTGTA	(de Hoog and van den Ende 1998)
			LS266	Reverse	GCATTCCCAAACAACTCGACTC	(Masclaux et al. 1995)
Translation elongation factor 1-alpha (*TEF1*)	54	30	EF1-983F	Forward	GCYCCYGGHCAYCGTGAYTTYAT	(Schoch et al. 2009)
			EF1-2218R	Reverse	ATGACACCRACRGCRACRGTYTG	(Schoch et al. 2009)

Table 3. *Curvularia* reference strains included in this study

Species	CBSNumber	*GAPDH*	ITS	*TEF1*
Bipolaris zeae	BRIP11512^{IsoPT}	KJ415408	KJ415538	KJ415454
Curvularia aeria	BRIP61232b	KU552162	–	–
C. alcornii	MFLUCC10-0703^{T}	JX276433	JX256420	JX266589
C. australiensis	BRIP12044^{T}	KJ415406	KJ415540	KJ415452
C. austriaca	CBS102694^{T}	MN688829	MN688802	MN688856
C. bannonii	BRIP16732^{T}	KJ415404	KJ415542	KJ415450
C. brachyspora	CBS186.50	KM061784	KJ922372	KM230405
C. buchloes	CBS246.49^{T}	KM061789	KJ909765	KM196588
C. caricae-papayae	CBS135941^{T}	HG779146	HG778984	–
C. chlamydospora	UTHSC07-2764^{T}	HG779151	HG779021	–
C. clavata	BRIP61680b	KU552167	KU552205	KU552159
C. coatesiae	BRIP24261^{T}	MH433636	MH414897	MH433659
C. eleusinicola	USJCC-0005	MT393583	MT262877	MT432925
C. elliptiformis	LC12004	MN264092	MN215659	MN263953
C. ellisii	CBS193.62^{T}	JN600963	JN192375	JN601007
C. eragrostidicola	BRIP12538^{T}	MH433643	MH414899	MH433661
C. eragrostidis	CBS189.48	HG779154	HG778986	–
C. frankliniae	BRIP72476a	OK655931	OK638995	OK655926
C. gladioli	CBS210.79	HG779123	HG778987	–

C. gudauskasii	DAOM165085	AF081393	–	–
C. harveyi	BRIP57412$^{IsoT/T}$	KJ415400	KJ415546	KJ415446
C. homomorpha	CBS156.60^{T}	JN600970	JN192380	JN601014
C. indica	CBS550.74	LT715837	–	–
C. iranica	IRAN3487C^{T}	MN266487	MT551122	MN266490
C. ischaemi	CBS630.82^{T}	JX276440	JX256428	–
C. kenpeggii	BRIP14530^{T}	MH433644	MH414900	MH433662
C. malina	CBS131274^{T}	KP153179	JF812154	KR493095
C. manamgodae	CGMCC3.19446^{T}	MN264110	MN215677	MN263971
C. mebaldsii	BRIP12900^{T}	MH433647	MH414902	MH433664
C. micrairae	BRIP17068a^{T}	–	OM421618	–
C. microspora	GUCC6272^{T}	MF139106	MF139088	MF139115
C. moringae	CBS146828	MW173105	MW175363	–
C. neergaardii	BRIP12919$^{IsoT/T}$	KJ415397	KJ415550	KJ415443
C. ovoidea	CBS854.72	LT715842.1	–	–
C. pallescens	CBS859.73	HF565455	HE861848	–
C. palmicola	MFLUCC14-04-4^{T}	–	MF621582	–
C. panici	BG10	–	MW151803	–
C. papendorfii	CBS308.67^{T}	KM083617	KJ909774	KM196594
C. patereae	CBS198.87^{T}	MN688837	MN688810	MN688864
C. perotidis	CBS350.90^{T}	KJ415394	JN192385	JN601021
C. prasadii	CBS143.64^{T}	KM061785	KJ922373	KM230408

C. protuberans	CGMCC3.19360/LC11996^{T}	MN264125	MN215693	MN263986
C. pseudobrachyspora	CPC28808^{T}	MF490841	MF490819	MF490862
C. pseudoellisii	CBS298.80^{T}	MN688845	MN688818	MN688870
C. pseudolunata	UTHSC09-2092^{T}	HF565459	HE861842	–
C. richardiae	BRIP4371$^{IsoLT/T}$	KJ415391	KJ415555	KJ415438
C. rouhanii	CBS144674^{T}	MG428694	KX139030	MG428687
C. sacchari-officinarum	CGMCC3.19331^{T}	MN264137	MN215705	MN263998
C. siddiquii	CBS196.62^{T}	MN688850	MN688823	–
C. simmonsii	USJCC-0002^{T}	MN053011	MN044753	MN053005
C. sporobolicola	BRIP23040b^{T}	MH433652	MH414908	MH433671
C. subpapendorfii	CBS656.74^{T}	KM061791	KJ909777	KM196585
C. tanzanica	BRIP71771^{HoloT}/IMI507176	MW388669	MW396857	–
C. tribuli	CBS126975^{T}	MN688852	MN688825	MN688875
C. trifolii	CBS173.55	HG779124	HG779023	–
C. tsudae	ATCC44764$^{PT/T}$	KC747745	KC424596	KC503940
C. variabilis	CPC28815^{T}	MF490844	MF490822	MF490865
C. warraberensis	BRIP14817^{T}	MH433653	MH414909	MH433672
Curvularia sp.	AR5117/JC2012	KP645349	HE861826	KP735698
Curvularia sp.	CBS274.52	JN600979	JN192387	JN601023
Curvularia sp.	BRIP17068b/DS2015B	MH433648	KP400654	MH433666
Curvularia sp.	UTHSC8809/BRIP23040b	HF565477	MH414908	–
Exserohilum turcicum	CBS690.71^{ET}	LT882581	LT837487	LT896618

[1]**ATCC**: American Type Culture Collection, Manassas, Virginia, USA; **Bp-Zj**: cultures in the Biotechnology Institute, Zhejiang University, Hangzhou, China; **BRIP**: Queensland Plant Pathology Herbarium, Brisbane, Australia; **CBS**: Westerdijk Fungal Biodiversity Institute, Utrecht, Netherlands; **CGMCC:** China General Microbiological Culture Collection, Chinese Academy of Sciences, Beijing, China; **CPC**: cultures of Pedro Crous, Westerdijk Fungal Biodiversity Institute; **DAOMC**: Plant Research Institute, Department of Agriculture, Ottowa, Canada; **GUCC**: culture collection at the Department of Plant Pathology, Agriculuture Collage, Guizhou University, China; **IRAN**: Iranian Fungal Culture Collection, Iranian Research Institute of Plant Protection, Tehran, Iran; **MFLUCC**: Mae Fah Luang University Culture Collection, Chiang Rai, Thailand; **USJCC** University of Jayewardenepura Culture Collection; **UTHSC**: Fungus Testing Laboratory, University of Texas Health Science Centre, San Antonio, Texas, USA.

[T] ex-type, [IsoPT] iso-paratype, [PT] paratype, [ET] ex-epitype, [HoloT] holotype, [IsoLT] iso-lectotype.

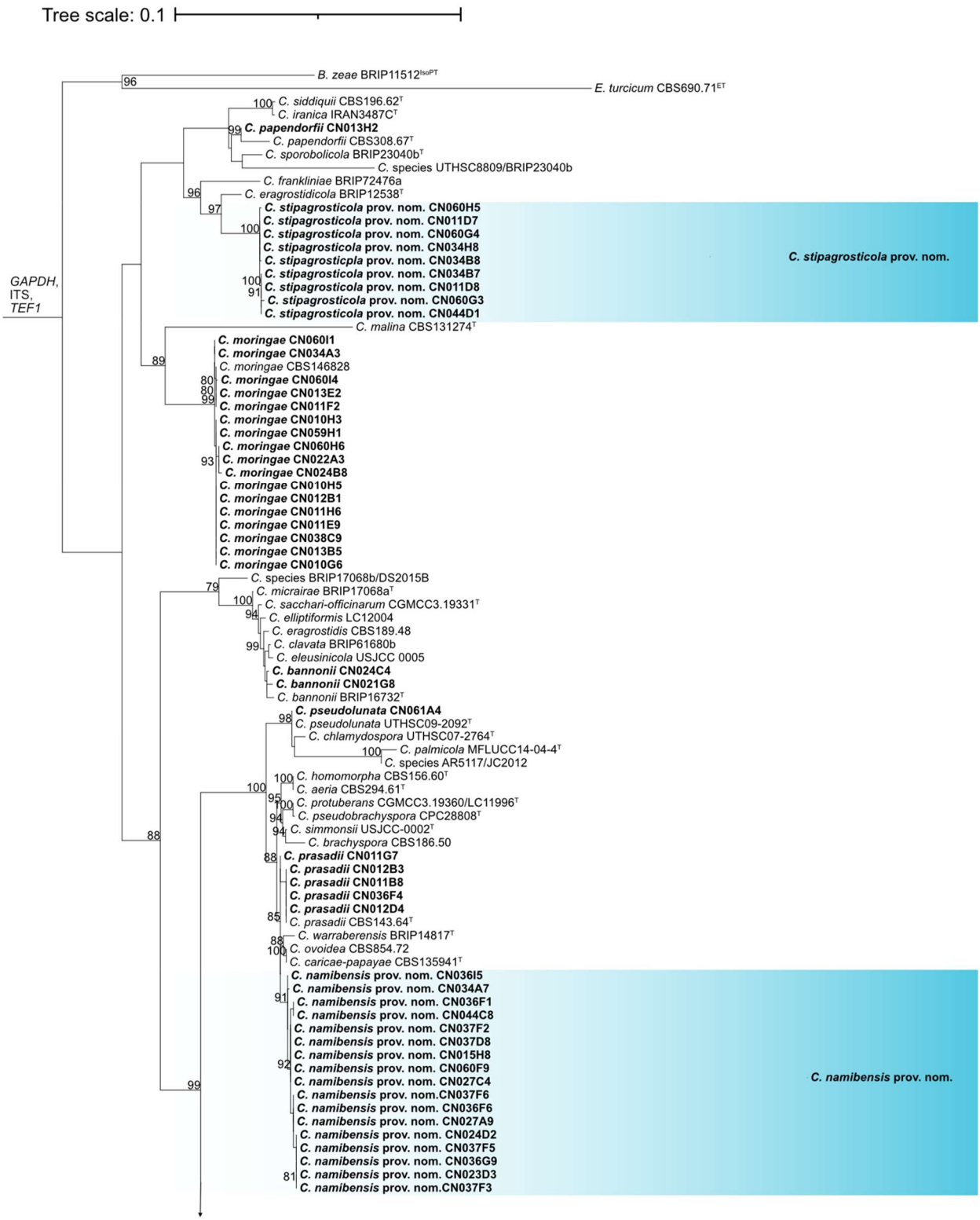

Figure 1. Phylogenetic tree based on a maximum-likelihood approach of the concatenated data of the *GAPDH*, ITS, and *TEF1* loci from phylogenetically related *Curvularia* species. The tree was rooted to *Exserohilum turcicum* and *Bipolaris zeae*. The taxonomic novelties proposed in this study are represented in bold and highlighted in blue, and additional strains included in this study are shown in bold. Bootstrap values above 75% are shown on the branch nodes.

^{T} ex-type, ^{IsoPT} iso-paratype, ^{PT} paratype, ^{ET} ex-epitype, ^{HoloT} holotype, ^{IsoLT} iso-lectotype

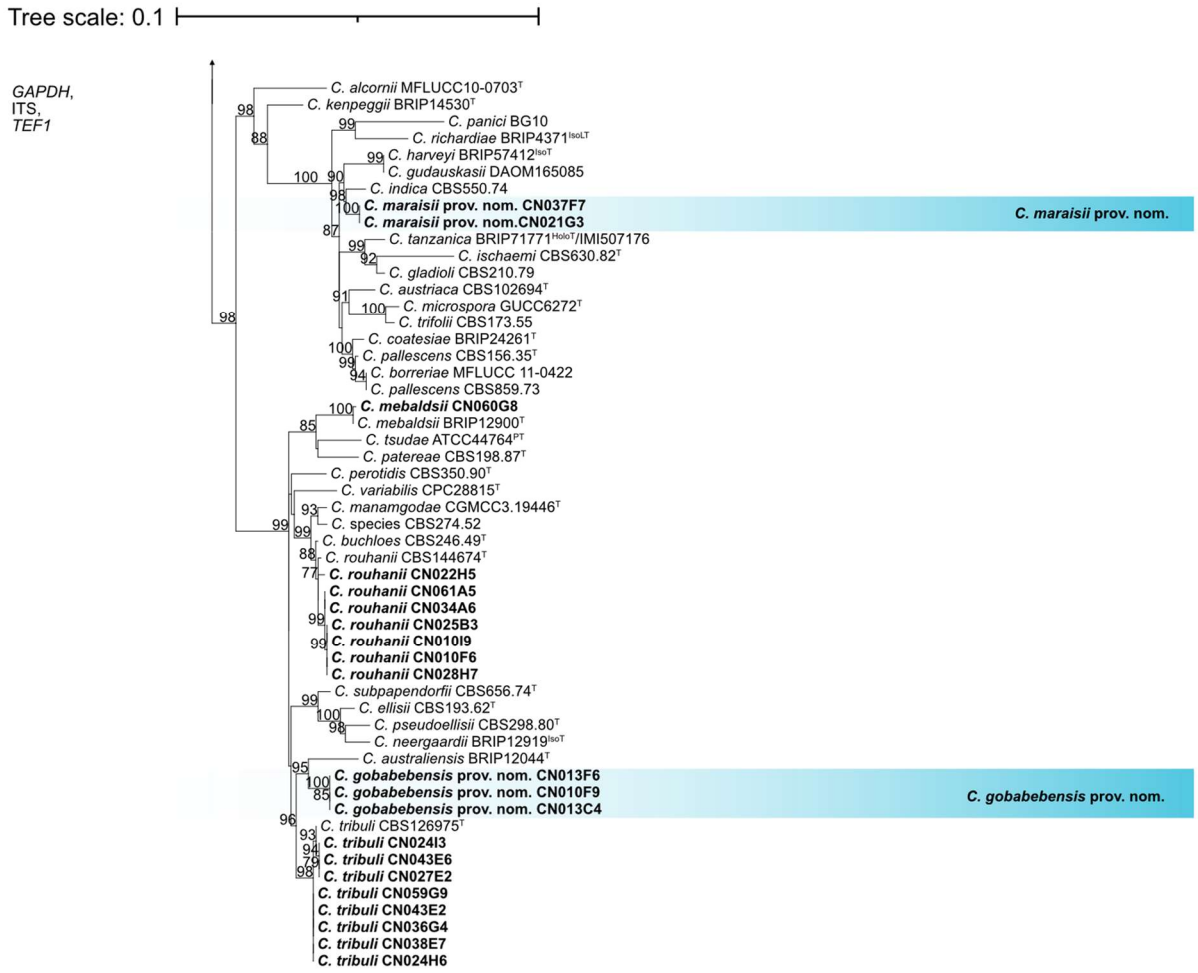

Figure 1. Continued

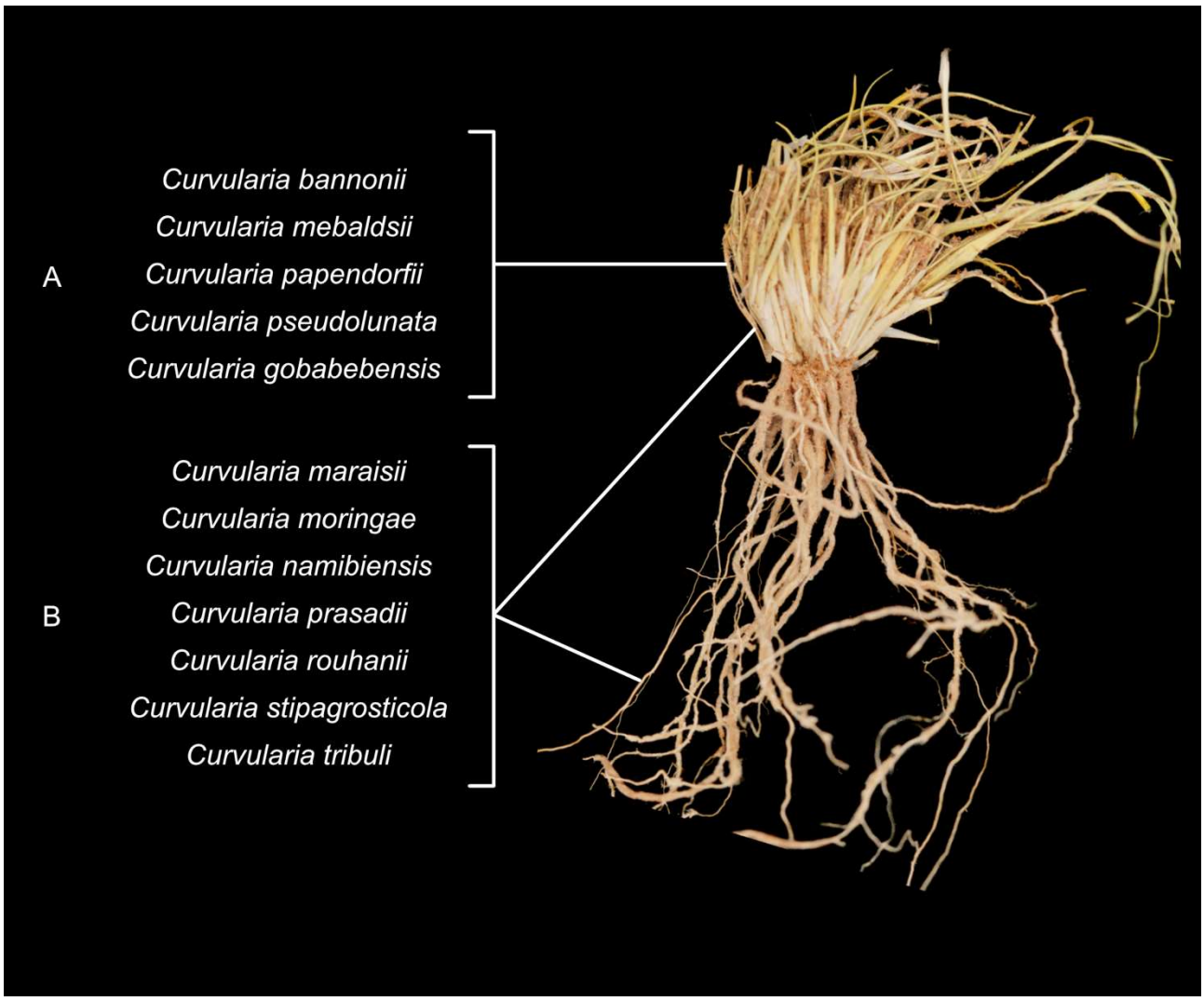

Figure 2. *Curvularia* isolates unique to and shared between rhizosphere and *Stipagrostis ciliata* samples. **A** Curvularia unique to *Stipagrostis ciliata* tissues; **B** *Curvularia* shared between rhizosphere and *Stipagrostis ciliata* samples.

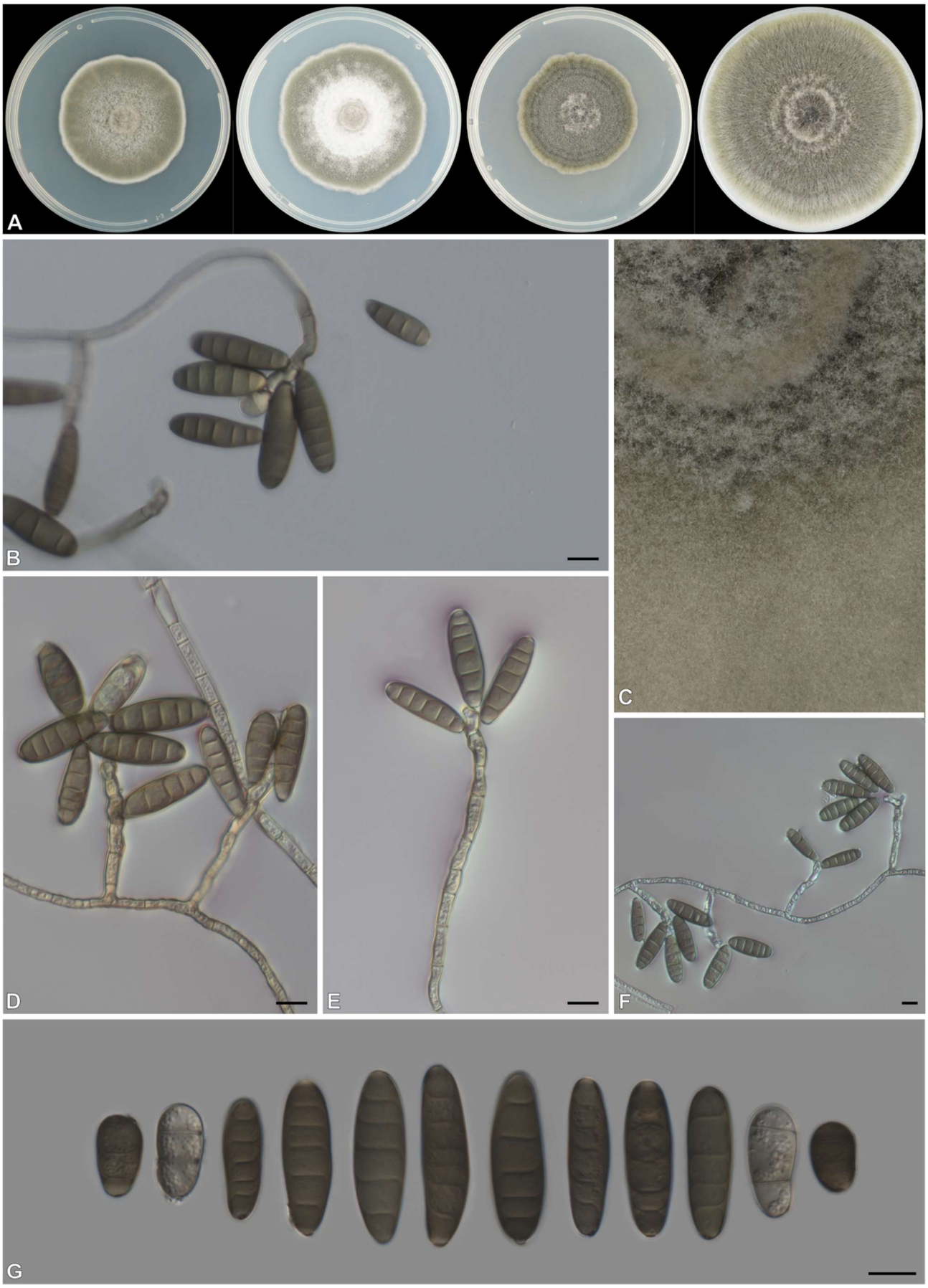

Figure 3. *Curvularia gobabebensis*; **A** Colony after incubation for 7 d on, from left to right, PDA in complete darkness, PDA exposed to a 12-hr UV light diurnal cycle, MEA exposed to

a 12-hr UV light diurnal cycle, and OA exposed to a 12-hr UV light diurnal cycle; **C** Colony texture **B, D–F** Conidiophores, conidiogenous cells and texture; **G** Conidia. Scale bars 10 μm.

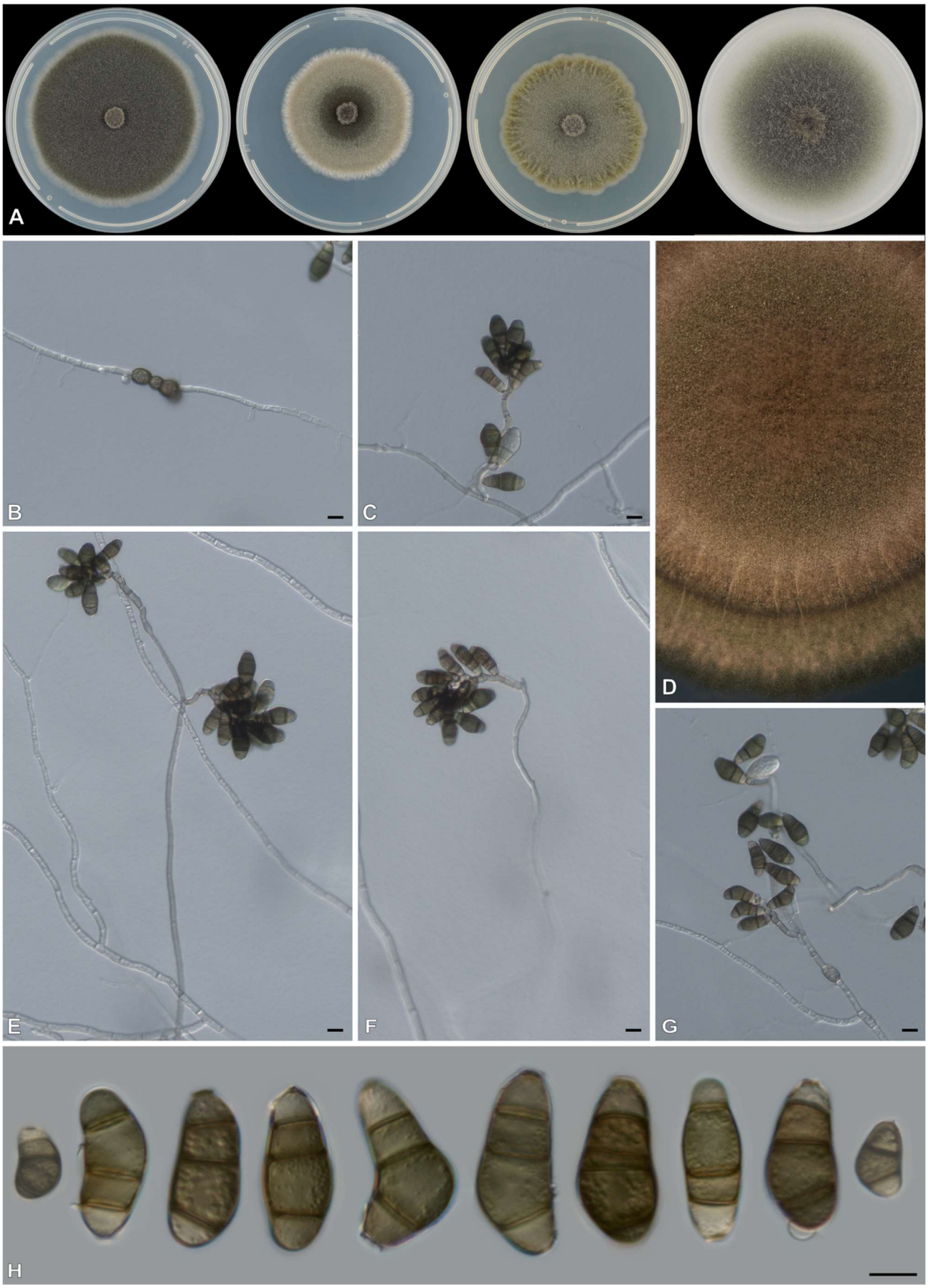

Figure 4. *Curvularia maraisii*; **A** Colony after incubation for 7 d on, from left to right, PDA in complete darkness, PDA exposed to a 12-hr UV light diurnal cycle, MEA exposed to a 12-

hr UV light diurnal cycle, and OA exposed to a 12-hr UV light diurnal cycle; **B** Chlamydospores; **D** colony texture; **C, E–G** Conidiophores, conidiogenous cells and conidia; **H** Conidia. Scale bars 10 μm.

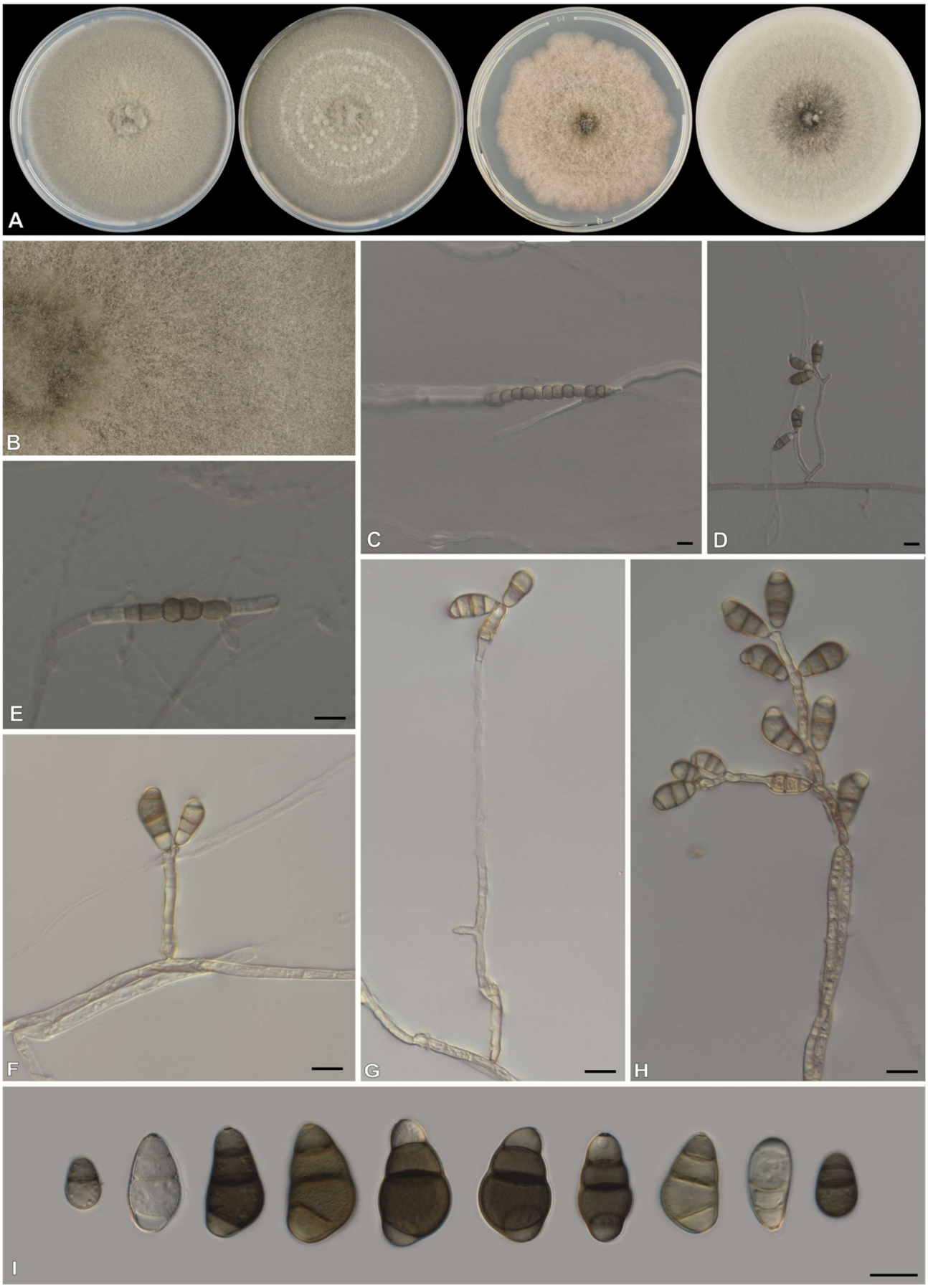

Figure 5. *Curvularia namibensis*; **A** Colony after incubation for 7 d on, from left to right, PDA in complete darkness, PDA exposed to a 12-hr UV light diurnal cycle, MEA exposed to a 12-

hr UV light diurnal cycle, and OA exposed to a 12-hr UV light diurnal cycle; **B** Colony texture; **C, E** Chlamydospores; **D, F–H** Conidiophores, conidiogenous cells and conidia; **I** Conidia. Scale bars 10 μm.

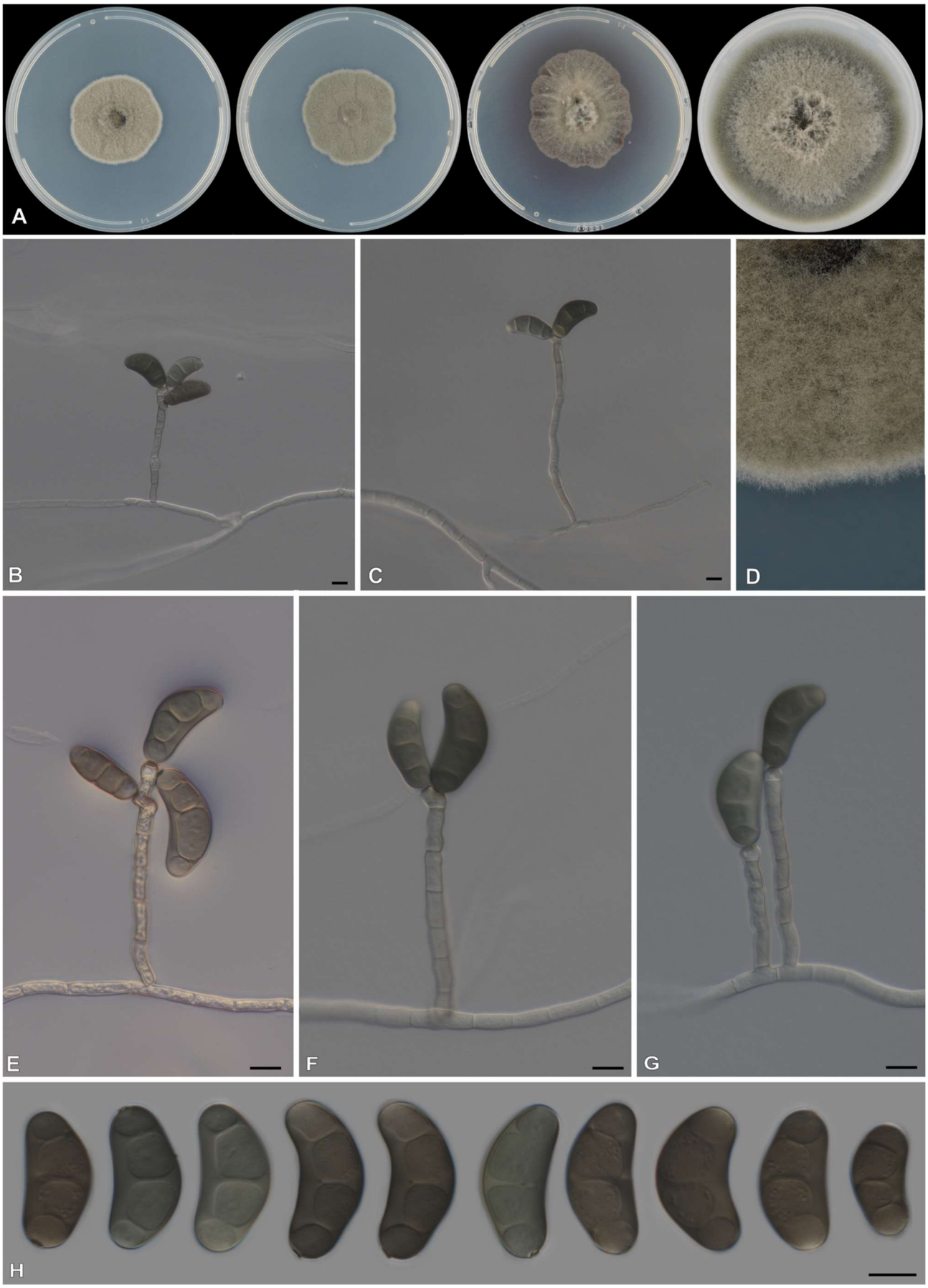

Figure 6. *Curvularia stipagrosticola*; **A** Colony after incubation for 7 d on, from left to right, PDA in complete darkness, PDA exposed to a 12-hr UV light diurnal cycle, MEA exposed to

a 12-hr UV light diurnal cycle, and OA exposed to a 1- hr UV light diurnal cycle; **D** colony texture; **B, C, E–G** Conidiophores, conidiogenous cells and conidia; **H** conidia. Scale bars 10 μm.

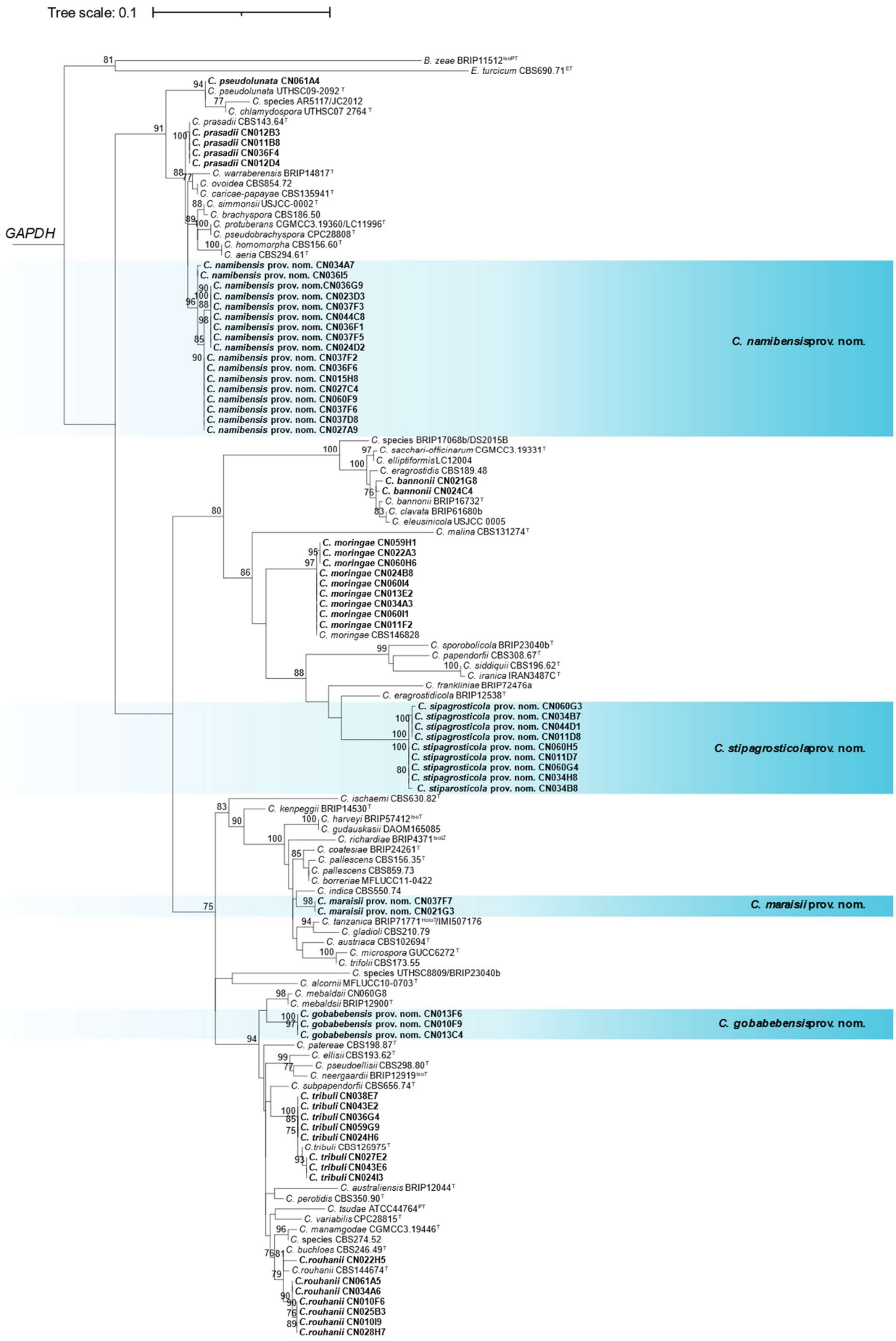
Tree scale: 0.1
GAPDH
B. zeae BRIP11512
E. turcicum CBS690.71
C. pseudolunata CN061A4
C. pseudolunata UTHSC09-2092
C. species AR5117/JC2012
C. chlamydospora UTHSC07 2764
C. prasadii CBS143.64
C. prasadii CN012B3
C. prasadii CN011B8
C. prasadii CN036F4
C. prasadii CN012D4
C. warraberensis BRIP14817
C. ovoidea CBS854.72
C. caricae-papayae CBS135941
C. simmonsii USJCC-0002
C. brachyspora CBS186.50
C. protuberans CGMCC3.19360/LC11996
C. pseudobrachyspora CPC28808
C. homomorpha CBS156.60
C. aeria CBS294.61
C. namibensis prov. nom. CN034A7
C. namibensis prov. nom. CN036I5
C. namibensis prov. nom.CN036G9
C. namibensis prov. nom. CN023D3
C. namibensis prov. nom. CN037F3
C. namibensis prov. nom. CN044C8
C. namibensis prov. nom. CN036F1
C. namibensis prov. nom. CN037F5
C. namibensis prov. nom. CN024D2
C. namibensis prov. nom. CN037F2
C. namibensis prov. nom. CN036F6
C. namibensis prov. nom. CN015H8
C. namibensis prov. nom. CN027C4
C. namibensis prov. nom. CN060F9
C. namibensis prov. nom. CN037F6
C. namibensis prov. nom. CN037D8
C. namibensis prov. nom. CN027A9
C. namibensis prov. nom.
C. species BRIP17068b/DS2015B
C. sacchari-officinarum CGMCC3.19331
C. elliptiformis LC12004
C. eragrostidis CBS189.48
C. bannonii CN021G8
C. bannonii CN024C4
C. bannonii BRIP16732
C. clavata BRIP61680b
C. eleusinicola USJCC 0005
C. malina CBS131274
C. moringae CN059H1
C. moringae CN022A3
C. moringae CN060H6
C. moringae CN024B8
C. moringae CN060I4
C. moringae CN013E2
C. moringae CN034A3
C. moringae CN060I1
C. moringae CN011F2
C. moringae CBS146828
C. sporobolicola BRIP23040b
C. papendorfii CBS308.67
C. siddiquii CBS196.62
C. iranica IRAN3487C
C. franklinae BRIP72476a
C. eragrostidicola BRIP12538
C. sipagrosticola prov. nom. CN060G3
C. stipagrosticola prov. nom. CN034B7
C. stipagrosticola prov. nom. CN044D1
C. stipagrosticola prov. nom. CN011D8
C. stipagrosticola prov. nom. CN060H5
C. stipagrosticola prov. nom. CN011D7
C. stipagrosticola prov. nom. CN060G4
C. stipagrosticola prov. nom. CN034H8
C. stiparosticola prov. nom. CN034B8
C. stipagrosticola prov. nom.
C. ischaemi CBS630.82
C. kenpeggii BRIP14530
C. harveyi BRIP57412
C. gudauskasii DAOM165085
C. richardiae BRIP4371
C. coatesiae BRIP24261
C. pallescens CBS156.35
C. pallescens CBS859.73
C. borreriae MFLUCC11-0422
C. indica CBS550.74
C. maraisii prov. nom. CN037F7
C. maraisii prov. nom. CN021G3
C. maraisii prov. nom.
C. tanzanica BRIP71771/IMI507176
C. gladioli CBS210.79
C. austriaca CBS102694
C. microspora GUCC6272
C. trifolii CBS173.55
C. species UTHSC8809/BRIP23040b
C. alcornii MFLUCC10-0703
C. mebaldsii CN060G8
C. mebaldsii BRIP12900
C. gobabebensis prov. nom. CN013F6
C. gobabebensis prov. nom. CN010F9
C. gobabebensis prov. nom. CN013C4
C. gobabebensis prov. nom.
C. patereae CBS198.87
C. ellisii CBS193.62
C. pseudoellisii CBS298.80
C. neergaardii BRIP12919
C. subpapendorfii CBS656.74
C. tribuli CN038E7
C. tribuli CN043E2
C. tribuli CN036G4
C. tribuli CN059G9
C. tribuli CN024H6
C. tribuli CBS126975
C. tribuli CN027E2
C. tribuli CN043E6
C. tribuli CN024I3
C. australiensis BRIP12044
C. perotidis CBS350.90
C. tsudae ATCC44764
C. variabilis CPC28815
C. manamgodae CGMCC3.19446
C. species CBS274.52
C. buchloes CBS246.49
C.rouhanii CN022H5
C.rouhanii CBS144674
C.rouhanii CN061A5
C.rouhanii CN034A6
C.rouhanii CN010F6
C.rouhanii CN025B3
C.rouhanii CN010I9
C.rouhanii CN028H7

Figure 7. Phylogenetic tree based on a maximum-likelihood approach of the *GAPDH* locus from phylogenetically related *Curvularia* species. The tree was rooted to *Exserohilum turcicum* and *Bipolaris zeae*. The taxonomic novelties proposed in this study are represented in bold and highlighted in blue, and additional strains included in this study are shown in bold. Bootstrap values above 75% are shown on the branch nodes.

^{T} ex-type, ^{IsoPT} iso-paratype, ^{PT} paratype, ^{ET} ex-epitype, ^{HoloT} holotype, ^{IsoLT} iso-lectotype

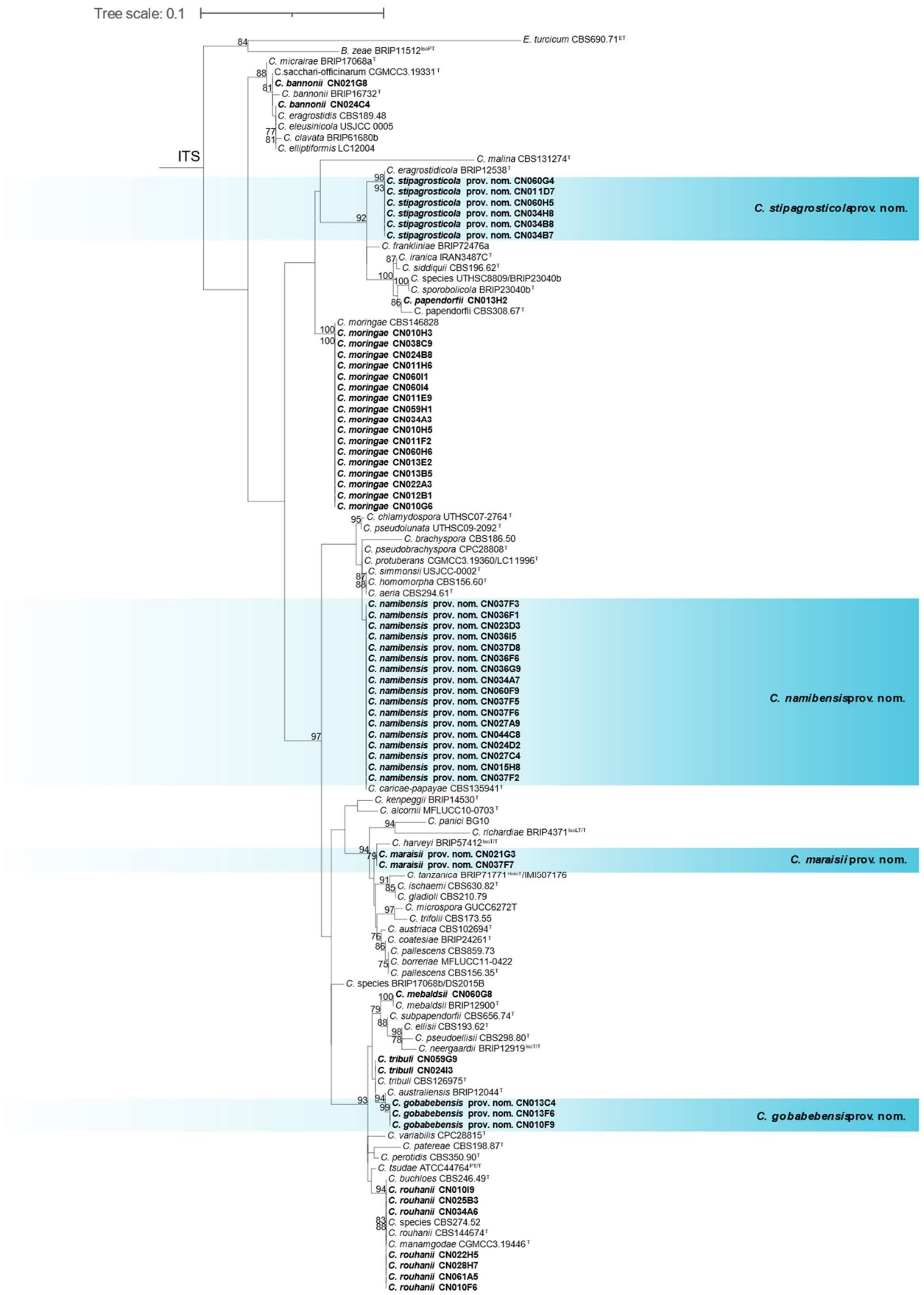
Tree scale: 0.1
ITS
E. turcicum CBS690.71ET
B. zeae BRIP11512IsoPT
C. micrairae BRIP17068aT
C.sacchari-officinarum CGMCC3.19331T
C. bannonii CN021G8
C. bannonii BRIP16732T
C. bannonii CN024C4
C. eragrostidis CBS189.48
C. eleusinicola USJCC 0005
C. clavata BRIP61680b
C. elliptiformis LC12004
C. malina CBS131274T
C. eragrostidicola BRIP12538T
C. stipagrosticola prov. nom. CN060G4
C. stipagrosticola prov. nom. CN011D7
C. stipagrosticola prov. nom. CN060H5
C. stipagrosticola prov. nom. CN034H8
C. stipagrosticola prov. nom. CN034B8
C. stipagrosticola prov. nom. CN034B7
C. stipagrosticola prov. nom.
C. franklinia BRIP72476a
C. iranica IRAN3487CT
C. siddiquii CBS196.62T
C. species UTHSC8809/BRIP23040b
C. sporobolicola BRIP23040bT
C. papendorfii CN013H2
C. papendorfii CBS308.67T
C. moringae CBS146828
C. moringae CN010H3
C. moringae CN038C9
C. moringae CN024B8
C. moringae CN011H6
C. moringae CN060I1
C. moringae CN060I4
C. moringae CN011E9
C. moringae CN059H1
C. moringae CN034A3
C. moringae CN010H5
C. moringae CN011F2
C. moringae CN060H6
C. moringae CN013E2
C. moringae CN013B5
C. moringae CN022A3
C. moringae CN012B1
C. moringae CN010G6
C. chlamydospora UTHSC07-2764T
C. pseudolunata UTHSC09-2092T
C. brachyspora CBS186.50
C. pseudobrachyspora CPC28808T
C. protuberans CGMCC3.19360/LC11996T
C. simmonsii USJCC-0002T
C. homomorpha CBS156.60T
C. aeria CBS294.61T
C. namibensis prov. nom. CN037F3
C. namibensis prov. nom. CN036F1
C. namibensis prov. nom. CN023D3
C. namibensis prov. nom. CN036I5
C. namibensis prov. nom. CN037D8
C. namibensis prov. nom. CN036F6
C. namibensis prov. nom. CN036G9
C. namibensis prov. nom. CN034A7
C. namibensis prov. nom. CN060F9
C. namibensis prov. nom. CN037F5
C. namibensis prov. nom. CN037F6
C. namibensis prov. nom. CN027A9
C. namibensis prov. nom. CN044C8
C. namibensis prov. nom. CN024D2
C. namibensis prov. nom. CN027C4
C. namibensis prov. nom. CN015H8
C. namibensis prov. nom. CN037F2
C. namibensis prov. nom.
C. caricae-papayae CBS135941T
C. kenpeggii BRIP14530T
C. alcornii MFLUCC10-0703T
C. panici BG10
C. richardiae BRIP4371IsoLT/T
C. harveyi BRIP57412IsoT/T
C. maraisii prov. nom. CN021G3
C. maraisii prov. nom. CN037F7
C. maraisii prov. nom.
C. tanzanica BRIP71771HoloT/IMI507176
C. ischaemi CBS630.82T
C. gladioli CBS210.79
C. microspora GUCC6272T
C. trifolii CBS173.55
C. austriaca CBS102694T
C. coatesiae BRIP24261T
C. pallescens CBS859.73
C. borreriae MFLUCC11-0422
C. pallescens CBS156.35T
C. species BRIP17068b/DS2015B
C. mebaldsii CN060G8
C. mebaldsii BRIP12900T
C. subpapendorfii CBS656.74T
C. ellisii CBS193.62T
C. pseudoellisii CBS298.80T
C. neergaardii BRIP12919IsoT/T
C. tribuli CN059G9
C. tribuli CN024I3
C. tribuli CBS126975T
C. australiensis BRIP12044T
C. gobabebensis prov. nom. CN013C4
C. gobabebensis prov. nom. CN013F6
C. gobabebensis prov. nom. CN010F9
C. gobabebensis prov. nom.
C. variabilis CPC28815T
C. patereae CBS198.87T
C. perotidis CBS350.90T
C. tsudae ATCC44764PT/T
C. buchloes CBS246.49T
C. rouhanii CN010I9
C. rouhanii CN025B3
C. rouhanii CN034A6
C. species CBS274.52
C. rouhanii CBS144674T
C. manamgodae CGMCC3.19446T
C. rouhanii CN022H5
C. rouhanii CN028H7
C. rouhanii CN061A5
C. rouhanii CN010F6

Figure 8. Phylogenetic tree based on a maximum-likelihood approach of the ITS locus from phylogenetically related *Curvularia* species. The tree was rooted to *Exserohilum turcicum* and *Bipolaris zeae*. The taxonomic novelties proposed in this study are represented in bold and highlighted in blue, and additional strains included in this study are shown in bold. Bootstrap values above 75% are shown on the branch nodes.

^{T} ex-type, ^{IsoPT} iso-paratype, ^{PT} paratype, ^{ET} ex-epitype, ^{HoloT} holotype, ^{IsoLT} iso-lectotype

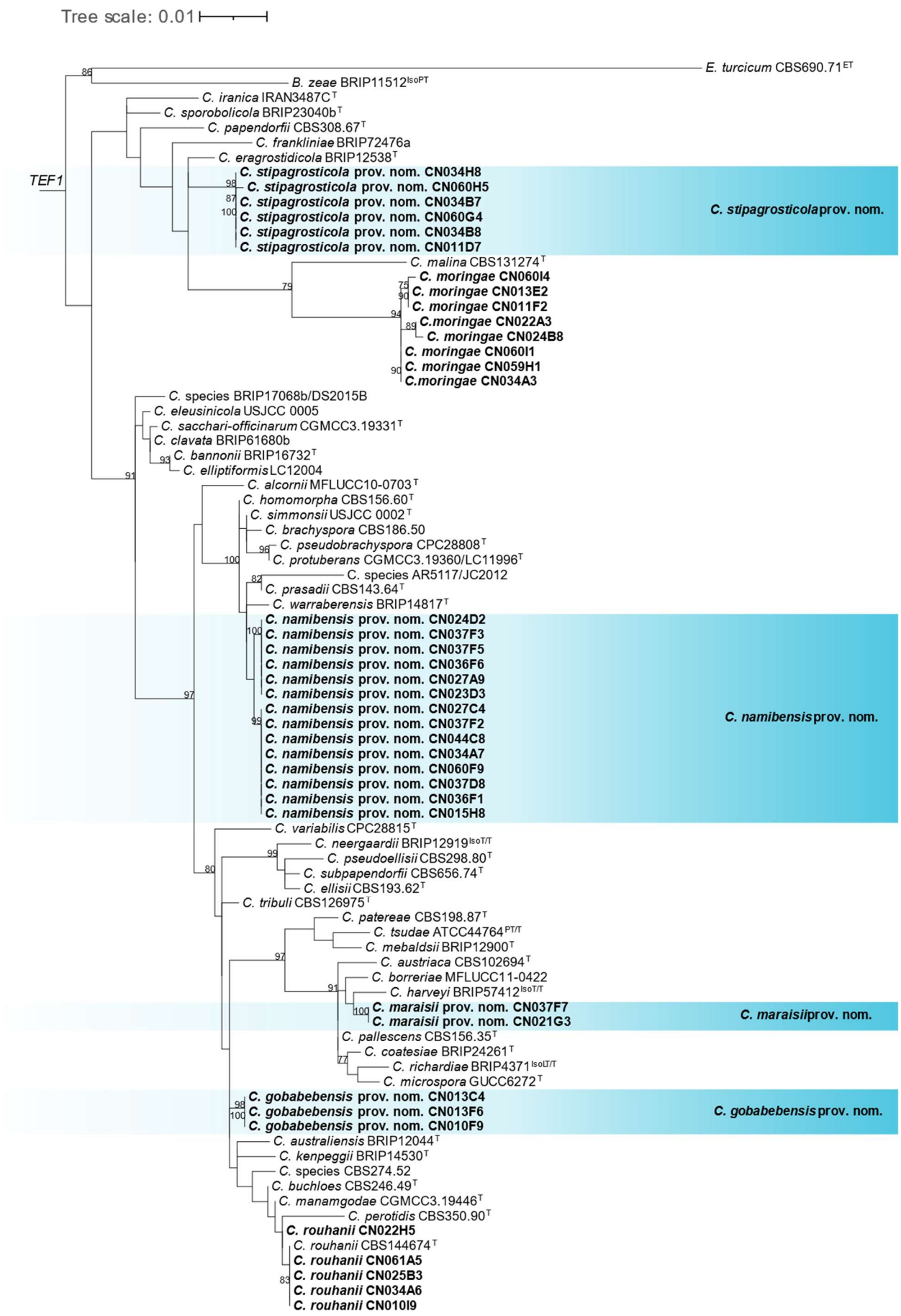
Tree scale: 0.01
TEF1
E. turcicum CBS690.71ET
B. zeae BRIP11512IsoPT
C. iranica IRAN3487CT
C. sporobolicola BRIP23040bT
C. papendorfii CBS308.67T
C. frankliniae BRIP72476a
C. eragrostidicola BRIP12538T
C. stipagrosticola prov. nom. CN034H8
C. stipagrosticola prov. nom. CN060H5
C. stipagrosticola prov. nom. CN034B7
C. stipagrosticola prov. nom. CN060G4
C. stipagrosticola prov. nom. CN034B8
C. stipagrosticola prov. nom. CN011D7
C. stipagrosticola prov. nom.
C. malina CBS131274T
C. moringae CN060I4
C. moringae CN013E2
C. moringae CN011F2
C.moringae CN022A3
C. moringae CN024B8
C. moringae CN060I1
C. moringae CN059H1
C.moringae CN034A3
C. species BRIP17068b/DS2015B
C. eleusinicola USJCC 0005
C. sacchari-officinarum CGMCC3.19331T
C. clavata BRIP61680b
C. bannonii BRIP16732T
C. elliptiformis LC12004
C. alcornii MFLUCC10-0703T
C. homomorpha CBS156.60T
C. simmonsii USJCC 0002T
C. brachyspora CBS186.50
C. pseudobrachyspora CPC28808T
C. protuberans CGMCC3.19360/LC11996T
C. species AR5117/JC2012
C. prasadii CBS143.64T
C. warraberensis BRIP14817T
C. namibensis prov. nom. CN024D2
C. namibensis prov. nom. CN037F3
C. namibensis prov. nom. CN037F5
C. namibensis prov. nom. CN036F6
C. namibensis prov. nom. CN027A9
C. namibensis prov. nom. CN023D3
C. namibensis prov. nom. CN027C4
C. namibensis prov. nom. CN037F2
C. namibensis prov. nom. CN044C8
C. namibensis prov. nom. CN034A7
C. namibensis prov. nom. CN060F9
C. namibensis prov. nom. CN037D8
C. namibensis prov. nom. CN036F1
C. namibensis prov. nom. CN015H8
C. namibensis prov. nom.
C. variabilis CPC28815T
C. neergaardii BRIP12919IsoT/T
C. pseudoellisii CBS298.80T
C. subpapendorfii CBS656.74T
C. ellisii CBS193.62T
C. tribuli CBS126975T
C. patereae CBS198.87T
C. tsudae ATCC44764PT/T
C. mebaldsii BRIP12900T
C. austriaca CBS102694T
C. borreriae MFLUCC11-0422
C. harveyi BRIP57412IsoT/T
C. maraisii prov. nom. CN037F7
C. maraisii prov. nom. CN021G3
C. maraisii prov. nom.
C. pallescens CBS156.35T
C. coatesiae BRIP24261T
C. richardiae BRIP4371IsoIT/T
C. microspora GUCC6272T
C. gobabebensis prov. nom. CN013C4
C. gobabebensis prov. nom. CN013F6
C. gobabebensis prov. nom. CN010F9
C. gobabebensis prov. nom.
C. australiensis BRIP12044T
C. kenpeggii BRIP14530T
C. species CBS274.52
C. buchloes CBS246.49T
C. manamgodae CGMCC3.19446T
C. perotidis CBS350.90T
C. rouhanii CN022H5
C. rouhanii CBS144674T
C. rouhanii CN061A5
C. rouhanii CN025B3
C. rouhanii CN034A6
C. rouhanii CN010I9

Figure 9. Phylogenetic tree based on a maximum-likelihood approach of the *TEF1* locus from phylogenetically related *Curvularia* species. The tree was rooted to *Exserohilum turcicum* and *Bipolaris zeae*. The taxonomic novelties proposed in this study are represented in bold and highlighted in blue, and additional strains included in this study are shown in bold. Bootstrap values above 75% are shown on the branch nodes.

^{T} ex-type, ^{IsoPT} iso-paratype, ^{PT} paratype, ^{ET} ex-epitype, ^{HoloT} holotype, ^{IsoLT} iso-lectotype

Summary

In the Namib desert a poorly understood phenomenon is found, known as “fairy circles”. These are almost circular, baren patches of land that are surrounded by a margin of flourishing *Stipagrostis ciliata* (*Poaceae*). Over the past 50 years, these circles have received considerable attention, however, no consensus has been reached regarding their maintenance or cause. One of the more recent hypotheses, is that they could result from the activity of microbial phytopathogens. In this study, we provide a comprehensive review of literature pertaining to the various hypotheses surrounding their formation and maintenance, their life-cycle, as well as their distribution. In this study, we surveyed the fungal diversity associated with *S. ciliata* tissues collected from fairy circles located at two sites in the Namib. For each fairy circle, five samples were collected from the almost barren inside, five from the lush margin, and five from the matrix vegetation that occurs between circles. Plant tissues were surface disinfested and plated onto Fusarium Selective Media (FSM), Malt Extract Agar (MEA) and Dichloran-Glycerol (DG18), supplemented with chloramphenicol and streptomycin. A total of 487 strains, representing 54 genera and 114 species were isolated and identified based on DNA sequence data of the beta-tubulin for *Penicillium*, calmodulin for *Aspergillus*, glyceraldehyde-3-phosphate dehydrogenase for *Bipolaris*, *Curvularia, Exserohilum* and other *Pleosporales*, internal transcribed spacer rDNA region (ITS) and/or 28S large subunit rDNA (LSU) for morphologically unidentified genera, RNA polymerase II second largest subunit for *Didymellaceae*, and/or translation elongation factor 1-alpha for *Trichoderm*a and *Fusarium*. The most prevalent genera identified included *Curvularia* (n = 73), *Fusarium* (n = 73), and *Monosporascus* (n = 41), with *Curvularia* including the largest number of species (n = 12). Four *Curvularia* species were considered novel based on comparisons with known species using both multi-locus sequence and morphological comparisons. Descriptions of these species are subsequently provided. Overall, this study indicates the rich fungal diversity present in the Namib desert that could play a role in the biology of the curious phenomenon, which certainly requires more explorations in future.